British Geological Survey
NATURAL ENVIRONMENT RESEARCH COUNCIL

# Geochemical interactions between supercritical $CO_2$ and the Utsira Formation: an experimental study

Reservoir Geosciences Programme
Saline Aquifer $CO_2$ Storage (SACS) Project
Commissioned Report CR/02/060

BRITISH GEOLOGICAL SURVEY

COMMISSIONED REPORT CR/02/060

# Geochemical interactions between supercritical $CO_2$ and the Utsira Formation: an experimental study

C.A. Rochelle, K. Bateman and J.M. Pearce



*Key words*

$CO_2$, carbon dioxide, $CO_2$ storage, SACS, Sleipner, Utsira Formation, experimental study, geochemistry, fluid-rock interaction.

*Bibliographical reference*

ROCHELLE, C.A., BATEMAN, K. AND PEARCE, J.M. 2002. Geochemical interactions between supercritical $CO_2$ and the Utsira Formation: an experimental study. *British Geological Survey Commissioned Report*, CR/02/060. 62 pp.



Keyworth, Nottingham British Geological Survey 2002

## BRITISH GEOLOGICAL SURVEY

The full range of Survey publications is available from the BGS Sales Desks at Nottingham and Edinburgh; see contact details below or shop online at www.thebgs.co.uk

The London Information Office maintains a reference collection of BGS publications including maps for consultation.

The Survey publishes an annual catalogue of its maps and other publications; this catalogue is available from any of the BGS Sales Desks.

*The British Geological Survey carries out the geological survey of Great Britain and Northern Ireland (the latter as an agency service for the government of Northern Ireland), and of the surrounding continental shelf, as well as its basic research projects. It also undertakes programmes of British technical aid in geology in developing countries as arranged by the Department for International Development and other agencies.*

*The British Geological Survey is a component body of the Natural Environment Research Council.*


**Keyworth, Nottingham NG12 5GG**

☎ 0115-936 3241 Fax 0115-936 3488
e-mail: sales@bgs.ac.uk
www.bgs.ac.uk
Shop online at: www.thebgs.co.uk

**Murchison House, West Mains Road, Edinburgh EH9 3LA**

☎ 0131-667 1000 Fax 0131-668 2683
e-mail: scotsales@bgs.ac.uk

**London Information Office at the Natural History Museum (Earth Galleries), Exhibition Road, South Kensington, London SW7 2DE**

☎ 020-7589 4090 Fax 020-7584 8270
☎ 020-7942 5344/45 email:
bgslondon@bgs.ac.uk

**Forde House, Park Five Business Centre, Harrier Way, Sowton, Exeter, Devon EX2 7HU**

☎ 01392-445271 Fax 01392-445371

**Geological Survey of Northern Ireland, 20 College Gardens, Belfast BT9 6BS**

☎ 028-9066 6595 Fax 028-9066 2835

**Maclean Building, Crowmarsh Gifford, Wallingford, Oxfordshire OX10 8BB**

☎ 01491-838800 Fax 01491-692345

*Parent Body*
**Natural Environment Research Council, Polaris House, North Star Avenue, Swindon, Wiltshire SN2 1EU**

☎ 01793-411500 Fax 01793-411501
www.nerc.ac.uk

# Foreword

This report is the published product of a study by the British Geological Survey (BGS), and forms part of the international SACS (Saline Aquifer $CO_2$ Storage) project. The SACS project aims to monitor and predict the behaviour of injected $CO_2$ in the Utsira Sand reservoir at the Sleipner field in the northern North Sea, using methods that include; time-lapse geophysics, modelling its subsurface distribution and migration, and simulating likely chemical interactions with the host rock.

This report aims to provide quantitative information on the shorter-term geochemical reactions of supercritical $CO_2$ with the Utsira formation. Laboratory experimental data have been produced to help constrain geochemical modelling activities. The experimental data also helps further our understanding of the longer-term fate of $CO_2$ that is injected into the Utsira formation.

# Acknowledgements

The authors would like to thank a number of BGS colleagues whose contributions have helped make this report possible. Humphrey Wallis and Steve Upton of the R&D workshops provided technical assistance and modified the pressure vessels used for the experiments. Pat Coombs helped with setting up the experimental systems used. Jon Bouch, Ellie Evans and Grenville Turner assisted with mineralogical analysis of the reacted samples of Utsira sand. Jo Wragg, Ben Charlton and Shaun Reeder analysed the fluid samples produced during this study.

# Contents

## FIGURES

**PLATES**



**TABLES**

# Summary

This report describes work undertaken at the British Geological Survey (BGS) that forms part of the international SACS (Saline Aquifer $CO_2$ Storage) project. The SACS project aims to monitor and predict the behaviour of injected $CO_2$ in the Utsira Sand reservoir at the Sleipner field in the northern North Sea, using methods that include; time-lapse geophysics, modelling its subsurface distribution and migration, and simulating likely chemical interactions with the host rock. This report describes a laboratory experimental study aimed at providing geochemical data to help constrain geochemical modelling activities, and to further our understanding of the longer-term fate of $CO_2$ injected into the Utsira formation.

The experimental study was undertaken in the Hydrothermal Laboratory of the BGS, where a range of measurements were made using actual Utsira sand core material and synthetic Utsira porewater. The experimental conditions chosen were mainly 37°C and 10 MPa (in-situ temperature and pressure in the Utsira formation at Sleipner), though some experiments were run at 70°C and 10 MPa to enhance the rates of reaction. Experiment durations ranged from one week to two years. Experiments were pressurised with either nitrogen or carbon dioxide. The former provided a 'non reacting' reference point from which to compare the more reactive experiments containing $CO_2$. However, they also helped provide confidence in the baseline conditions within the Utsira formation prior to $CO_2$ injection. The $CO_2$ experiments provided direct information on how $CO_2$ reacted with the Utsira sand and its porewater.

Most of the observed reactions are deduced from fluid chemical changes and involve dissolution of a carbonate phase (probably shell fragments), a significant proportion of which appear to have dissolved over a 2 year period under in-situ conditions (37°C, 10 MPa). However, sand porosity is approximately 40%, and as carbonates are a minor component of the whole rock (3.9% of the total rock volume), significant dissolution is unlikely to change overall porosity by a large degree. Dissolution of silicate minerals was a much slower process, and was still ongoing (though at a reduced rate) after 2 years of reaction. There was no direct evidence for the formation of appreciable quantities of secondary precipitates. Overall however, observed $CO_2$-water-rock reactions have resulted in relatively little dissolution of the Utsira sand. From a geochemical standpoint, and just considering the host rock, the results of this study indicate that the Utsira sand would appear to be a suitable host for injected $CO_2$.

# 1 Introduction

During underground $CO_2$ storage operations in deep reservoirs, the $CO_2$ can be trapped in three main ways (with descriptors from Bachu *et al.*, 1994):

- as 'free' $CO_2$, most likely as a supercritical phase (physical trapping)
- dissolved in formation water (hydronamic trapping)
- precipitated in carbonate phases such as calcite (mineral trapping)

During the early stages of storage, 'physical trapping' is likely to be most important trapping mechanism. However, over time, hydrodynamic trapping and eventually mineral trapping will make significant contributions to the long-term containment of $CO_2$. This study focuses on the reactions between $CO_2$, porewater and host rock within the Utsira formation. It therefore covers aspects related to both hydrodynamic trapping and mineral trapping, though further details relevant to hydrodynamic trapping are given in Rochelle and Moore (2002). Within this study, identification of geochemical reactions was through detailed mineralogical and fluid chemical analyses of experimental products.

Within an underground $CO_2$ storage operation there will be a region of free $CO_2$ (e.g. the $CO_2$ 'bubble') overlying original formation porewater. The $CO_2$ will dissolve into the formation water at a rate controlled by factors such as; the rate of $CO_2$ injection, the rate of $CO_2$ dissolution into the porewater, the surface area available for reaction, the rate of diffusion of the $CO_2$ into the porewater away from the porewater-$CO_2$ interface, and the degree of mixing of the two fluids. Therefore, in different parts of the formation there will exist porewaters with a range of dissolved $CO_2$ concentrations. Within a relatively small experimental programme it is not possible to simulate all possible dissolved $CO_2$ concentrations, so the two 'end-members' of the range have been chosen for investigation. The first of these is the '$CO_2$-free' case where little reaction is expected, and the second is the '$CO_2$-saturated' case where maximum $CO_2$ is dissolved into the porewater. It is anticipated that maximizing aqueous $CO_2$ concentrations will maximize the degree of fluid-rock reaction and provide a 'limiting case' for study.

The experimental programme was constrained by the limited Sleipner baseline geochemical data available at the start of the study. For example, the only fluid chemical data available for the Utsira porewater was a single incomplete analysis from the Oseberg field some 200 km north of Sleipner (Gregersen et al., 1998). It was recognised therefore, that the porewaters at Oseberg might not be representative of those at Sleipner. As well as identifying $CO_2$-enhanced reactions, the experimental study also sought to further our understanding of the baseline Utsira porewater geochemistry.

# 2 Description of the experiments

## 2.1 EXPERIMENTAL EQUIPMENT

Laboratory experiments were conducted within The Hydrothermal Laboratory of the British Geological Survey, Keyworth. Two main approaches were utilised during this study:

- Numerous low maintenance 'batch' experiments of variable duration.

- A single, higher maintenance 'column' experiment, having a 0.5 ml $h^{-1}$ flow rate over a period of 8 months.

Prior to performing the experiments, it was necessary to design and construct equipment that would perform well. Although dry supercritical $CO_2$ is relatively inert, in the presence of water or NaCl solution it is much more reactive. Previous studies (Schremp and Roberson, 1975) have shown that steel will corrode and standard O-ring seals will blister and fail. To minimise both corrosion and experimental failure, exposed surfaces were chosen so as to be as inert as practicable. Therefore, the wetted parts of stainless steel vessels (steel types 316 and EN54) were generally lined with PTFE (polytetrafluoroethene), high pressure tubing was made of 316 stainless steel or PEEK™ (polyaryletherketone), O-ring seals were made of Viton®, high pressure columns were made of PEEK™ and pressurised sampling containers were made of titanium.

### 2.1.1 'Batch' equipment

In order to obtain a better understanding of rock-water-$CO_2$ interactions, long-term 'batch' experiments have been performed. This type of equipment is relatively simple and free from day-to-day maintenance. As a consequence, it is well-suited for running over prolonged time periods. Indeed, it has also been used successfully in previous studies of $CO_2$-water-rock reaction (Czernichowski-Lauriol et al., 1996; Gunter et al., 1993).

There were two main aims for the 'batch' experimental programme:

- To study the evolution of porewater chemistry over time. This is achieved by setting up a series of identical experiments and terminating them at ever-increasing timescales. Changing fluid chemistry can then be followed as a series of 'snapshots', which can be used to indicate the direction of reaction, overall rates of reaction, or the time required to approach steady-state conditions.
- To investigate whether the Oseberg porewater was indeed representative of the Utsira porewater at Sleipner. This is achieved by setting up an identical series of experiments to that above, but this time using nitrogen (inert) rather than $CO_2$ as the pressurising medium. If the starting experimental porewater composition is broadly in equilibrium with the Utsira sand, then very little change in fluid chemistry should be observed. These experiments also served as 'blanks' with which to compare the $CO_2$ experiments.

The experiments were aimed at simulating the in-situ conditions, and so were undertaken at 10 MPa pressure and 37°C (Gregersen et al., 1998). However, at these relatively low temperatures reactions are slow. It was decided therefore, to perform a few experiments at 70°C and 10 MPa. This higher temperature (approximately double the in-situ temperature) was chosen as it should increase the reaction rate by approximately an order of magnitude. There are also several experimental studies at 70°C which have generated potentially useful kinetic data (e.g. Knauss and Wolery, 1986, 1988), and this might aid the modelling of the batch experiments at this temperature. Although somewhat of a simplification, in some respects the 10 times faster reaction at 70°C can be envisaged as broadly equivalent to 10 times longer reaction at 37°C. As such, the 70°C experiments might give an indication as to the direction of reactions over longer timescales.

A schematic diagram of a typical 'batch' apparatus is shown in Figure 1. For the $CO_2$ experiments 150 ml vessels were used, whereas 100 ml vessels were used for the $N_2$ experiments. Water saturated with $CO_2$ is relatively reactive, and this is especially so for saline fluids. For this reason PTFE (polytetrafluoroethylene) liners or 'cups' were used in all

vessels. Assembly of the apparatus involved first weighing out a sub-sample of dried Utsira sand (10 g for the $CO_2$ experiments and 6 g for the $N_2$ experiments) into the PTFE liners, followed by an aliquot of synthetic Utsira porewater (100 g for the $CO_2$ experiments, 60 g for the $N_2$ experiments). A 10:1 fluid:rock mass ratio was used for all the experiments. Finally a magnetic stirrer bead was added, the liner placed into the appropriate steel vessel, fresh O-rings inserted into their grooves, and the lid securely fastened down. The vessel was then placed into a Gallenkamp PlusII thermostatically-controlled oven (accurate to better than ± 0.5°C) and connected to the appropriate pressure line, and a schematic diagram of a single vessel arrangement is shown in Figure 2.

A maximum of 6 vessels (at any one time) were connected together via their $CO_2$ inlet lines. The $CO_2$ input lines were placed at the top of the vessels so that aqueous fluids (denser than supercritical $CO_2$) could not move between vessels. This arrangement meant that only a single pump was needed to maintain the $CO_2$ pressure at 10 MPa. The pump used was an ISCO 260D syringe pump. This type of pump had the advantage of a relatively large volume (260 ml), a high pressure capability (50 MPa), and modes of operation that included maintaining a constant pressure. This was particularly useful for the 'batch' experiments, especially at the start of each run when the $CO_2$ was being warmed (increasing in volume) and dissolving in the porewater (decreasing in volume). Full details of the 'batch' experiments are given in Table 1.

Mixing of $CO_2$, porewater and rock was achieved via the stirrer bead in each vessel. Although the base of the stainless steel pressure vessel was in the order of 1 cm thick, it still allowed for good 'coupling' between the magnetic stirrer and the stirrer bead. However, stirring presented a dilemma. Lots of stirring would result in good mixing, but it could also mechanically degrade the sample of Utsira sand. Conversely, little stirring would keep the Utsira sand sample relatively pristine, but mixing would not be good. It was decided to adopt a compromise between these two extremes, and have several short periods of stirring a day, with a stirring speed just high enough to agitate the sand grains. Two minutes of stirring were used every 4 hours, which was controlled via an electronic time switch. Previous studies (Toews et al., 1995) indicate that stable $CO_2$ concentrations can be obtained in high pressure water-$CO_2$ experiments within timescales as short as 30 minutes, though slightly longer timescales may be more realistic (Ellis and Golding, 1963; Stewart and Munjal, 1970; Czernichowski-Lauriol et al, 1996). However, given the relatively long duration of the batch experiments, it is reasonable to assume that the aqueous fluid within them is saturated with $CO_2$ at the pressure and temperature of the experiment.

The 'blank' experiments pressurised by nitrogen were not controlled by a high precision pump, but instead utilised a regulator connected to a gas cylinder. Control of regulators at 10 MPa is somewhat coarse, and might easily be ± 5%. This was not considered a major problem as the nitrogen was not a 'reactive' part of the system. However, this was not the case for the $CO_2$ experiments and an accurate pump had to be used as the pressure of $CO_2$ had a direct influence on dissolved $CO_2$ activity, pH etc.

In general, few problems were found with the equipment, and it performed well over up to 24 months of continuous use. However, design improvements to make the system even more 'user friendly' could include:

- Sample valve/dip tube. Any unwanted movement of aqueous fluid up the dip tube is likely to corrode the sample valve and possibly hinder sampling (see later comments). Replacement of the entire dip tube assembly with a filter in the head of the vessel would stop aqueous fluids reaching the sample valve. However, this change would require inversion of the vessel during sampling.

- Pressure seals. Each pressure vessel contained a pair of Viton® O-ring 'face seals'. Once a seal was made these performed well, but were subject to possible sudden failure if the temperature or pressure decreased (e.g. during a power cut). 'Face seals' are less well able to cope with any movement of metal surfaces, and O-ring extrusion can result. Replacing the pair of 'face seal' O-rings with a single 'edge seal' O-ring would increase reliability and halve the number of seals.

The sampling procedure used was the same for both $CO_2$-pressurised and $N_2$-pressurised experiments. In essence, it involved withdrawing a sample of $CO_2$-saturated aqueous fluid up the dip tube shown in Figure 1, and along $^1/_8$ inch diameter PEEK (polyetherethylketone) pressure tubing. This resulted in a cooling of the sample to room temperature (approximately 20°C). This was advantageous, in that the solubility of $CO_2$ increases at lower temperatures (e.g. Kuk and Montagna, 1983). Consequently, the cooled aqueous solution was below saturation with $CO_2$, and hence less prone to degassing during sampling. After flushing the pipe work with a few ml of sample, the $CO_2$-rich aqueous sample was then withdrawn into a titanium floating piston sampler (internal volume of approximately 22 ml) (see Figure 2). In order to prevent degassing of $CO_2$, this had to be done under constant pressure conditions. This was achieved by isolating all the other 'batch' experiments and using the $CO_2$ pressurising pump to maintain constant pressure conditions. The de-ionised water on the non-sample end of the floating piston was then either withdrawn via a pump, or allowed to slowly drip out via a needle valve (see Figure 3). Degassing of $CO_2$ was further prevented by keeping the sampler outside the oven. $CO_2$ has a higher solubility at lower temperatures (e.g. Kuk and Montagna, 1983; Rochelle and Moore, 2002) and cooling to room temperature will tend to make the sampled fluid slightly under-saturated and less prone to degassing. Degassing was also minimised by sampling the fluid slowly. Too rapid sampling would result in localised reduction in pressure (especially within the filter shown in Figure 1) and possible degassing.

Samples for straightforward cation and anion analysis were degassed as the titanium sampler was opened. However, some samples were taken for the analysis of total dissolved carbon. This involved reacting some of the $CO_2$-rich solution with 4M NaOH solution at the experimental pressure, in the same way as for $CO_2$ solubility experiments (for more details see Rochelle and Moore, 2002).

Most fluid samples were taken as above. However, in a few experiments it was found that a few drops of the aqueous fluid had seeped through the 'sampling valve' (see Figure 1) and corroded it to the extent that it was permanently shut. Being unable to sample via this valve, the only way to access the fluid was to invert the vessel and drain off fluid via the '$CO_2$ inlet valve'. This procedure meant that $CO_2$ pressure could not be maintained, and would have fallen slightly during sampling as the volume of water inside the vessel decreased as it was withdrawn. This procedure was also undertaken outside the oven. Some heat would have been lost from the vessel, and would have also caused some reduction in pressure. However, given the thermal inertia of the steel, and the relatively short duration of the sampling procedure, it is thought that the effects of cooling would not unduly alter the fluid chemistry or cause major secondary mineral precipitation.

Once sufficient fluid samples had been obtained, as much as possible of the remaining fluid inside the vessel was also removed (also at pressure). This was to minimise the potential for carbonate mineral precipitation as an artefact of sampling. Initially this was achieved by using a heavy liquid (dichloromethane) to displace the aqueous fluid (Gunter et al., 1993). However, it was found that secondary phase precipitation did not occur over the relatively short duration of the sampling procedure. For the majority of experiments therefore, as much

aqueous fluid as possible was removed via the dip tube prior to depressurisation. The sold sample could then be recovered.

### 2.1.2 Column equipment

This experiment was aimed at understanding how the front of dissolved $CO_2$ (and associated chemical reactions) will propagate in an open system, and also to investigate the impact of mineral reaction kinetics on flowing systems. A schematic diagram the apparatus is shown in Figure 3. It consists of 4 lengths of PEEK tubing (each 60 cm long), making a total length of 2.4 m. Each column has an internal diameter of 0.7 cm, and was packed with Utsira sand to an average porosity of approximately 42% (based on the difference between wet and dry weights, and assuming an overall solid density similar to quartz). Each column contained approximately 41 g of Utsira sand, with the total dry weight of Utsira sand being 166.028 g.

The experimental temperature of 70 °C (approximately double the in-situ temperature) was chosen to increase the reaction rate by approximately an order of magnitude compared to the in-situ temperature of 37 °C. It was hoped that this would maximise the degree of reaction in the limited time available, whilst not causing the formation of unrepresentative secondary products. This temperature was also the same as for some of the batch experiments which should allow for closer comparison. Finally, there are also several experimental studies at 70 °C which have generated kinetic data (e.g. Knauss and Wolery, 1986, 1988), and this might aid the modelling of the column experiment at this temperature. The fluid used was the same synthetic Utsira porewater used for the batch experiments, and was pre-saturated with $CO_2$ under the experimental conditions before being pumped into the column. A flow rate of 0.5 ml $h^{-1}$ was used throughout the experiment.

The sampling procedure used was the similar to that used for batch experiments. Fluid from the column was diverted into a floating piston sampler (internal volume of approximately 22 ml) under constant pressure conditions (see Figure 3). The de-ionised water on the non-sample end of the floating piston was then withdrawn at a constant rate via a pump. When the sampler was full fluid was diverted to waste and the sampler removed from the system. The fluid samples were prepared for analysis as detailed in section 2.3.2.

The fluid pressure was monitored at the inlet and outlet of the column (via pressure transducers $P_1$ and $P_2$ in Figure 3). This was done to investigate whether any pressure gradient existed across the column whilst the $CO_2$-rich porewater flowed through it. If there was a pressure gradient, any changes in it during the experiment might be due to mineral dissolution/precipitation that altered permeability.

## 2.2 STARTING MATERIALS

### 2.2.1 Utsira sand

Preparation

4 pieces of frozen Utsira Sand core were received from Reservoir Laboratories, Trondheim, Norway. Together they formed approximately 1 m of the 7 m of total core available. When received, the core was packed into a ‘cooler box’ for transportation, and was kept frozen by dry ice. Upon receipt, the core was kept frozen in a large freezer.

Initial visual inspection of the core revealed an outer zone impregnated by drilling mud, approximately 1 cm thick. In some sections of the core there was also a curved ‘fracture-like’ structure containing drilling mud that paralleled the axis of the core. It is thought that this might have resulted from ‘slumping’ of the sediment prior to it being frozen in the core tube.

Two samples of Utsira sand were taken for use in the experiments (BGS mineralogical identification numbers E641A - 420 g and E642 - 280 g), and they were treated in an identical manner (see Pearce et al. [1999, 2002] for a fuller description of the samples). The outer portions of the samples were discarded so as to remove the worst of the drilling mud contamination. However, analysis of the residual porewaters had already shown that they were heavily contaminated with drilling fluids (especially K). The first task involved washing as much of this material out of the sediment as possible so as to return the sand to close to its original state. The washing medium used was a synthetic Utsira porewater (SUP) based on the composition from the Oseberg field (Gregersen et al., 1998). A weight of SUP equal to the weight of the damp Utsira sand was added, the mixture stirred, and left for 15 minutes. This was repeated 3 times. The fourth addition of SUP was left for 4 hours, and a final addition of SUP left for 24 hours. It is anticipated that these 5 washings will have removed all of the residual drilling fluid. It is also anticipated that leaving the sample for 24 hours will have caused the majority of any ion-exchanged K to re-enter solution.

The final steps in the solid sample preparation involved filtering the sample using a Buchner funnel and then adding half the sample weight of de-ionised water. The sample was then dried at approximately 35°C. The final washing using de-ionised water was done to minimise the formation of salt crystals during drying. The formation of these (and their subsequent dissolution in the experiments) would have made the porewater chemistry of the actual experiments slightly more concentrated than required. Once dry, the samples of Utsira sand were stored in airtight containers prior to use.

The washed and dried Utsira sand samples were given individual BGS Hydrothermal Laboratory identification numbers. HTL 127 was produced from E641A, and Pearce et al. (2002) quote a surface area of 0.9 $m^2g^{-1}$ for this sample. HTL 127 was used in all the batch experiments. HTL 128 was produced from E642, and Pearce et al. (2002) quote a surface area of 0.3 $m^2g^{-1}$ for this sample. HTL 128 was used in the flow experiment.

Analysis

More detailed descriptions of the Utsira sand used in this study are given in Pearce et al. (1999, 2002) and only a summary is presented here. The Utsira sand is a medium grained, moderately to well sorted, very poorly cemented and friable subarkosic sand. It comprises predominant quartz with minor plagioclase, K-feldspar, calcite (probably shell fragments) and common bioclastic debris including foraminifera, radiolaria and sponge spicules. Some detrital grains are covered in a thin, <10 μm, clay coating which XRD indicates comprises mainly smectite with minor illite and chlorite. Although the smectite may be derived from drilling mud, the lack of sharply defined peaks, indicating a crystalline smectite, appears to preclude this. Pyrite is a minor but commonly distributed authigenic mineral occurring as framboidal aggregates, especially within foraminifera tests. The most notable diagenetic modification is the development of two minor zeolites, phillipsite and clinoptilolite. Phillipsite is the dominant of the two zeolites. Both zeolites have developed through precipitation directly from porewaters with the dissolution of radiolaria and sponge spicules providing a source of biogenic silica. Although common, the zeolites only form a very small component of the sand and do not represent a significant modification to porosity and permeability. A summary composition of the Utsira sand is given in Table 2.

### 2.2.2 Fluids

Three fluids were used in the experiments: $CO_2$, $N_2$ and synthetic Utsira porewater.

$CO_2$

The $CO_2$ used in this study was sourced from high purity (99.99%) liquid $CO_2$ (Air Products, 4.5 Grade). This liquid $CO_2$ was obtained in a cylinder fitted with a dip tube and pressurised with 2000 psi (approximately 14 MPa) of helium. However, the actual experimental pressure was controlled by ISCO syringe pumps, which had their pressure transducers periodically 'zeroed' to minimise drift. As the liquid $CO_2$ was piped to the experiments in the ovens, the increase in temperature would have converted it into a supercritical state.

$N_2$

The $N_2$ used was obtained from BOC Gases and classified as 'oxygen free' (99.998% pure). It was delivered in a cylinder pressurised to 200 bar. A single-stage regulator was used to control the $N_2$ pressure to the required 10 MPa (100 bar) for the 'blank' experiments.

Synthetic Utsira porewater

At the start of the experimental programme it was decided to make up a single, 25 l stock solution of synthetic Utsira porewater (SUP), and that this would be used for all the experiments. The 'recipe' for this is given in Table 3, and was based upon the only analysis of the Utsira porewater available at the start of the study - from the Oseberg field (Gregersen et al., 1998). This synthetic porewater was close to seawater composition and was used in the majority of the experiments. Three analyses of the initial solution were made, and these averaged to give a representative composition (see Appendix I) of the starting fluid for the experiments.

It is noteworthy that the Utsira is a relatively shallow formation. Porewaters within deep aquifers or associated with hydrocarbon fields (Abbotts, 1991) could be significantly more saline that the SUP used in these experiments. The effect of higher salinity would be to lower the concentration of dissolved $CO_2$ in solution and hence possibly reduce the amount of $CO_2$/rock reaction.

Partly as a quality assurance check, it was also decided to periodically analyse the stock solution which was kept in the laboratory. Data for this are given in Appendix I. Most analytes show uniform concentrations over time (within analytical uncertainties). However, bicarbonate concentration does decrease over the 2 years of the experimental programme, possibly as a result of slow conversion to $CO_2$ and loss to the atmosphere. This is not considered an important aspect for the experimental programme as bicarbonate concentrations change radically once 10 MPa of $CO_2$ is applied to the synthetic porewater in the experiments. However, it is noted that slight re-equilibration might occur in the $N_2$ 'blank' experiments.

## 2.3 PREPARATION OF EXPERIMENTAL PRODUCTS

### 2.3.1 Solid products

#### 2.3.1.1 BATCH EXPERIMENTS

Once the pressure vessel was opened, the PTFE liner containing the (usually only slightly damp) sample of reacted Utsira sand was washed 3 times in de-ionised water (3 x 20 ml for the $CO_2$ experiments, and 3 x 12 ml for the N2 experiments). The sample was allowed to settle for 5 minutes between washings. A final wash of acetone (20 ml for the $CO_2$ experiments, and 12 ml for the $N_2$ experiments) was used to remove traces of water, and the sample allowed to dry at 37°C. Once dry, the sample was placed in an airtight container prior to mineralogical analysis.

#### 2.3.1.2 COLUMN EXPERIMENT

On completion of the column experiment, the entire column assembly (4 linked 60 cm columns) was flushed with isopropyl alcohol in order to displace the synthetic Utsira porewater (SUP). This was done to minimise salt formation when the columns were dried and prepared for mineralogical analysis, as this might have obscured observation of subtle mineralogical features. Prior to analysis, each column was sliced up into 2.5 cm long sections, and the reacted sand removed and dried.

### 2.3.2 Fluid samples

For most of the experiments, two types of samples were taken. One involved depressurisation (and hence loss of $CO_2$), but the solution was relatively simple to analyse. The other involved capture of the dissolved $CO_2$ using alkaline solutions, but the resulting mixture made it less easy to analyse.

Depressurisation sample

Each of the reacted fluids was split into several sub-samples. A sub-sample of 1 ml was taken for immediate analysis of pH. Another sub-sample was taken using a polythene syringe and filtered using a 0.2 μm 'Anotop'® syringe filter. 12 ml of this sample was placed into a polystyrene tube and acidified with 0.12 ml of concentrated 'ARISTAR'® nitric acid. This was later analysed for major and trace cations by inductively coupled plasma - optical emission spectroscopy (ICP-OES). A further 4 ml of this filtered sample was taken for analysis of anions by ion chromatography (IC).

Details of elements/species analysed, their detection limits and associated analytical errors are given in Table 4. The errors are based on long-term internal quality control standards. Most analytes were significantly above their detection limits, so the error bars shown on the data plots mentioned in Section 3 represent ± 5% unless otherwise stated.

For a very limited number of samples, a sub-sample was depressurised/degassed into a flask filled with water in order to measure the volume of $CO_2$ released (and hence give an indication of dissolved $CO_2$ content).

Alkali preserved sample

This involved first filling the floating piston sampler (Figure 2) half full of 4M NaOH solution. The alkali conditions would ensure that all dissolved C species (mainly $CO_{2(aq)}$, $H_2CO_3$ and $HCO_3^-$) were converted into $CO_3^{2-}$. After standing for approximately 10 minutes the sample could be depressurised with minimal degassing. This sample was used for determination of total dissolved inorganic carbon, of which approximately 99% is likely to be dissolved $CO_2$ (van Eldik and Palmer, 1982). This was essentially the same procedure as used in the $CO_2$ solubility experiments (Rochelle and Moore, 2002).

Dilution factors between $CO_2$-saturated synthetic porewater and 4M NaOH solution were calculated based on $Cl^-$, the 4M NaOH solution effectively containing none of this element.

## 2.4 ANALYTICAL TECHNIQUES

Standard methods of analysis of solid and liquid samples were employed in this study. In brief, appropriate fluid samples were taken for chemical analysis of major cations using inductively coupled plasma - optical emission spectroscopy (ICP-OES), and for all major anions using ion chromatography (IC). Mineralogical analyses were conducted as detailed in Pearce et al. (1999, 2002).

pH measurements were made on cooled and depressurised samples using an Orion® 900A pH meter calibrated using Whatman® NBS traceable buffers at pH 7, 10 and 13. However, for the longest duration batch experiments (24 months), another (somewhat experimental) technique was also applied. This technique effectively monitors the colour change of an aqueous pH indicator solution (in this case bromophenol blue) using a UV-visible spectrometer. Although this technique is somewhat more complex than conventional methods, it has the advantage that it can be used at elevated temperatures and pressures (i.e. at in-situ conditions) (Toews et al., 1995). Determination of pH is based upon calibration against known citric acid/NaOH pH buffers. Further details of the exact technique used can be found in Faanu (2001).

# 3 Results and discussion

## 3.1 MINERALOGY

### 3.1.1 Batch experiments

A more detailed description of the mineralogical observations of the reacted Utsira sand is given in Pearce et al. (2002) and only a summary is presented here.

All samples studied were fine to medium grained, well-sorted sands, ranging between approximately 100-300 μm in diameter. They are dominated by subangular to very well rounded grains of quartz. The latter grains typically have pitted surfaces, which are equally common in $CO_2$ experiments as the $N_2$ experiments, indicating that they probably represent a primary feature of the sand. Plagioclase and alkali feldspar occur in subordinate amounts (< *c*.15%), and are typically weakly corroded in both sets of experiments. Bioclasts are a minor component (< 1%) and comprise shell and echinoderm spine fragments. They are commonly microporous with etch marks/borings, though there is no systematic difference in the degree of etching between samples from the $CO_2$ and $N_2$ experiments. Indeed it is possible to find both lightly and highly corroded bioclasts within the same sample. Rare mica plates show no evidence for alteration. Disseminated fines occur in all the samples and comprise a mixture of clay, finely crystalline authigenic alkali feldspar, Ca-carbonate and very rare framboidal pyrite. Again, there is no apparent difference in the relative abundances of this material between the $CO_2$ and $N_2$ experiments.

In spite of the observed changes in solution chemistry (see following sections), which suggests mineral dissolution (and in particular a Ca-carbonate phase), SEM analysis provides no evidence that any such reactions occurred. Pitting and corrosion features are observed on all the main detrital components of the sand (quartz, feldspar and Ca-carbonate bioclasts), with apparently equal prominence in both the samples reacted in a $CO_2$-rich environment and those from the blanks. These features are therefore taken to represent primary features of the Utsira Sand. Furthermore, it is possible to find both lightly and highly corroded bioclasts within the same sample from either $CO_2$-reacted experiments or blank experiments. This indicates that changes in fluid chemistry must be attributable to reactions whose extent is lost within the 'noise' of natural mineralogical variation within the sand.

Visual observations during extraction and washing of the reacted solids indicated (very tentatively) that the abundance of larger shell fragments might decrease with increased reaction time. Also, solids from experiments that were of longer duration, or contained $CO_2$, appeared to have more fines associated with them. These observations could indicate dissolution/precipitation reactions, but they might also represent a certain degree of

mechanical abrasion. Stirring was conducted for only 2 minutes every 4 hours in an attempt to reduce damage to the solids, but it is likely that some will have occurred. The very tentative visual observations were not confirmed by the SEM observations above, though these were hampered by natural variability within the sample.

Two precipitate samples were examined. These were formed after the experiments were depressurised, and occurred as small quantities of very thin and delicate crusts that floated on the surface of the solution. The first sample of precipitate was formed 'accidentally', being a product of a failed experiment. However, later experiments had an aliquot of fluid removed, and this was left to stand for a precipitate to form. Precipitation rates were relatively fast, with crusts appearing within 1 day, though they grew in thickness over the following 2-3 days. The crusts studied came from Run 842 ($CO_2$ experiment, 37°C, 10 MPa, 760 days duration, precipitation at 37°C and 0.1 MPa) and Run 997 ($CO_2$ experiment, 37°C, 10 MPa, 7 days duration, precipitation at 37°C and 0.1 MPa). In both instances this material is Ca-carbonate. The upper surfaces of the precipitate were relatively flat, but the morphology of the lower surfaces was quite different (Plates 1 and 2). The precipitate from Run 842 is in the form of blocky rhombs up to 50 μm long, whereas that from Run 997 is in the form of acicular prisms up to 30 μm long. The acicular prism morphology is similar to that of aragonite. However, the small quantities of precipitate preclude more detailed identification.

### 3.1.2 Column experiment

As per the batch experiments above, a more detailed description of the mineralogical observations of the reacted Utsira sand is given in Pearce et al. (2002) and only a summary is presented here.

Several 2.5 cm long samples were taken along the 240 cm length of the column for mineralogical analysis. The reacted solids were very similar to those from the batch experiments described above. Indeed, none of the original phases showed any definite variability in abundance or character along the length of the column. Quartz, feldspar and bioclastic grains all displayed pitting and corrosion features, but these are no more strongly developed than features seen in samples from the batch experiments described above, and are therefore interpreted to represent primary characteristics of the sands. Thus, any reactions which have occurred in response to exposure to $CO_2$ appear to be below the resolution of the SEM technique. However, minor amounts of very small (approximately 10 μm across) halite crystals were observed. These were probably a product of only partial removal of the synthetic Utsira porewater prior to drying.

## 3.2 FLUID CHEMISTRY

Analytical data for all experiments are given in Appendixes I and II. These data are described in the following sections, which are arranged depending on the particular type of experiment involved. Where plots of experimental data are used, the composition of actual Utsira porewaters are also shown. These come from samples at Oseberg (Gregersen et al., 1998) and from analyses of a sample taken from the Brage field (adjacent to Oseberg). Uncertainty bars on the plots represent ±5%, an average uncertainty for the analytes of this study.

Interpretation of the experiments was done by considering data from a group of similar experiments rather than by concentrating on individual experiments. In this way, general patterns could be observed, and undue emphasis would not be placed a single (possibly erroneous) data point. This approach should increase the robustness of the conclusions, and ensure that 'real' changes are being observed, rather than experimental artefacts.

### 3.2.1 'Batch' experiments at 37 ° C

Most experiments conducted within this study were of this type, because the experiments were straightforward and conditions represent those in-situ within the Utsira at Sleipner. Certain of the data show variations over time, and are described in the following paragraphs. Of particular note, are the variations in concentrations of the Group II metals (especially Ca, Sr and Ba).

$Cl^-$

$Cl^-$ is generally considered conservative, and its concentrations (Figure 4) do show a broadly uniform composition over time (approximately 18500 mg $l^{-1}$), with no difference between the $CO_2$ experiments and the $N_2$-pressurised 'blank' experiments. The starting fluid was also very similar to both the Brage and Oseberg compositions. The six longest experiments (all over 400 days duration) possibly show a very slight increase in concentration towards longer timescales, but this is a very tentative observation as the increases fall within the ± 5% uncertainty used.

The $Cl^-$ data show that the presence of $CO_2$ does not appear to alter the behaviour of $Cl^-$ as both $CO_2$ and $N_2$ experiments behave similarly. The data also show that there may possibly be very slight evaporation of some water leading to slightly raised concentrations over longer timescales (a very tentative observation). The $CO_2$ enters the vessel as an anhydrous supercritical phase, and water will dissolve into it. Over time there will inevitably be various slight leakages of $CO_2$ (immediately replaced by the pump controlling $CO_2$ pressure), and this is also likely to take some water out of the vessel. However, if evaporation and leakage is actually occurring it is only very minor.

Na

Na is the next most abundant element in solution after Cl. The starting fluid Na concentration is very similar to both the Brage and Oseberg porewaters (Figure 5). There appears to be no great difference between the $CO_2$ experiments and the $N_2$ experiments, though both appear to have a steady increase in Na over time, from approximately 10300 mg $l^{-1}$ to approximately 11500 mg $l^{-1}$ after 2 years reaction. This degree of increase is not reflected in the $Cl^-$ plots.

The Na data show that the presence of $CO_2$ does not appear to alter the behaviour of Na as both $CO_2$ and $N_2$ experiments behave similarly. The steady increase in Na concentrations appear not be attributed to fluid concentration as a result of evaporation, as this is not reflected in the $Cl^-$ data. It would therefore appear likely that Na is being released from the Utsira sand as a result of fluid-rock reaction (either mineral dissolution or ion exchange). The rate of this release is approximately 50 mg $l^{-1}$ per month for a 10:1 fluid:rock ratio, or approximately 8 x $10^{-12}$ mol $g^{-1}s^{-1}$. What remains unresolved however, is why Na is being released, especially in the $N_2$ experiments. It would be expected that (pre $CO_2$ injection) porewaters at Sleipner were in approximate equilibrium with minerals within the Utsira formation. As such, the $N_2$ experiments might be expected to show no changes in fluid chemistry. Possible reasons for the observed changes in chemistry might include:

- The Oseberg and Brage Na concentrations are not representative of that at Sleipner, and the experiments reflect slow re-equilibration to the higher Sleipner concentrations.
- Extraction and subsequent handling of the sample has in some way slightly altered (increased) the reactivity of the Utsira sand (though this seems unlikely).

K

In broad terms, the $CO_2$ and $N_2$ experiments show similar K data (Figure 6). Data for the 30 and 96 day experiments appear somewhat lower than might be expected compared to the remainder of the experiments, and less emphasis is placed on these data (note later comments regarding unusual $SiO_2$ concentrations for these two samples). The remainder of the data show an initial increase in the first few weeks, followed by a relatively uniform concentration of approximately 275 mg $l^{-1}$. The experimental data lie between the Brage and Oseberg compositions.

The K data show that the presence of $CO_2$ does not appear to alter the behaviour of K as both $CO_2$ and $N_2$ experiments appear very similar. The initial increase in K seen in the majority of the experiments may represent ion exchange reactions. The original Utsira sand sample was heavily contaminated with drilling fluid, which was particularly rich in K. Although care was taken during starting material preparation to remove as much of the drilling fluid as possible (see Section 2.2.1), it was less easy to 'undo' all ion-exchange reactions initiated by the drilling fluid. Re-equilibration of the K ion-exchange reactions appears to have taken up to 2 months at 37°C.

Ca

Of all the analytes monitored during the study, Ca shows the largest variation (Figure 7), with the $CO_2$ and $N_2$ experiments showing very different profiles. The concentration of dissolved Ca rose very rapidly in the $CO_2$ experiments from approximately 430 mg $l^{-1}$ to approximately 1650 mg $l^{-1}$ within just 8 days, with a slower increase to approximately 1840 mg $l^{-1}$ after 96 days. This was followed by an apparent decrease in concentration to a steady-state value of approximately 1700 mg $l^{-1}$. The $N_2$ experiments show a very different profile, with Ca concentrations only slightly changed (relatively) from the starting fluid. The steady-state concentration is approximately 300 mg $l^{-1}$, some 130 mg $l^{-1}$ less than the starting fluid.

The Ca data show relatively fast equilibration between the SUP and the Utsira sand for both experiment types. It is most likely that this is a result of reaction of carbonate shell fragments, carbonate minerals having much faster reaction rates than silicate minerals (e.g. Chou et al., 1989; Knauss and Wolery 1986, 1988). The $CO_2$ and $N_2$ experiments show very different behaviour, graphically illustrating the linkage between $CO_2$ and Ca activity through carbonate equilibrium. Although on the scale used in Figure 7 Ca concentrations in the $N_2$ experiments appear only slightly changed, they actually fell by approximately 30%. The reason why this steady-state concentration was achieved rather than staying at the starting value, might relate to dissolved gas concentrations in the Utsira. The analysis of the Utsira porewater from the Oseberg field (Gregersen et al., 1998) does indicate that some dissolved $CO_2$ is present (approximately 1.9 x $10^{-4}$ mole $l^{-1}$). The $N_2$ experiments did not have any extra $CO_2$ added, and so there was probably a slight shift in equilibrium between the in-situ Utsira porewater and the $N_2$ experiments through:

$$CaCO_3 + CO_2 + H_2O = Ca^{2+} + 2\,HCO_3^- \qquad [1]$$

Thus there would appear to have been potential for limited some carbonate mineral precipitation/overgrowths within the $N_2$ experiments.

Through equation [1] it is possible to make a broad assessment of how much carbonate mineral (probably shell fragments) has dissolved in the $CO_2$ experiments. In the following calculations all the carbonate is assumed to be calcite. The maximum amount of Ca dissolved was equivalent to approximately 1400 mg $l^{-1}$ after 96 days reaction, though this decreased to approximately 1270 mg $l^{-1}$ after 760 days. This later figure is equivalent to 0.32 g of calcite per $CO_2$ 'batch' experiment. Point counting data (Pearce et al., 1999, 2002) show that

approximately 6.7% of the solid material within the Utsira sand is calcite. Assuming (for simplicity) that all the minerals in the Utsira sand are roughly the same density, then the 10 g sample of Utsira sand in each experiment would contain approximately 0.67 g of calcite. Consequently, approximately half of the carbonate material in the Utsira sand sample dissolved in the $CO_2$ experiments.

The rate of carbonate mineral dissolution was initially relatively rapid, with some 1220 mg $l^{-1}$ of Ca released in just 8 days. However, it is likely that by day 8 the rate of release was already decreasing. Unfortunately data are not available for timescales of less than 8 days. Therefore a rate will be calculated based upon 1220 mg $l^{-1}$ in 8 days, but this is likely to be an underestimate. As such, the result will be a minimum rate of initial reaction, and will provide a limiting value. This rate of release of Ca is equivalent to 4.4 x $10^{-10}$ mol $g^{-1}s^{-1}$, for the 10 g of Utsira sand reacting with 100 ml of $CO_2$-saturated synthetic Utsira porewater. The surface area of the Utsira sand sample used was 0.9 $m^2g^{-1}$, which gives and overall Ca release rate equivalent to 4.0 x $10^{-14}$ mol $cm^{-2}s^{-1}$.

It is interesting to compare the above release rate information from previous studies, though some rather large assumptions have to be used. Let us assume that the total surface area is equally distributed between all mineral phases within the Utsira sand (a rather large assumption), that all the carbonate phase is calcite, and that all Ca released into solution comes from calcite. Given that 6.7% of the sand sample is calcite, this would equate to a calcite dissolution rate of approximately 3 x $10^{-15}$ mol $cm^{-2}s^{-1}$. At 25°C and atmospheric pressure, Chou et al. (1989) and Busenberg and Plummer (1986) give calcite and aragonite dissolution rates in the pH 3-5 region of approximately 1 x $10^{-9}$ mol $cm^{-2}s^{-1}$. Using an activation energy of 46 kJ $mol^{-1}$ (Sjoberg and Rickard, 1984), this would equate to a dissolution rate of approximately 2 x $10^{-9}$ mol $cm^{-2}s^{-1}$ at 37°C. It would appear therefore, that the rate of dissolution of the carbonate phase within the batch experiments is significantly slower than in more idealised systems. This difference may in part be due to some of the rather large simplifications and assumptions used in the calculations. However, it may also reflect the difference in results between very simple idealised experiments, and more complex 'dirty' experiments. It is possible that the lower stirring rate used in this study has led to an increased impact of 'transport control' over 'surface reaction control', and a consequent decrease in the observed release rate of Ca. It is noted that a similar process has been identified in silicate mineral dissolution, where dissolution rates measured in (poorly mixed) natural systems are commonly several orders of magnitude slower than in 'idealised' laboratory systems (e.g. Velbel, 1993).

Sr

In general, the Sr profiles have many similarities with the Ca profiles. Both $CO_2$ and $N_2$ experiments show an initial fast increase to maximum concentrations within the first 60-100 days, followed by a subsequent decrease to lower steady-state concentrations (Figure 8). However, there is possible evidence that might suggest slow increase in Sr concentration over longer timescales. The $CO_2$ experiments have higher steady-state Sr concentrations (approximately 16 mg $l^{-1}$) compared to the $N_2$ experiments (approximately 7 mg $l^{-1}$). Finally, the $CO_2$ experiments have steady-state concentrations above the starting fluid (10 mg $l^{-1}$), whereas the $N_2$ experiments fall below this.

The similarity between the profiles of Sr and Ca suggests that both elements are being controlled by a similar process - namely carbonate phase dissolution/precipitation. Sr is a common trace constituent within both shell fragments and inorganic calcite and so it would be expected to be released in a similar way to Ca. In the $CO_2$ experiments approximately 1270 mg $l^{-1}$ of Ca was released compared to some 6 mg $l^{-1}$ of Sr. This would equate to a molar ratio

within the solid phase of approximately 460:1, assuming both elements were sourced from the same phase and were released in stoichiometric proportions.

Fe

The Fe profiles have many similarities with both the Ca and Sr profiles. Both $CO_2$ and $N_2$ experiments show an initial fast increase to maximum concentrations within the first 60-100 days, followed by a subsequent slow decrease (Figure 9). Steady-state conditions would appear to have not been attained, though Fe concentrations in the longer-term experiments are broadly comparable with porewaters from Brage and Oseberg.

The similarity between the Fe, Sr and Ca data suggests that all elements are being controlled by a similar process - namely carbonate phase dissolution/precipitation. Fe is also a common trace constituent within both shell fragments and inorganic calcite and so it would be expected to be released in a similar way to Ca. However, unlike Ca and Sr, Fe is redox sensitive. Release of $Fe^{2+}$ from $FeCO_3$ within the carbonate solid would have initiated redox reactions and oxidation to $Fe^{3+}$. This is much less soluble than $Fe^{2+}$ and probably precipitated out within the experiments as an oxyhydroxide phase such as goethite (FeOOH).

Ba

The Ba profiles are somewhat different to that of Ca, Sr or Fe. In general, there is an initial increase in concentration within the first 60 days, followed by a subsequent decrease to lower steady-state concentrations (Figure 10). Steady-state concentrations lie above the starting concentrations. However, what is different to Ca, Sr and Fe is that the longer-term steady-state concentration for the $N_2$ experiments (approximately 2.5 mg $l^{-1}$) is greater than that for the $CO_2$ experiments (approximately 1 mg $l^{-1}$).

The initial rapid release of Ba into solution is very similar to that of Ca, Sr and Fe, and again suggests control by carbonate phase dissolution. However, $BaSO_4$ is a common additive to drilling mud, so there is at least the potential for some to have been sourced from this. The lower Ba solubility in the $CO_2$ experiments indicates some $CO_2$-mediated process. It is tentatively suggested that although the high $CO_2$ activity might have caused approximately half of the calcite in the Utsira sand sample to dissolve, it might also have initiated $BaCO_3$ precipitation (or at least a very Br-rich carbonate phase). This subsequent precipitation would have resulted in the lower Ba concentrations in solution.

Steady-state Ba concentration for both the $CO_2$ and $N_2$ experiments lie between the Brage and Oseberg porewater compositions. However, with so little information about the Brage sample, it is hard to know if its relatively high concentration (approximately 6 mg $l^{-1}$) is 'real', or if it reflects Ba input from other sources such as drilling fluids.

Mg

The Mg profiles are somewhat different to the other Group II metals considered so far. There is no initial increase in concentration. Indeed, the opposite would appear to happen, and there is a slight decrease in concentration over the first 120 days for both $CO_2$ and $N_2$ experiments (Figure 11). Over longer timescales however, concentrations appear to increase, and after 760 days of reaction they are approximately back to the starting fluid concentration (approximately 630 mg $l^{-1}$). There is no evidence for steady-state conditions having been reached after 760 days.

The behaviour of Mg is notable in that it does not appear to be controlled by a carbonate phase (unlike the other Group II metals). The $CO_2$ and $N_2$ experiments behave very similarly (within the 5% limits chosen), so the processes controlling Mg availability do not appear to be

highly sensitive to the presence of $CO_2$. It is tentatively suggested that Mg might be controlled by ion-exchange reactions on clays.

$SiO_2$

No information was available on the concentration of dissolved $SiO_2$ in the Oseberg porewater (Gregersen et al., 1998), and as a consequence, the synthetic Utsira porewater used as the starting fluid in the experiments was $SiO_2$-free. For both the $CO_2$ and $N_2$ experiments, $SiO_2$ concentrations increased throughout the two years of the experimental programme (Figure 12). $SiO_2$ concentrations within the $CO_2$ experiments were approximately double those within the $N_2$ experiments. However, all experimental $SiO_2$ concentration data are far lower than the measured Brage porewater datum (approximately 50 mg $l^{-1}$).

The majority of the $SiO_2$ data follow a general trend of a fast initial increase, later slowing towards a steady-state value. Some data are exceptions to this however. Data at 30 and 96 days appear unusually low (by about 50%) for both the $CO_2$ and $N_2$ experiments. The samples were re-analysed several times and the same results obtained, which tends to rule out a Si versus $SiO_2$ atomic/molecular weight conversion error (factor of about 2). A dilution error is ruled out as other analytes should show a similar problem - they do not (though K data for these 2 samples are a little depressed). It was not possible to resolve this apparent problem, and less emphasis was placed on these two data points.

The $SiO_2$ data points after 600 hours of reaction present a little uncertainty. It is not clear if:

- The 654 day data are slightly lower than extrapolations through the rest of the data

or

- The 760 day data are slightly higher than extrapolations through the rest of the data

What is apparent however, is that $SiO_2$ solubility is lower in the $N_2$ experiments (steady-state concentration in the order of 10 mg $l^{-1}$) and higher in the $CO_2$ experiments (steady-state concentration in the order of at least 25-30 mg $l^{-1}$).

$SiO_2$ solubility in the Brage porewater is far higher than in the $N_2$ experiments. The reasons for this are unclear. Although it is possible that 2 years of reaction time has not been sufficient for full equilibration in the experiments, it is also possible that the controls on $SiO_2$ are different at Brage and Sleipner. For example, there may be larger quantities of biogenic $SiO_2$ at Brage, and this poorly crystalline material leads to locally higher $SiO_2$ solubilities.

The rate of $SiO_2$ release can be calculated for the $CO_2$ experiments over the time period of 1 week to 4 months. This amounted to 6.1 mg $l^{-1}$ over 110 days for 10 g of Utsira sand and 100 ml of porewater. For a surface area of 0.9 $m^2g^{-1}$, this is equivalent to approximately 1 x $10^{-13}$ mol $g^{-1}s^{-1}$. It is interesting to compare the above release rate information from previous studies, though some rather large assumptions have to be used. Let us assume that the total surface area is equally distributed between all mineral phases within the Utsira sand (a rather large assumption), and that all $SiO_2$ released into solution comes from quartz. Given that approximately 76.4% of the sand sample is quartz, this would equate to a quartz dissolution rate of approximately 8 x $10^{-14}$ mol $cm^{-2}s^{-1}$. This compares to a more idealised quartz dissolution rate of approximately 1 x $10^{-16}$ mol $cm^{-2}s^{-1}$ between pH 3-7 (Brady and Walther, 1990). It would appear that $SiO_2$ was being released into solution faster than what might have been expected. This suggests that another (more minor) Si-rich phase is undergoing dissolution and a faster rate than quartz. This phase could be K-feldspar or mica, both of which have been identified in the Utsira sand (Pearce et al, 1999, 2002). However, biogenic silica could also be a possible source. This is likely to be amorphous, and hence have a dissolution rate much faster than quartz.

Al

Most Al concentrations are in the order of 0.5 mg $l^{-1}$ (Figure 13). There are however, 2 data points at 96 and 118 days where concentrations are approximately 2 mg $l^{-1}$ ($N_2$ experiment) and 1.5 mg $l^{-1}$ ($CO_2$ experiment) respectively. The two longest duration experiments have Al concentrations of 0.1 mg $l^{-1}$ or lower.

The $CO_2$ and $N_2$ experiments appear to behave similarly, so the processes controlling Al availability does not appear to be highly sensitive to the presence of $CO_2$. It is unclear why the two data points at 96 and 118 days should give such elevated concentrations, though comparison with the other data points suggests that these values are probably unduly high. It is possible that rupture of the filter membrane during sampling could have allowed very small-scale (possibly colloidal) Al-rich particulates into the fluid sample, and less emphasis is therefore placed on these two data points. Unfortunately, mineralogical observations are unable to identify which phases are undergoing dissolution/precipitation. However, it is noted that kaolinite has been identified previously as a reaction product of feldspar-$CO_2$ interaction within experimental (Czernichowski-Lauriol et al., 1996) and natural analogue systems (Pearce et al., 1996).

It is worth noting that sampling for, and analysis of, low concentrations of Al can be problematic. At very low concentrations, sample contamination cannot always be avoided. This could come from the equipment used, or even from colloidal material that manages to pass through the fine filters used. Within this study we attempted to minimise such problems, but it is acknowledged that the Al data should be treated with a little caution.

S

The release of S to solution differs between the $CO_2$ and $N_2$ experiments, with the $CO_2$ experiments having approximately twice the S concentrations of the $N_2$ experiments (Figure 14). Their profiles however are similar in shape, with an initial relatively fast increase in the first 120 days, followed by a slower increase after that. In the $CO_2$ experiments, concentrations are approximately 40 mg $l^{-1}$ after 120 days, with a slower (if somewhat more complex) increase to 60 mg $l^{-1}$ after 760 days. In the $N_2$ experiments concentrations rise to approximately 17 mg $l^{-1}$ after 120 days, with a slower increase to 24 mg $l^{-1}$ after 760 days.

The experimental data show that $CO_2$ does have a large impact on increasing S in solution, though the exact mechanism by which it does this is not clear. The only S-rich phase identified in the Utsira sand by Pearce et al. (1999) is pyrite, but this is only a trace component (0.05%). Oxidation of this material would result in increases in aqueous S (probably as $SO_4^{2-}$). However, for the $CO_2$ experiments to have liberated approximately twice as much S compared to the $N_2$ experiments would require a pyrite dissolution mechanism aided by $CO_2$ in some way. It is possible that this could have been by stabilising Fe carbonate species in solution, or by the slightly more acidic conditions aiding the sulphide oxidation reaction.

There is however, a problem with the pyrite oxidation hypothesis. In the $CO_2$ experiments, 0.05% pyrite would equate to 0.005 g, or $4.2 \times 10^{-5}$ moles of pyrite, or $8.3 \times 10^{-5}$ moles of S in the solid phase. This quantity of S would give a maximum possible amount available to go into solution of only 27 mg $l^{-1}$. Clearly there has to be another source of S in the Utsira sand. The analysis undertaken by Pearce el al. (1999) examined some 1300 grains, and it is unlikely that some relatively abundant S-rich phase has not been accounted for (such as anhydrite for example). However, S might exist as a trace component within another phase. The profiles of S, with a relatively rapid release within the first 120 days, mirrors the behaviour of Ca and Sr. It is therefore likely that significant S is associated with the carbonate phase, possibly locked

up within shell fragments. The presence of $CO_2$ appears to have initiated significant dissolution of carbonate, which could explain why more S is liberated in the $CO_2$ experiments.

For the $CO_2$ experiments, initial total dissolved S increased from 17.8 to 38.5 mg $l^{-1}$ from day 8 to day 118. This equates to a linear rate of release of 6.8 x $10^{-13}$ mol $g^{-1}s^{-1}$. For a surface area of 0.9 $m^2g^{-1}$, this is equivalent to approximately 6.1 x $10^{-13}$ mol $g^{-1}s^{-1}$. After 118 days the pattern of S release is somewhat more complex, as it appears relatively unchanged up to 430 days reaction, but then starts to increase again. It is unclear if this is a 'real' observation, or an artefact of the experiments. However, assuming a linear increase from 38.5 to 64.2 mg $l^{-1}$ between 120 and 760 days, gives release rate of 1.4 x $10^{-13}$ mol $g^{-1}s^{-1}$. For a surface area of 0.9 $m^2g^{-1}$, this is equivalent to approximately 1.3 x $10^{-13}$ mol $g^{-1}s^{-1}$.

For the $N_2$ experiments, initial total dissolved S increased from 10.8 to 16.0 mg $l^{-1}$ from day 8 to day 118. This equates to a linear rate of release of 1.7 x $10^{-13}$ mol $g^{-1}s^{-1}$. For a surface area of 0.9 $m^2g^{-1}$, this is equivalent to approximately 1.5 x $10^{-13}$ mol $g^{-1}s^{-1}$. After 118 days the release rate of S was much slower. It increased from 16.0 to 24.1 mg $l^{-1}$ between 120 and 760 days months, giving a release rate of 4.6 x $10^{-14}$ mol $g^{-1}s^{-1}$. For a surface area of 0.9 $m^2g^{-1}$, this is equivalent to approximately 4.1 x $10^{-14}$ mol $g^{-1}s^{-1}$.

Total inorganic carbon

Total inorganic carbon measurements were obtained by alkali preservation of the fluid sample. This method of sampling preserved all dissolved carbon species as carbonate, be they $HCO_3^-$, true carbonic acid, or dissolved $CO_2$. The results are fairly uniform over time (Figure 15), with the $CO_2$ experiments containing appreciably more carbon compared to the $N_2$ experiments.

The relative uniformity of the results is expected, as $CO_2$ solubility and equilibrium are achieved relatively rapidly, probably in just a few hours (Czernichowski-Lauriol et al., 1996; Ellis and Golding, 1963; Stuart and Munjal, 1970). The average solubility of $CO_2$ in the synthetic Utsira porewater is in the order of 1.1 mol $l^{-1}$ which is very close to the value obtained from $CO_2$ solubility experiments (Rochelle and Moore, 2002). This is not altogether unexpected because the two sets of experiments used the same synthetic saline porewater, whose overall salinity did not change appreciably even after reaction with the Utsira sand.

$HCO_3^-$

Bicarbonate concentrations are highly variable for the $CO_2$ experiments, which is to be expected as they will tend to reflect different degrees of degassing between sampling and analysis (Figure 16). Due to the large amount of degassing and subsequent partial re-equilibration, the measured concentrations will not reflect in-situ concentrations. As such, the results from the $CO_2$ experiments will not be utilised further, other than to say that they are generally higher than the $N_2$ experiments. The $N_2$ experiments however, are less prone to such variations because a high $CO_2$ pressure is not being used. $HCO_3^-$ concentrations in these experiments show an initial decrease, followed by a slight peak to approximately 360 mg $l^{-1}$ after 59 days, and lastly a decrease to 90 mg $l^{-1}$ after 760 days.

The profile of $HCO_3^-$ concentrations appears to tie in with Ca, and it is assumed that they are both linked via the carbonate equilibrium in equation [1]. It is interesting to note that the final $HCO_3^-$ concentrations in the $N_2$ experiments (90 mg $l^{-1}$) are very much lower than in the Brage or Oseberg porewaters (700-840 mg $l^{-1}$). This might be explained by the in-situ Utsira porewaters containing a small amount of dissolved $CO_2$. The presence of a small amount of dissolved $CO_2$ would be to shift the position of equation [2] in favour of more $HCO_3^-$. This would also fit in with the observations for Ca (see earlier section).

pH

Most pH measurement was taken in the lab at approximately 20°C and 0.1 MPa pressure. These conditions are quite different from those within the experiments, and some deviation from in-situ values is to be expected. Measured pH values are approximately 6.6 for the $CO_2$ experiments and approximately 7.8 for the $N_2$ experiments (Figure 17). The Oseberg and Brage porewater pH values lie within this range.

These measured pH values are of limited use until they have been re-calculated to in-situ conditions using computer models. However, they do demonstrate the impact of dissolved $CO_2$ in lowering pH via:

$$CO_2 + H_2O = HCO_3^- + H^+ \quad [2]$$

That the Oseberg and Brage porewaters have a lower pH than the $N_2$ experiments tends to confirm information from the Ca and $HCO_3^-$ data that the in-situ Utsira porewaters do have a certain quantity of dissolved $CO_2$ within them.

Data for the two 24 month batch experiments in Appendix I also include measurements of in-situ pH using an experimental technique. Although the technique appeared to work well on test solutions, there was relatively little real sample to analyse. This, coupled with problems of maintaining constant temperature and pressure, means that these data should be treated with caution. Any slight depressurisation (especially in the $CO_2$ experiment sample) would have resulted in a pH value that was too high. However, the technique shows great promise, and could be developed into a practicable 'day-to-day' standard analytical method.

### 3.2.2 'Batch' experiments at 70°C

These experiments were conducted at approximately twice the actual in-situ temperature. Although not exactly representative of conditions at Sleipner, the elevated temperature would tend to make the rates of reaction approximately an order of magnitude faster. This would aid observations of mineral dissolution/precipitation reactions. They would also serve as a useful 'halfway house' between the 37°C batch experiments and the 70 °C column experiment, and would help in the interpretation of the latter. However, as they are not representative of in-situ conditions, only the more important points are brought out in the following sections. Analytical data for these experiments are given in Appendix I.

Several analytes have unusually high concentrations in the experiments of 14 days duration. The effect is most noticeable for the $N_2$ experiment, but the $CO_2$ experiment is also affected. This appears to be an artefact of the experiments and is probably caused by evaporative loss of water into the $N_2$ or $CO_2$ phase. If the experiments were to leak appreciable $N_2$ or $CO_2$, then water would also be lost. This process appears to have continued throughout the experiments, with the pump and gas cylinder continually supplying dry gas to the experiments to maintain pressure. Significant water loss on this scale has caused concentrations of elements dissolved in the aqueous phase to increase markedly. For this reason, only limited emphasis is placed on data from these experiments. However, the experiments are useful in that they clearly show that it is possible to identify experiments showing unrepresentative results.

$Cl^-$

$Cl^-$ concentrations (Figure 18) show an overall steady increase over time from approximately 18660 mg $l^{-1}$ to approximately 20230 mg $l^{-1}$ over 9 months, and are similar fro both $CO_2$ and $N_2$ experiments. This 8% increase is probably associated with a very slow and steady loss of water (as opposed to the relatively large amount of fast evaporation mentioned above). The

effect of this was not really noticeable at 37°C, even though the experiments were of longer duration. Two factors might influence this:

- Higher temperatures are associated with greater movement (energy) of gas molecules, and so the rate of escape might be expected to increase at higher temperatures.
- Higher temperatures could have led to a softening of the Viton® seals. Although they continued to contain the 10 MPa pressure, they might have been more susceptible to partial extrusion and a reduction is sealing efficiency.

Na

Na concentrations (Figure 19) also show a steady increase over time, from approximately 10310 mg $l^{-1}$ to approximately 12550 mg $l^{-1}$ over 266 days, and are similar for both $CO_2$ and $N_2$ experiments. The increase this time is in the order of 22%. However, unlike $Cl^-$ above, the rate of increase does not appear to be linear, with the two data points at 266 days appearing to have slightly higher concentrations than might otherwise be expected from the rest of the data. It would appear therefore, that increases in Na concentrations are a joint function of evaporative water loss (as per $Cl^-$) and release from the Utsira sand (as per the 37°C experiments).

K

K concentrations (Figure 20) show steady increases over time, from approximately 225 mg $l^{-1}$ to approximately 320 mg $l^{-1}$ over 266 days, and are similar for both $CO_2$ and $N_2$ experiments. The rate of increase appears linear and is in the order of 42%. This is a large increase even accounting for evaporative water loss. The 37°C experiments showed some evidence for ion-exchange reactions and release of K, though this process appears to have been complete after approximately 60 days of reaction. The steady increase in K therefore, might represent dissolution of part of the Utsira sand. Subtraction of the effects of evaporative water loss, would give an increase in K of approximately 34% over 266 days due to fluid-rock reaction. This would equate to a rate of release of approximately 9.6 x $10^{-13}$ mol $g^{-1}s^{-1}$. For a surface area of 0.9 $m^2g^{-1}$, this is equivalent to approximately 8.6 x $10^{-13}$ mol $g^{-1}s^{-1}$.

Ca

Ca concentrations (Figure 21) show an unusual profile for both the $CO_2$ and $N_2$ experiments. For the $CO_2$ experiments there is an initial rapid increase in concentration, followed by an equally rapid fall. This is thought to represent initial dissolution of shell fragments followed by attainment of steady-state conditions. The $N_2$ experiments appear to reach a steady-state value relatively quickly, at about half the concentration of the $CO_2$ experiments. However, after 266 days of reaction, Ca concentrations for both the $CO_2$ and $N_2$ experiments are significantly greater than after 109 days reaction. The reasons for this are not clear, and interpretation of the data is made difficult by the relatively few number of analyses at these longer timescales.

There are similarities between the Ca data and the concentration profiles of Sr (Figure 22), Fe (Figure 23) and Mn (Figure 24). Unfortunately, the resolution of the data does not fully allow for interpretation of what is happening within the first 50 days of the experiments. However, two observations can be made:

- Concentrations in the $CO_2$ experiments are higher than in the $N_2$ experiments.
- Concentrations are generally lower at the start of the experiments (though there is some variability) and move towards higher concentrations after several months of reaction.

The similarities between the Sr, Fe, Mn and Ca data suggest that a similar mechanism is involved in their release, namely dissolution of carbonate minerals - probably shell fragments. This process is enhanced by the presence of $CO_2$, and is the same conclusion as for the 37°C experiments. However, longer-term control of Sr, Fe and Mn concentrations, could be by other phases (e.g. oxyhydroxides in the case of Fe and Mn).

Ba

Ba concentration profiles are different to Ca, Sr, Fe and Mn. In general there is an initial increase over the first 109 days, followed by a decrease thereafter (Figure 25). The difference in behaviour of Ba compared to Ca, Sr and Fe (± Mn) is a similar observation to the 37°C experiments. However, unlike the 37 °C experiments (which showed increased Ba solubility in the $N_2$ experiments compared to the $CO_2$ experiments) at 70°C Ba solubility appears to be broadly similar for both $CO_2$ and $N_2$ experiments. The Ba profiles suggest dissolution of a phase containing Ba (possibly carbonate) with subsequent re-precipitation.

Mg

Mg concentration profiles are again different to the rest of the Group II metals (as per the 37°C experiments. Most of the data (neglecting the $CO_2$ experiment at 109 days which appears to be anomalous) show generally similar behaviour between the $CO_2$ and $N_2$ experiments. Mg concentrations are approximately unchanged throughout the experimental programme (Figure 26).

$SiO_2$

$SiO_2$ concentration profiles show increases over time (Figure 27) for both $CO_2$ and $N_2$ experiments. However, the rate of increase in the $CO_2$ experiments may be falling after 266 days reaction. For the $N_2$ experiments, the single data point at 266 days suggests a falling $SiO_2$ concentration and hence possible precipitation of a Si-rich phase. However, this is only a single data point, and care should be taken not to read too much into it without other data to confirm such a decrease.

$SiO_2$ concentration profiles over the first 109 days show that the $CO_2$ experiments have slightly higher concentrations compared to the $N_2$ experiments, however the rate of increase is similar in both cases. The increase is in the order of 24 mg $l^{-1}$ over a 100 day period. This equates to approximately 4.5 x $10^{-13}$ mol $g^{-1}s^{-1}$, which is about twice the observed release rate at 37°C. For a surface area of 0.9 $m^2g^{-1}$, this is equivalent to a release rate of approximately 4.1 x $10^{-13}$ mol $cm^{-2}s^{-1}$.

If it is assumed that the total surface area is equally distributed between all mineral phases within the Utsira sand (a rather large assumption), and that all $SiO_2$ released into solution comes from quartz. Given that approximately 76.4% of the sand sample is quartz, this would equate to a quartz dissolution rate of approximately 3 x $10^{-13}$ mol $cm^{-2}s^{-1}$. This compares to a measured quartz dissolution rate at 70°C of approximately 1 x $10^{-15}$ mol $cm^{-2}s^{-1}$ between pH 4-6 (Knauss and Wolery, 1988). It would again appear that $SiO_2$ was being released into solution faster than what might be expected. This suggests that another (more minor) Si-rich phase is undergoing dissolution and a faster rate than quartz. This phase could be K-feldspar or mica, both of which have been identified in the Utsira sand (Pearce et al, 1999, 2002). However, biogenic silica could also be a possible source. This is likely to be amorphous, and hence have a dissolution rate much faster than quartz.

The observed doubling of release rate on going from 37°C to 70°C is smaller than the order of magnitude increase predicted from previous kinetics studies on common silicate minerals (Knauss and Wolery, 1986, 1988). However, the experimental methods used in this study

were not the same as the somewhat more 'ideal system' kinetics experiments. It is entirely possible that the lower stirring rate used in this study has led to an increased impact of 'transport control' over 'surface reaction control', and a consequent decrease in the observed release rate of $SiO_2$. The impact of this would have been greater for the 70 °C experiments compared to the 37°C experiments as the release rate is higher at more elevated temperatures.

Al

Al concentration profiles are similar for both $CO_2$ and $N_2$ experiments (Figure 28) showing that the reaction mechanism is insensitive to the presence of $CO_2$. This is similar to the 37°C experiments. Concentration profiles show an initial increase for the first 14 days of reaction, followed by a decrease towards 0.06 mg $l^{-1}$ after 266 days. These concentration profiles suggest dissolution of some Al-rich phase, followed by precipitation of a secondary phase which controls Al solubility. Unfortunately, mineralogical observations are unable to identify which phases are undergoing dissolution/precipitation.

S

The profiles for S concentration are not as clear as for the 37°C experiments (Figure 29). Unlike the 37°C experiments where S release was enhanced by the presence of $CO_2$, for the 70°C experiments there is no great difference between the $CO_2$ and $N_2$ experiments. There appears to be a fast initial increase in S concentrations over the first 14 days of reaction, followed by a slower decrease. However, data from the 266 days experiments suggest a later increase in S concentrations. Interpretation of such a profile is not straightforward, and suggests that more than one reaction (dissolution/precipitation) mechanism is active in the experiments. It is possible that there may be initial release of S from a relatively reactive phase, and that this dominates the early part of the reaction. However, there might also be slower release from another phase, which dominates over longer timescales. Such a two-step mechanism is consistent with observations from the 37°C experiments, where both carbonate (containing S as a trace component) and pyrite dissolution were implicated.

Total inorganic carbon

Total inorganic carbon measurements were obtained by alkali preservation of the fluid sample as per the 37°C experiments. Unfortunately, sample availability meant that this was not possible for all experiments at 70°C and only a limited set of data were obtained (Figure 30). Although the $CO_2$ experiment data point at 14 days appears unduly high, the two remaining data points suggest concentrations in the order of 0.8 mol $l^{-1}$. This is equivalent to approximately 3.5 g of $CO_2$ per 100 g of $H_2O$, and is close to that obtained for $CO_2$ solubility studies (Rochelle and Moore, 2002).

$HCO_3^-$

Bicarbonate concentrations are highly variable for the $CO_2$ experiments, which is to be expected, as they will tend to reflect variable amounts of degassing between sampling and analysis. This is apparent in the two groups of data points, one set with concentrations of approximately 1800 mg $l^{-1}$ (analysed soon after sampling) and another set with concentrations of approximately 400 mg $l^{-1}$ (analysed after standing for some time) (Figure 31). However, the $N_2$ experiments contain relatively little bicarbonate and $CO_2$ degassing is not a problem. $HCO_3^-$ concentrations are therefore much more uniform for the $N_2$ experiments, and mostly below 100 mg $l^{-1}$.

pH

As for the 37 °C experiments, the measured pH values (Figure 32) are of limited use until they have been re-calculated to in-situ conditions using computer codes. However, they do

demonstrate the impact of dissolved $CO_2$ in lowering pH via equation [3]. Even though much degassing will have occurred, it is apparent that the lower pH values are associated with the higher $HCO_3^-$ measurements, i.e. the $CO_2$ experiments.

### 3.2.3 'Column' experiment at 70 °C

This experiment (like the batch experiments at 70 °C) was conducted at approximately twice the actual in-situ temperature. Although not exactly representative of conditions at Sleipner, the elevated temperature will tend to make the rates of reaction approximately an order of magnitude faster. This will aid the determination of mineral dissolution/precipitation reactions. During the 10 month duration of the experiment, a total of 33 individual fluid samples were collected. Analytical data for these samples are given in Appendix II.

The fluid pressure was monitored at the inlet and outlet of the column (Figure 33). This was done to investigate whether any pressure gradient existed across the column whilst the $CO_2$-rich porewater flowed through it. If there was a pressure gradient, any changes in it during the experiment might be due to mineral dissolution/precipitation that altered permeability. However, for most of the time during the experiment the pressure differential across the column was less than 0.1MPa (1 bar). This suggests that there has been little reaction resulting in loss of permeability of the column.

$Cl^-$

$Cl^-$ concentrations (Figure 34) show that there is little or no difference between the starting SUP fluid and the reacted fluid (within errors). The $Cl^-$ concentrations are comparable with those observed in the batch experiments.

Na

Na concentrations (Figure 34) could be described as approximately unchanged, as a single concentration value can be fitted within virtually all of the error bars. However, if the actual errors were less than those indicated, then the trends in the data show a rapid initial increase (from approximately 4.8-5.2 x $10^{-2}$ mol $l^{-1}$ (11000-12000 mg $l^{-1}$) - as per the batch experiments). Thereafter, there appears to be a slight, but general decrease throughout the remainder of the experiment. By the end of the experiment, Na concentrations are close to that of the starting $CO_2$-equilibrated SUP fluid.

If this tentative identification of Na release from the Utsira sand is indeed, the process appears to have been completed within the 10 month duration of the experiment. The relatively short timescale of this process (months rather than years), might suggest either sluggish ion-exchange reactions or relatively rapid dissolution of some minor phase within the Utsira sand.

K

K concentrations (Figure 35) show an initial rapid increase (first 20 days) before decreasing back to value close to that of the $CO_2$-equilibrated SUP fluid. This initial increase may represent ion-exchange reactions. The original Utsira sand sample was heavily contaminated with K-rich drilling fluid. Although this was carefully washed with SUP several times, complete re-equilibration does not appear to have been achieved, and a small amount of 'excess' K appears to have remained on the sand.

Ca

Ca concentrations (Figure 36) show one of the more interesting trends in this study. Initially there was a rapid increase in concentration from approximately 7.5 x $10^{-3}$ to 3.7 x $10^{-2}$ mol $l^{-1}$ (300 to 1500 mg $l^{-1}$) (first 10 days). This was followed by a slow decrease in concentration throughout the rest of the experiment.

The Ca data suggests that there is relatively fast release of Ca to solution, probably through dissolution of carbonate shell fragments present in the Utsira sand. Over the 10 months of the experiment the rate of Ca release decreased, possibly due to the consumption of a significant proportion of the shell fragments and/or a reduction of their reactive surface area.

The rate of release of Ca as a result of carbonate mineral dissolution from the Utsira sand was initially relatively rapid, peaking at about 3 x $10^{-2}$ mol $l^{-1}$. Given a flow rate of 0.5 ml $h^{-1}$, this is equivalent to a rate of release of 4.2 x $10^{-9}$ mol $s^{-1}$ for the 166.028 g of Utsira sand in the column. The surface area of the Utsira sand sample used was 0.3 $m^2g^{-1}$, which gives an overall Ca release rate equivalent to 7.6 x $10^{-16}$ mol $cm^{-2}s^{-1}$.

It is interesting to compare the above release rate information from previous studies, though some rather large assumptions have to be used. Let us assume that the total surface area is equally distributed between all mineral phases within the Utsira sand (a rather large assumption), that all the carbonate phase is calcite, and that all Ca released into solution comes from calcite. Given that 6.7% of the sand sample is calcite, this would equate to a calcite dissolution rate of approximately 5 x $10^{-17}$ mol $cm^{-2}s^{-1}$.

At 25°C and atmospheric pressure, Chou et al. (1989) and Busenberg and Plummer (1986) give calcite (and aragonite) dissolution rates in the pH 3-5 region of approximately 1 x $10^{-9}$ mol $cm^{-2}s^{-1}$. Using an activation energy of 46 kJ $mol^{-1}$ (Sjoberg and Rickard, 1984), this would equate to a dissolution rate of approximately 1 x $10^{-8}$ mol $cm^{-2}s^{-1}$ at 70°C. It would appear therefore, that the rate of dissolution of the carbonate phase within the column experiments is significantly slower than in more idealised systems. This difference may in part be due to some of the rather large simplifications and assumptions used in the calculations. However, it may also reflect the difference in results between very simple idealised experiments with good fluid-mineral mixing at 'far from equilibrium conditions', and more complex 'dirty' experiments that have a longer fluid-mineral contact time and are thus considerably closer to equilibrium. Reaction rates decrease markedly as equilibrium is approached.

Sr

The Sr concentration profile (Figure 36) is similar to that of Ca above, with a rapid large initial release followed by a slow decease. However, the actual Sr concentrations are much lower than for Ca. This similar pattern of behaviour suggests (as per the batch experiments) that both Ca and Sr are being controlled by the same processes (i.e. carbonate dissolution). This is very probable as Sr is a common trace element within both shell fragments and abiogenic carbonate minerals.

Ba

Ba concentrations (Figure 36) show a slightly different profile to that of Ca and Sr. After an initial rapid decrease in concentration, there is a slower rise to approximately 9.5 x $10^{-5}$ mol $l^{-1}$ (13 mg $l^{-1}$) after about 50 days. After this there is a much slower decrease in concentration to an approximately steady-state value of about 6.6 x $10^{-5}$ mol $l^{-1}$ (9 mg $l^{-1}$) after 200 days reaction.

Two possible sources of Ba within the sample could be envisaged. Some may have been as a trace constituent within shell fragments (as per Sr). However, no initial rapid release of Ba was observed, as might have been expected if Ba behaved in the same way as Ca and Sr. A second possibility is that it is present as a fine-grained contaminant, which originated from the drilling mud (possibly as $BaSO_4$). However, if this were the source of the dissolved Ba, its fine-grained nature would tend to lead to rapid reaction and early release. The profile of Ba concentrations therefore, remains problematic.

Mg

Compared to the other Group II elements, Mg concentrations (Figure 35) are relatively constant. However, in detail, they show a slight, but progressive decrease over the first third of the experiment. Thereafter, the long term trend is for a slow increase in concentration up to approximately 2.7 x $10^{-2}$ mol $l^{-1}$ (650 mg $l^{-1}$), which is similar to that of the starting SUP fluid. This trend is very different to Ca, Sr and Ba, and suggests that Mg concentrations are not being controlled by carbonate reactions. It is thought that the slight changes in Mg concentration might be due to ion-exchange reactions, though there is no hard evidence to back this up.

$SiO_2$

$SiO_2$ concentrations (Figure 37) show an initial very rapid release of $SiO_2$ (up to approximately 9.2 x $10^{-4}$ mol $l^{-1}$ (55 mg $l^{-1}$)) followed by a decrease towards a steady-state value of approximately 5.0 x $10^{-4}$ mol $l^{-1}$ (30 mg $l^{-1}$) after about 180 days. It should be noted that due to lack of information on silica concentrations in the Oseberg porewater, the SUP was prepared with no dissolved $SiO_2$. The fluid was therefore almost certainly out of equilibrium with respect to a solid Si phase (e.g. quartz). The initially enhanced release rate may reflect dissolution of more 'reactive' sites on such a phase, with the later steady release rate reflecting more uniform dissolution.

Given a flow rate of 0.5 ml $h^{-1}$, the initial release of $SiO_2$ is equivalent to a rate of 1.3 x $10^{-10}$ mol $s^{-1}$ for the 166.028 g of Utsira sand in the column. The surface area of the Utsira sand sample used was 0.3 $m^2g^{-1}$, which gives an initial $SiO_2$ release rate equivalent to 2.3 x $10^{-17}$ mol $cm^{-2}s^{-1}$. The later steady-state $SiO_2$ release rate was equivalent to 7 x $10^{-11}$ mol $s^{-1}$ for the 166.028 g of Utsira sand in the column. The surface area of the Utsira sand sample used was 0.3 $m^2g^{-1}$, which gives a steady-state $SiO_2$ release rate equivalent to 1.3 x $10^{-17}$ mol $cm^{-2}s^{-1}$.

If it is assumed that the total surface area is equally distributed between all mineral phases within the Utsira sand (a rather large assumption), and that all $SiO_2$ released into solution comes from quartz. Given that approximately 76.4% of the sand sample is quartz, this would equate to a quartz dissolution rate of approximately 1 x $10^{-18}$ mol $cm^{-2}s^{-1}$. This compares to a measured quartz dissolution rate at 70°C of approximately 1 x $10^{-15}$ mol $cm^{-2}s^{-1}$ between pH 4-6 (Knauss and Wolery, 1988). It would appear therefore, that the rate of quartz dissolution (if indeed this was the important Si-rich phase – see comments in the previous section regarding the batch experiments) within the flow experiment is significantly slower than in more idealised systems. This difference may in part be due to some of the rather large simplifications and assumptions used in the calculations. However, it may also reflect the difference in results between very simple idealised experiments with good fluid-mineral mixing at 'far from equilibrium conditions', and more complex 'dirty' experiments that have a longer fluid-mineral contact time and are thus considerably closer to equilibrium. Reaction rates decrease markedly as equilibrium is approached. It is noted that a similar process has been identified in (poorly mixed) natural systems where silicate mineral dissolution rates are commonly several orders of magnitude slower than in 'idealised' laboratory systems (e.g. Velbel, 1993).

Al

Al concentrations (Figure 37) are somewhat erratic. There is an initial rapid tenfold decrease followed by a general rise in concentration up to approximately 7.4 x $10^{-6}$ mol $l^{-1}$ (0.2 mg $l^{-1}$) after about 150 days. After this, there was a decrease to approximately 3.7x$10^{-6}$ mol.$l^{-1}$ (0.1 mg $l^{-1}$), which continued until the end of the experiment. Although the apparently unduly high concentrations at approximately 40 and 240 days are probably artefacts (e.g. due to sample

contamination or other sampling problems), it is hard to explain the rest of the trends. However, processes such as clay mineral dissolution might be a possible cause of higher concentrations earlier in the experiment.

S

S concentrations (Figure 38) show an initial very rapid increase up to approximately 1.7 x $10^{-3}$ mol $l^{-1}$ (53 mg $l^{-1}$), followed by a large decrease over the next 20 days. Thereafter, the concentrations remain at a steady-state value of approximately 2.2 x $10^{-4}$ mol $l^{-1}$ (7 mg $l^{-1}$) for the remainder of the experiment.

One possible source of S in the experiments is pyrite, and this was identified in the Utsira sand (Pearce et al., 1999), but only as a trace component. Oxidation of this may have released the S as $SO_4^{2-}$. However, small amounts of S may also have been present within organic compounds in carbonate shell fragments. As these dissolved the S would have been released.

Given a flow rate of 0.5 ml $h^{-1}$, then the initial release of S is equivalent to a rate of 2.4 x $10^{-10}$ mol $s^{-1}$ for the 166.028 g of Utsira sand in the column. The surface area of the Utsira sand sample used was 0.3 $m^2g^{-1}$, which gives an initial S release rate equivalent to 4.3 x $10^{-17}$ mol $cm^{-2}s^{-1}$. The later steady-state S release rate was equivalent to 3 x $10^{-11}$ mol $s^{-1}$ for the 166.028 g of Utsira sand in the column. The surface area of the Utsira sand sample used was 0.3 $m^2g^{-1}$, which gives a steady-state S release rate equivalent to 5.4 x $10^{-18}$ mol $cm^{-2}s^{-1}$.

Fe

Fe concentrations (Figure 39) are somewhat erratic, and show no obvious trends. It should be noted that redox conditions were not controlled during the experiment. Therefore, for some samples, it is possible that ingress of atmospheric oxygen may have converted $Fe^{2+}$ to $Fe^{3+}$, with subsequent removal from solution by precipitation. However, it is also noted that the concentrations in some samples are significantly higher than in the SUP starting fluid. This suggests that at least some dissolution of a Fe-rich phase was occurring. Several phases can be identified within the Utsira sand that could have been the source of the Fe. These include; pyrite, Fe oxide, clays, and carbonates. However, the high pressure tubing used in the flow equipment was made of 316 stainless steel. Although generally considered unreactive, stainless steels can be subject to pitting corrosion (Ryan et al., 2002). Some sections of the high pressure tubing were cut and studied visually, but no significant corrosion was observed. However, subtle pitting corrosion would have been difficult to identify within narrow-bore tubing, and this might have provided another possible source of Fe.

Mn

Mn concentrations (Figure 39) show an initial rapid increase, followed by a quick decline within the first 20 days. Thereafter, concentrations stabilise at approximately 1.1 x $10^{-5}$ mol $l^{-1}$ (0.6 mg $l^{-1}$). This pattern is most similar to that of S, though it is unclear why these elements should behave in a similar way. It is possible that this is just coincidence, and that the vast majority of mobile Mn is being removed from the column on a similar timescale to S.

Cr

Cr concentrations (Figure 39) show that steady state release was attained within the first 10 days of reaction and remained at approximately 1.2 x $10^{-5}$ mol $l^{-1}$ (0.6 mg $l^{-1}$) throughout the rest of the experiment. It is possible that Cr could have been sourced from the stainless steel high pressure tubing, though there were no visual signs of corrosion (see comments for Fe).

$HCO_3^-$

Bicarbonate concentrations (Figure 40) show an increasing trend over time, with concentrations of over 1.3 x $10^{-2}$ mol $l^{-1}$ (800 mg $l^{-1}$) by the end of the experiment. Some inter-sample variation in concentration is observed, probably caused by a combination of sample degassing and standing time prior to analysis. Degassing of the aqueous fluid during sampling will have resulted in disequilibria, and the initiation of slow conversion of bicarbonate to $CO_2$. This means that the measured bicarbonate concentrations may not absolutely reflect the in-situ concentrations. It is worth noting that all the samples were analysed at the end of the experiment, and therefore early samples might have had longer to re-equilibrate (reducing bicarbonate concentrations). Consequently, later samples are more likely to be closer to in-situ values.

pH

It should be noted that pH measurement was taken in the lab at approximately 20 °C and 0.1 MPa pressure (atmospheric pressure) on depressurised and degassed samples. These conditions are quite different from those within the experiments, and thus cannot be regarded as indicative of in-situ pH. Consequently, the pH data should be taken as an indicator of trends rather than of absolute values. Measured pH values on depressurised and degassed samples (Figure 41) show a large increase from the input SUP fluid (pH of approximately 6.5) to a pH value of approximately 6.3.

# 4. Conclusions

An experimental study has been undertaken to react samples of Utsira sand from Sleipner with a synthetic Utsira porewater based upon a composition from the Oseberg field. A range of experiments have been conducted in either 'batch' and 'flow through' equipment at a pressure of 10 MPa and temperatures of either 37°C or 70°C. Durations ranged from one week to two years. These have revealed changes in fluid chemistry associated mainly with dissolution of primary minerals. Overall however, observed $CO_2$-water-rock reactions have resulted in relatively little dissolution of the Utsira sand.

Batch experiments at 37°C and pressurised by $N_2$ showed relatively few changes in aqueous chemistry relative to the starting fluid. To a first approximation therefore, the initial assumption that the Utsira porewater from the Oseberg field was similar to the Utsira porewater at Sleipner would appear to have been valid. However, closer inspection of the data reveals some differences, possibly indicating that the in-situ Utsira porewater contains a small quantity dissolved $CO_2$, and this was not accounted for in the $N_2$ experiments. The $N_2$ experiments have also given information on in-situ dissolved Al, Si and S concentrations, data absent from the original Oseberg analyses. These data will help refine models of the original geochemical 'baseline' at Sleipner.

Batch and flow experiments at 37°C and pressurised by $CO_2$ show the impact that storage operations will have on the porewater chemistry. Dissolution of carbonate phases led to large increases in solubility of Group II metals (and in particular Ca, Sr and Fe). This process appears to have been relatively rapid, and for the 10:1 fluid:rock ratio batch experiments, was essentially complete after 2 months of reaction. Dissolution of silicate minerals was a much slower process, and was still ongoing (though at a reduced rate) after 2 years of reaction.

In spite of the observed changes in solution chemistry, which suggests mineral dissolution (and in particular a Ca-carbonate phase), mineralogical analysis provided little evidence that

any such reactions occurred. Pitting and corrosion features are observed on all the main detrital components of the sand (quartz, feldspar and Ca-carbonate bioclasts), with apparently equal prominence in both the samples reacted in a $CO_2$-rich environment and those from the $N_2$ 'blanks'. These features are therefore taken to represent primary features of the Utsira Sand. Furthermore, it is possible to find both lightly and highly corroded bioclasts within the same sample from either $CO_2$-reacted experiments or blank experiments. This indicates that observed changes in fluid chemistry must be attributable to mineral dissolution reactions whose extent is lost within the 'noise' of natural mineralogical variation within the sand.

There are however, still a few outstanding questions. These can be summarised as follows:

- Why does Ba solubility behave in an opposite way to Ca, Sr, Fe and Mn and show lower solubility in the presence of $CO_2$?
- What phase controls Mg solubility?
- What phase controls Al solubility?
- Apart from pyrite, what other phase contains S, and which phases are controlling the release of S to solution?

The experiments appear to show that the Utsira sand is only likely to undergo limited reaction with the injection of $CO_2$. Most of the observed reactions involve dissolution of a carbonate phase (much of which is probably shell fragments), half of which was observed to dissolve over a 2 year period under in-situ conditions (37°C, 10 MPa). However, sand porosity is approximately 40%, and as carbonates only constitute 3.9% of the total rock volume, dissolution of half of them will not change overall porosity by a large degree. There was no direct evidence for the formation of appreciable quantities of secondary precipitates, though when reacted solutions were degassed and held at atmospheric pressure without any preservation for at least 24 hours some minor calcium carbonate precipitate was observed.

Overall therefore, observed $CO_2$-water-rock reactions have resulted in relatively little dissolution of the Utsira sand. From a geochemical standpoint, and just considering the host rock, the results of this study indicate that the Utsira sand would appear to be a suitable host for injected $CO_2$.

# References

Abbotts, I.L. (1991). United Kingdom oil and gas fields, 25 years commemorative volume. Geological Society of London Memoir, 14.

Bachu, S., Gunter, W.D. and Perkins, E.H. (1994). Aquifer disposal of $CO_2$: hydrodynamic and mineral trapping. Energy Conversion and Management, 35, 269-279.

Brady, P.V. and Walther, J.V., 1990. Kinetics of quartz dissolution at low temperatures. Chemical Geology, 82, 253-264.

Busenberg, E. and Plummer, L.N. (1986). A comparative study of the dissolution and crystal growth kinetics of calcite and aragonite. In 'Studies in Diagenesis' (F.A. Mumpton ed.), U.S. Geological Survey Bulletin 1578, 139-168.

Chou, L., Garrels, R.M. and Wollast, R., 1989. Comparative study of the kinetics and mechanisms of dissolution of carbonate minerals. Chemical Geology, 78, 269-282.

Czernichowski-Lauriol, I., Sanjuan, B., Rochelle, C., Bateman, K., Pearce, J. and Blackwell, P. (1996). Area 5: Inorganic Geochemistry, Chapter 7 in 'The underground disposal of carbon dioxide' (S. Holloway ed.). Final report for the CEC, contract number JOU2-CT92-0031. Published by the British Geological Survey.

Ellis, A.J. and Golding, R.M. (1963). The solubility of carbon dioxide above 100°C in water and in sodium chloride solutions. American Journal of Science, 261, 47-60.

Faanu, A. (2001). Spectroscopic determination of pH. MSc project report, University of Nottingham.

Gregersen, U., Johannessen, P.N., Møller, J.J., Kristensen, L., Christensen, N.P., Holloway, S., Chadwick, A., Kirby, G., Lindeberg, E. and Zweigel, P. (1998). Saline Aquifer $CO_2$ Storage (S.A.C.S.) Phase Zero 1998.

Gunter, W.D., Perkins, E.H., Bachu, S., Law, D., Wiwchar, B., Zhou, Z. and McCann, T.J., 1993. Aquuifer disposal of $CO_2$-rich gases. Alberta Research Council report, C-1993-5.

Knauss, K.G., and Wolery, T.J., 1986. Dependence of albite dissolution kinetics on pH and time at 25°C and 70°C, Geochim. Cosmochim. Acta, 50, p. 2481-2497.

Knauss, K.G., and Wolery T.J., 1988. The dissolution kinetics of quartz as a function of pH and time at 70°C. Geochim Cosmochim Acta, 52, p. 1493-1501.

Kuk, M.S. and Montagna, J.C. (1983). Solubility of oxygenated hydrocarbons in supercritical carbon dioxide. In: 'Chemical Engineering at Supercritical Fluid Conditions', Ann Arbor Science, Ann Arbour, MI, USA, 101-111.

Pearce, J.M., Holloway, S., Wacker, H., Nelis, M.K., Rochelle, C. and Bateman, K., 1996. Natural occurrences as analogues for the geological disposal of carbon dioxide. Energy Conversion and Management, 37, 6-8, 1123-1128.

Pearce, J.M., Kemp, S.J., Bouch, J., Turner, G.H. and Evans, E.J. (2002). A petrographic study of the Utsira Formation and its reaction with $CO_2$-rich fluids during hydrothermal experiments. British Geological Survey report, CR/02/071.

Pearce, J.M., Kemp, S.J. and Wetton, P.D. (1999). Mineralogical and Petrographical characterisation of a 1m core from the Utsira Formation, central North Sea. British Geological Survey technical report, WG/99/24C.

Rochelle, C.A. and Moore, Y.A. (2002). The solubility of $CO_2$ into pure water and synthetic Utsira porewater. British Geological Survey Commissioned Report, CR/02/052. 23 pp.

Ryan, M.P., Williams, D.E., Chater, R.J., Hutton, B.M. and McPhall, D.S. (2002). Why stainless steel corrodes. Nature, 415, 770-774.

Schremp, F.W., and Roberson, G.R., 1975. Effect of supercritical carbon dioxide ($CO_2$) on construction materials. Soc. of Petroleum Engineers Journal, June edition, p. 227-233.

Sjoberg, E.L. and Rickard, D.T. (1984). Temperature dependence of calcite dissolution kinetics between 1 and 62°C at pH 2.7 to 8.4 in aqueous solution. Geochim Cosmochim Acta, 48, p. 485-493.

Stewart, P.B. and Munjal, P.K. (1970). The solubility of carbon dioxide in pure water, synthetic sea water and synthetic sea-water concentrates at –5 to 25°C and 10 to 45 atm pressure. Journal of Chemical Engineering Data, 15(1), 67-71.

Suto, Y., Liu, L., Hashida, T. and Yamasaki, N. (2000). Measurement of $CO_2$ solubility in simulated underground water at depth for the carbon dioxide sequestration. In 'Proceedings of joint Sixth International Symposium on Hydrothermal Reactions and Fourth International Conference on Solvo-Thermal Reactions' (K. Yanigisawa and Q. Feng eds), July 25-28, 2000, Kochi, Japan.

Takenouchi, S. and Kenedy, G.C. (1965). The solubility of carbon dioxide in NaCl solutions at high temperatures and pressures. American Journal of Science, 263, 445-454.

Teng, H. and Yamasaki, A. (1998). Solubility of liquid $CO_2$ in synthetic sea water at temperatures from 298 K to 293 K and pressures from 6.44 MPa to 29.49 MPa, and densities of the corresponding aqueous solutions. Journal of Chemical Engineering Data, 43, 2-5.

Toews, K.L., Shroll, R.M. and Wai, C.M. (1995). pH-defining equilibrium between water and supercritical $CO_2$. Influence on SFE of organics and metal chelates. Analytical Chemistry, 67, 4040-4043.

van Eldik, R. and Palmer, D.A. (1982). Effects of pressure on the kinetics of the dehydration of carbonic acid and the hydrolysis of $CO_2$ in aqueous solution. Journal of Solution Chemistry, 11(5), 339-346.

Weast, R.C. (1972/1973). Handbook of Chemistry and Physics, 53rd edition. Published by The Chemical Rubber Co.

Velbel, M.A. (1993). Constancy of silicate-mineral weathering-rate ratios between natural and experimental weathering: Implications for hydrologic control of differences in absolute rates. Chemical Geology, 105, 89-99.

Wiebe, R. and Gaddy, V.L. (1941). Vapour phase composition of carbon dioxide-water mixtures at various temperatures and at pressures up to 700 atmospheres. Journal of the American Chemical Society, 63, 475.

Figure 1 Schematic diagram showing a typical batch reactor.

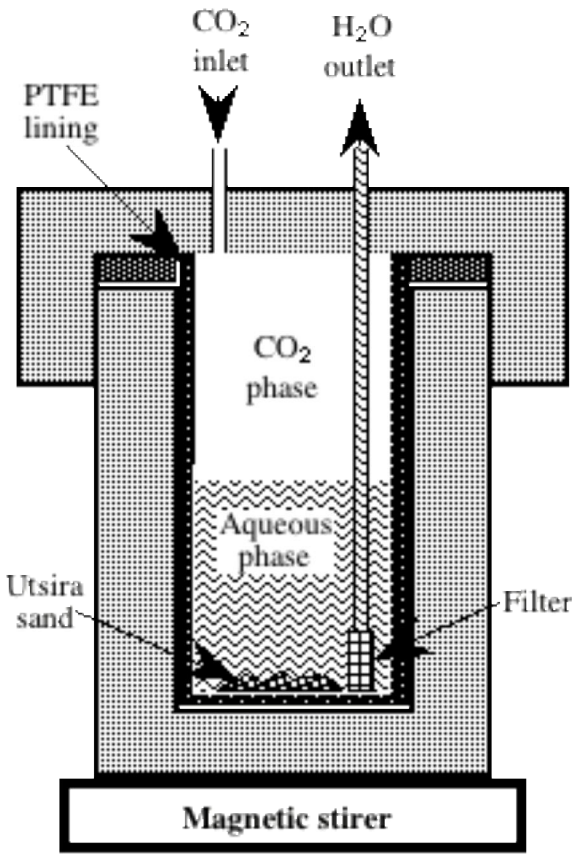

Figure 2 Schematic diagram showing the sampling of a batch reactor.

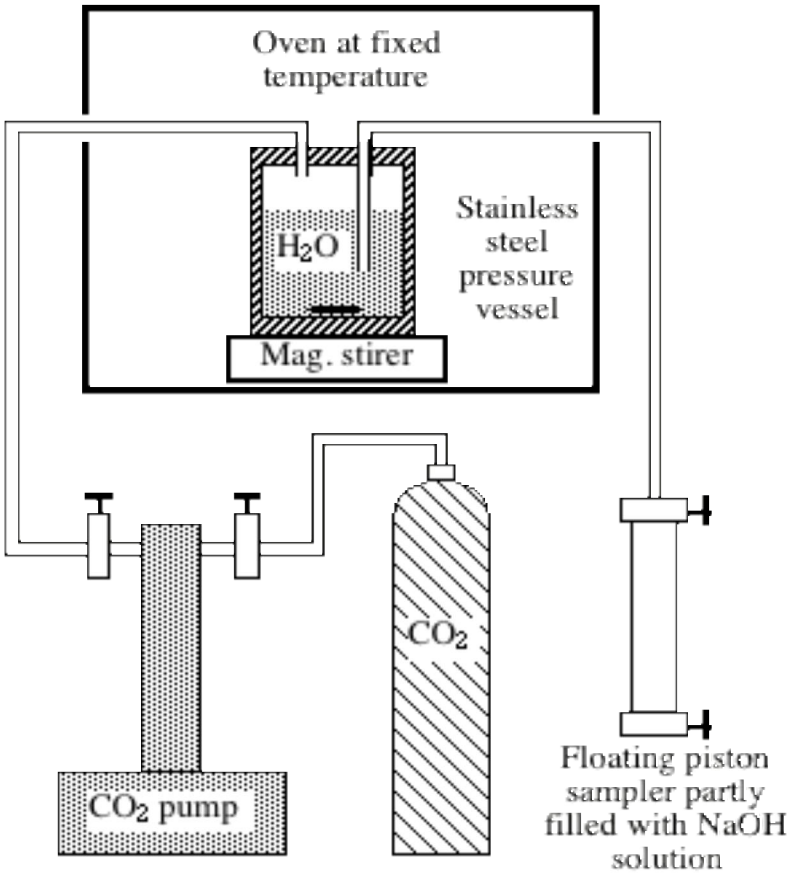

Figure 3 Simplified schematic of column experiment layout.

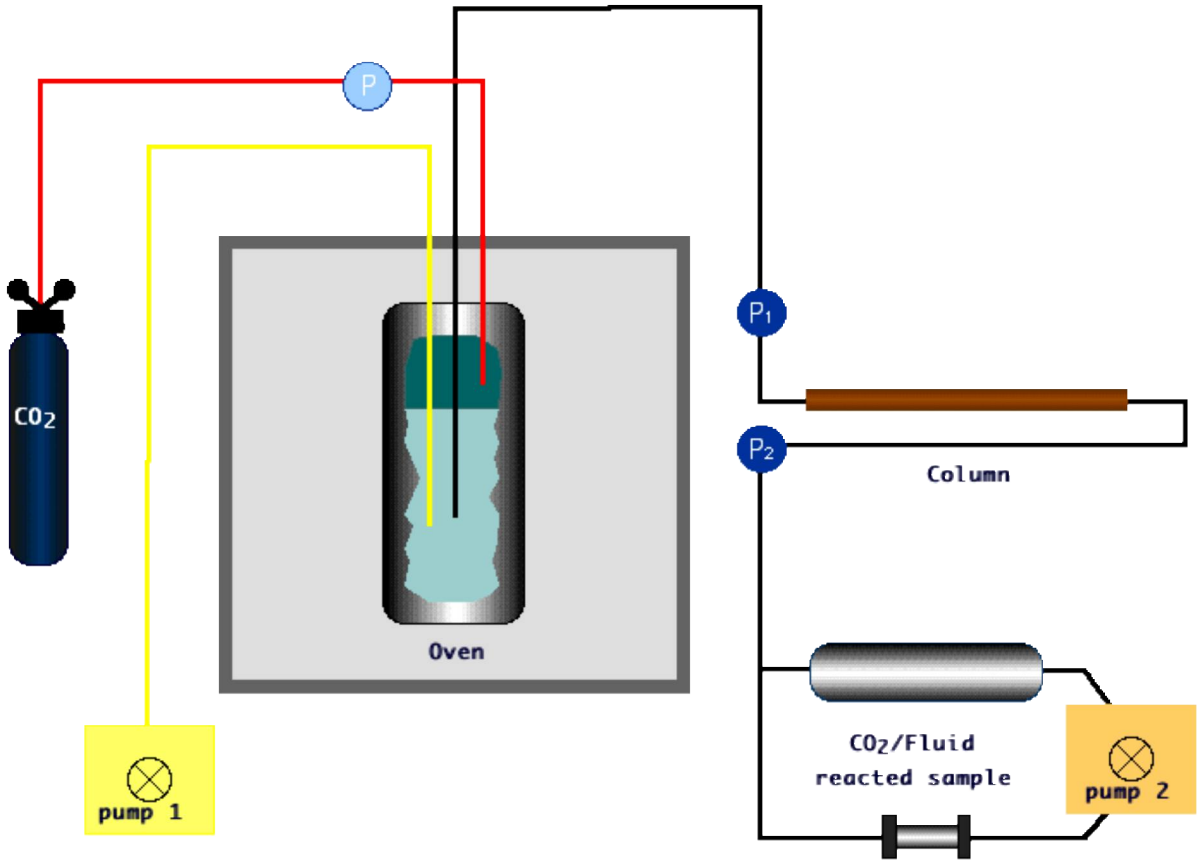

Figure 4 $Cl^-$ variation over time. Batch reactors, 37°C, 10 MPa.

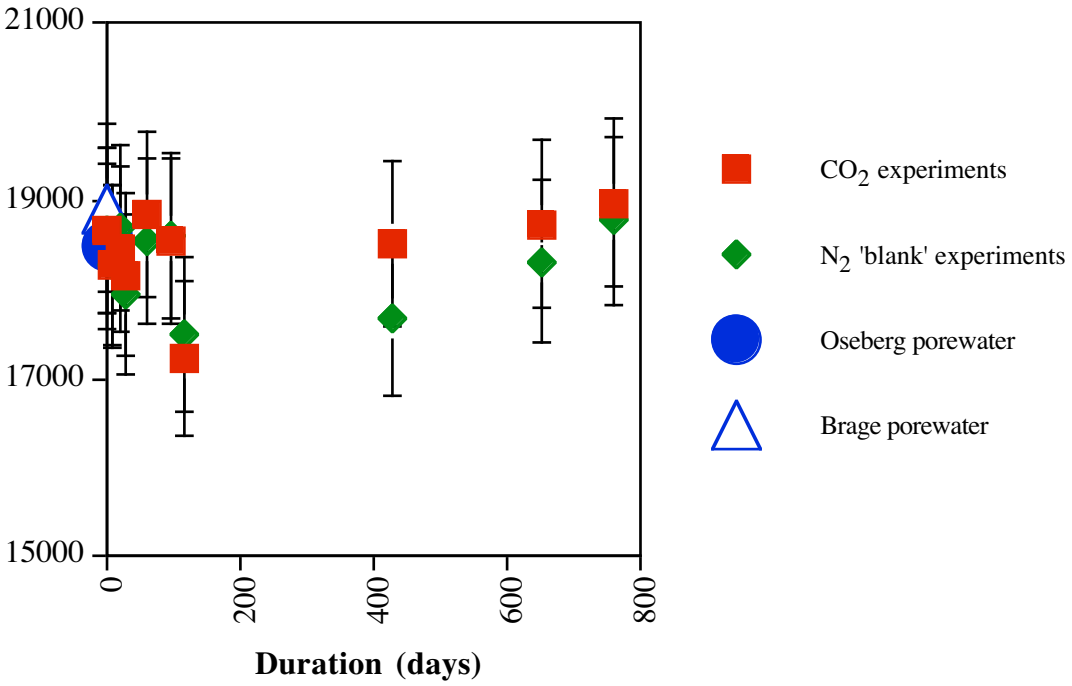


Figure 5 Na variation over time. Batch reactors, 37°C, 10 MPa.

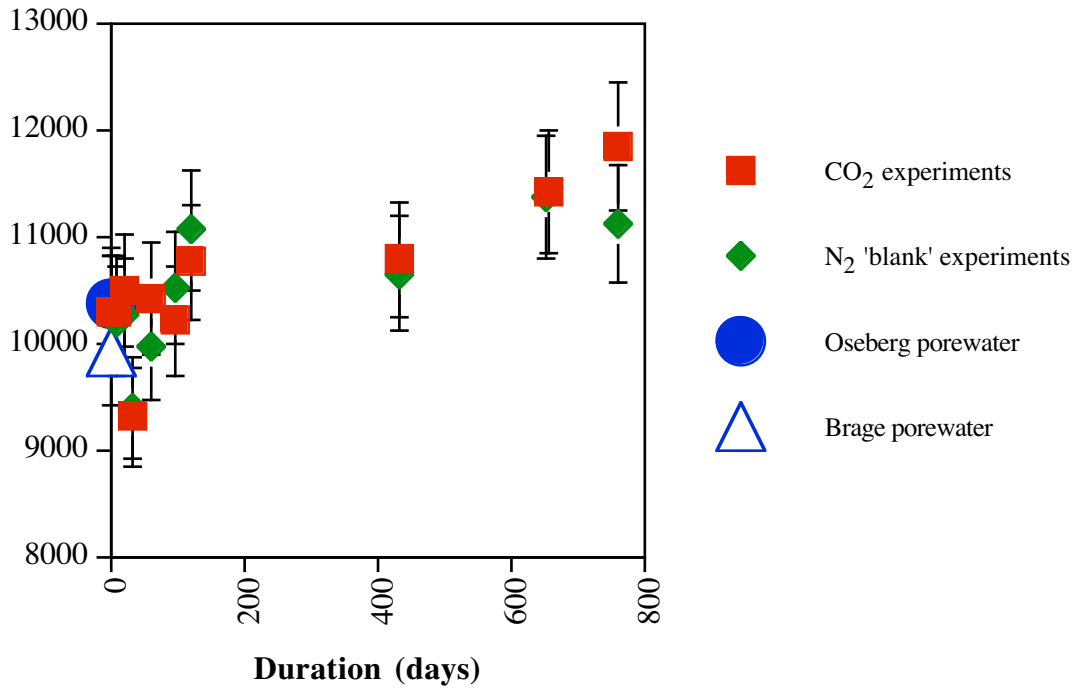

Figure 6 K variation over time. Batch reactors, 37°C, 10 MPa.

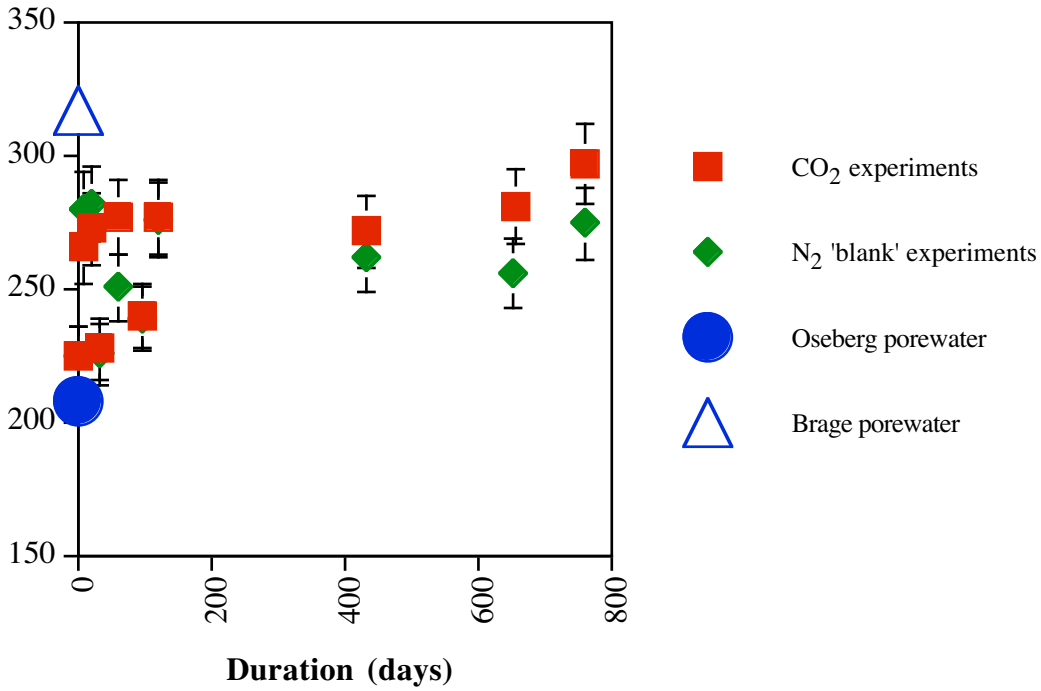


Figure 7 Ca variation over time. Batch reactors, 37°C, 10 MPa.

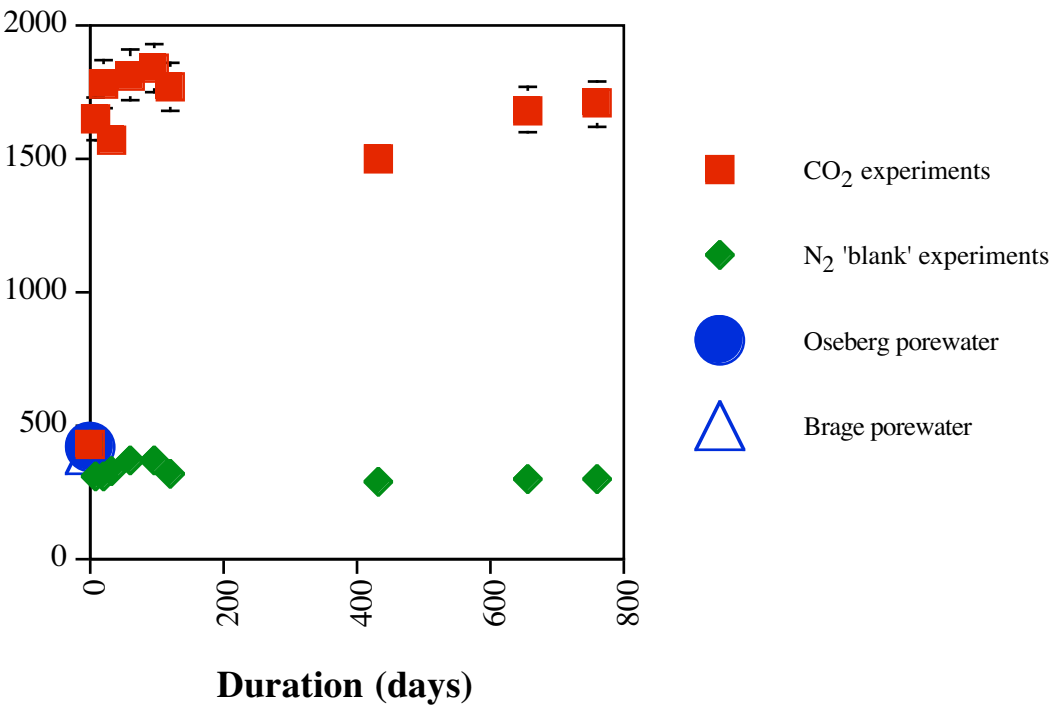

Figure 8 Sr variation over time. Batch reactors, 37°C, 10 MPa.

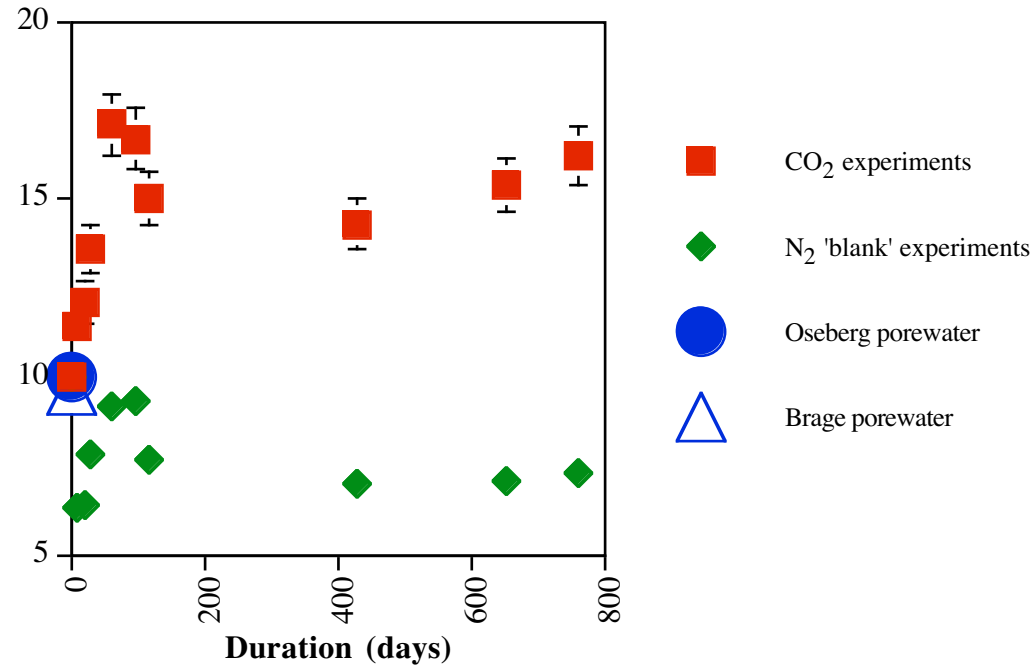


Figure 9 Fe variation over time. Batch reactors, 37°C, 10 MPa.

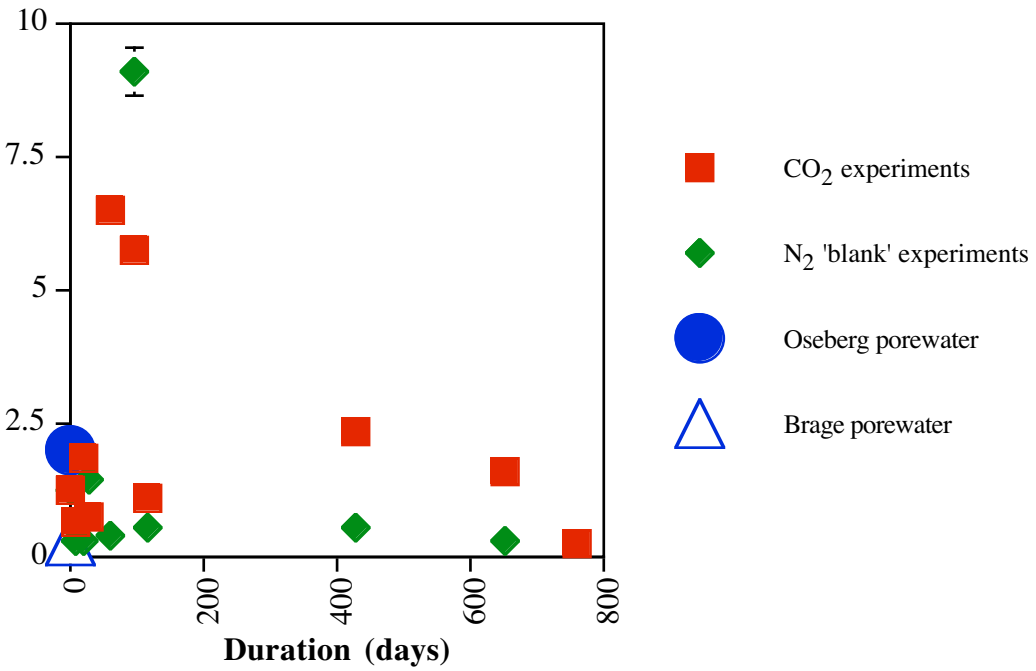

Figure 10 Ba variation over time. Batch reactors, 37°C, 10 MPa.

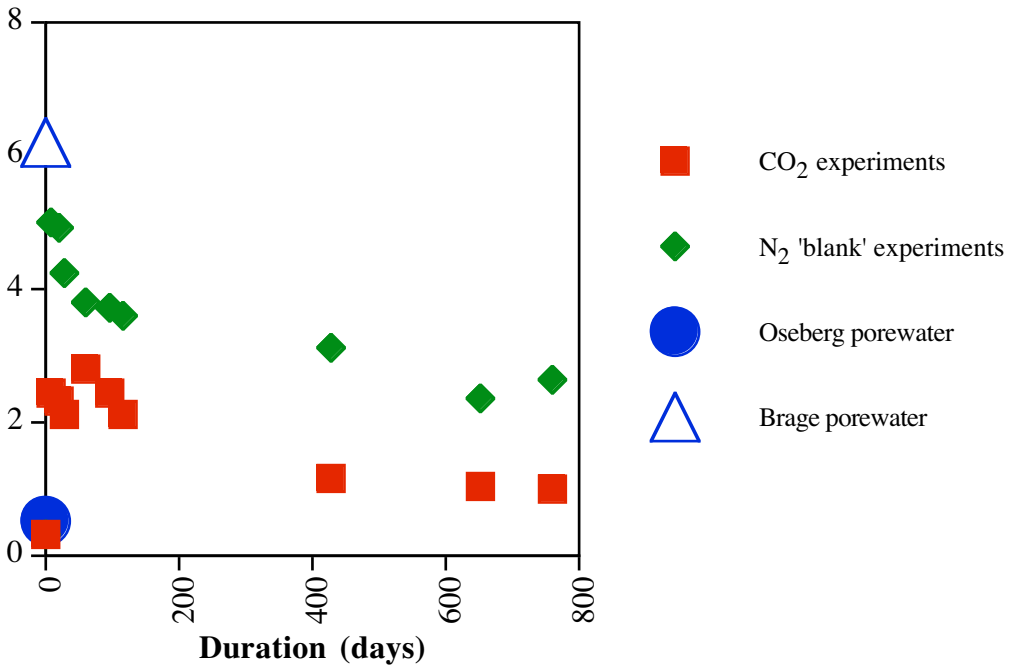


Figure 11 Mg variation over time. Batch reactors, 37°C, 10 MPa.

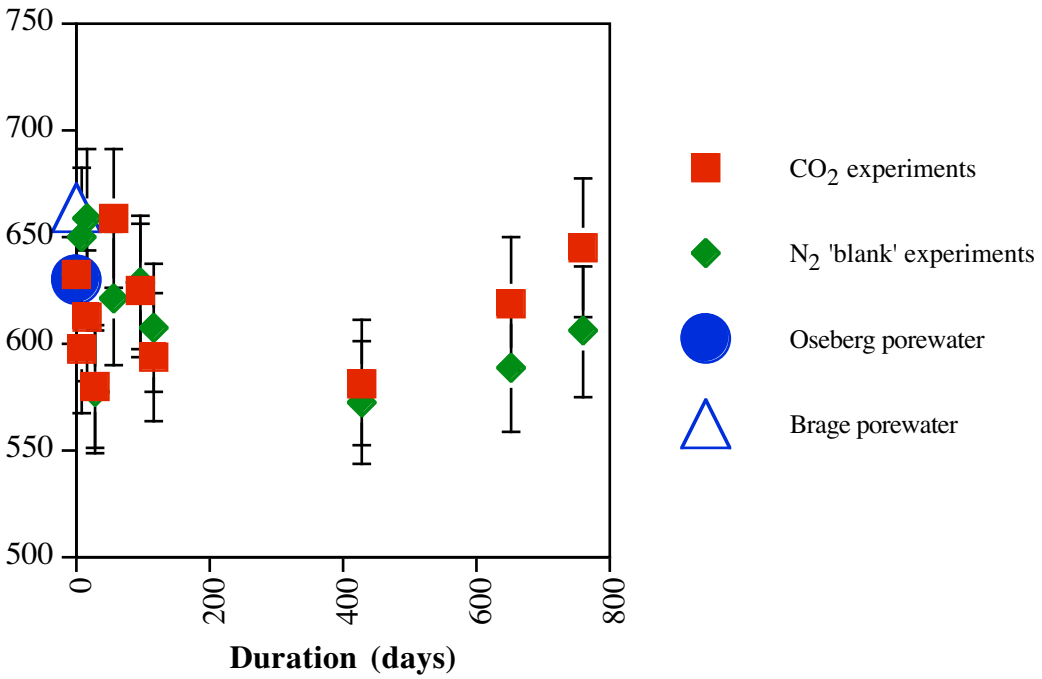

Figure 12 $SiO_2$ variation over time. Batch reactors, 37°C, 10 MPa.

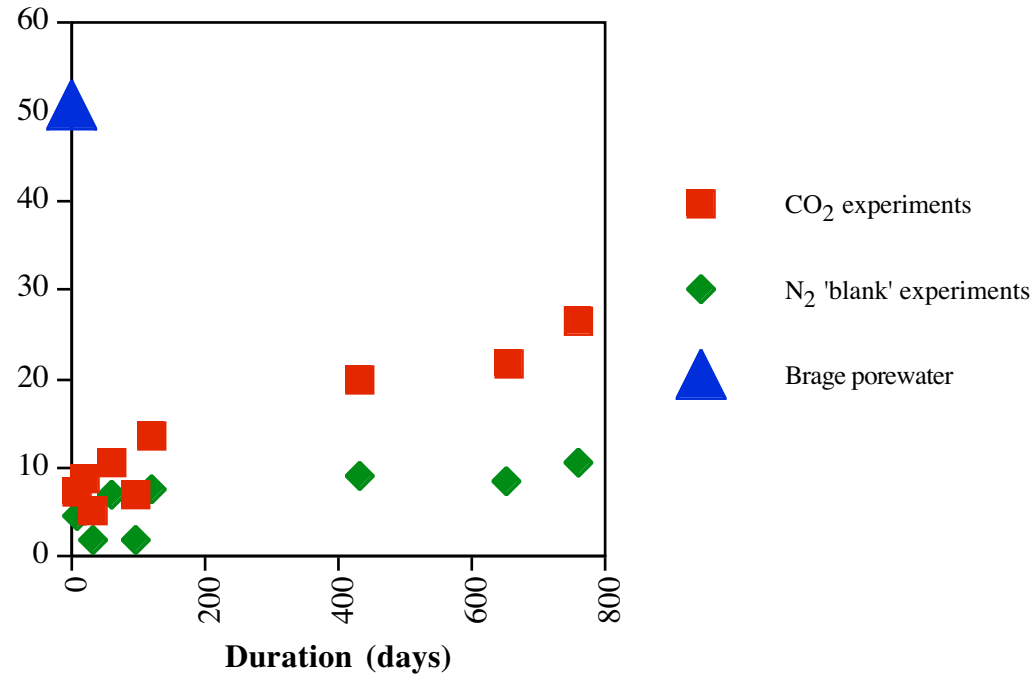


Figure 13 Al variation over time. Batch reactors, 37°C, 10 MPa.

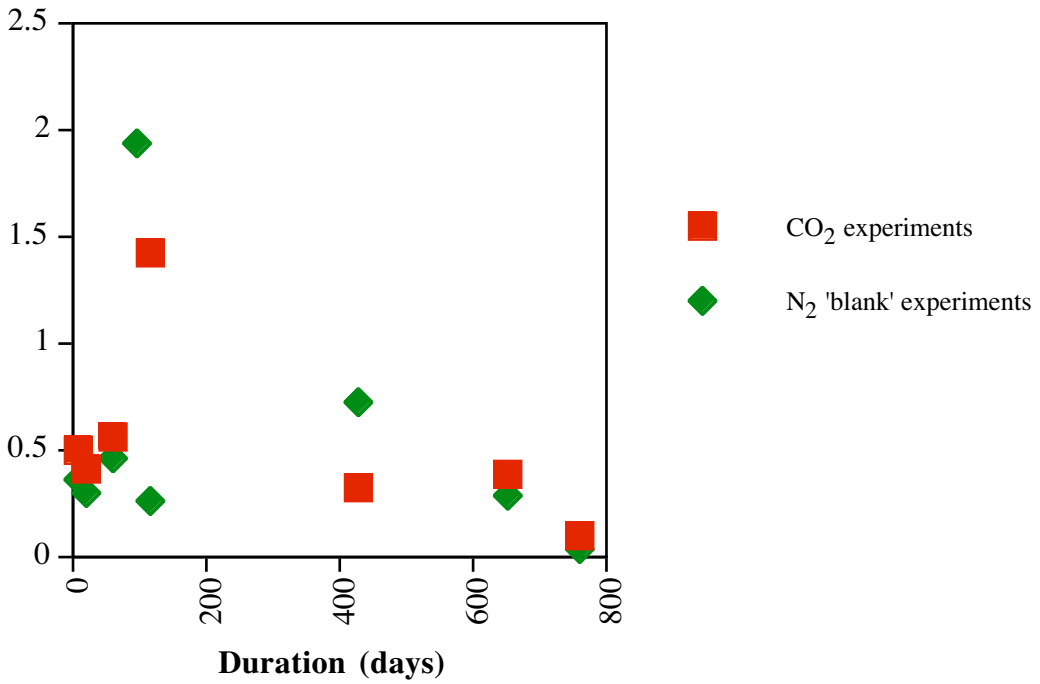

Figure 14 Total S variation over time. Batch reactors, 37°C, 10 MPa.

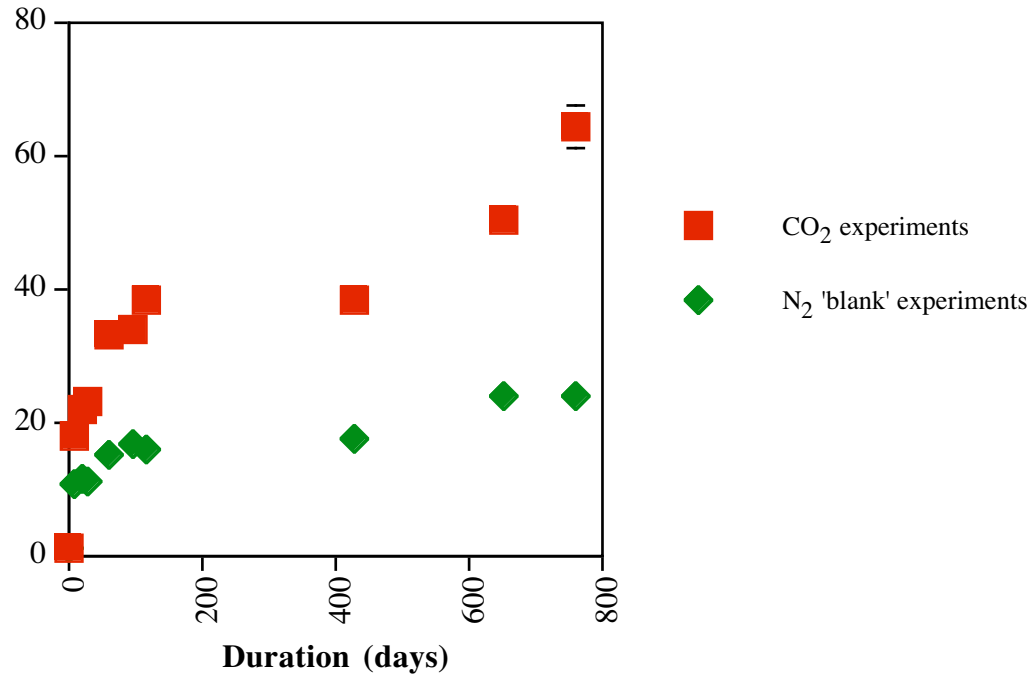


Figure 15 $CO_3^{2-}$ variation over time. Batch reactors, 37°C, 10 MPa.

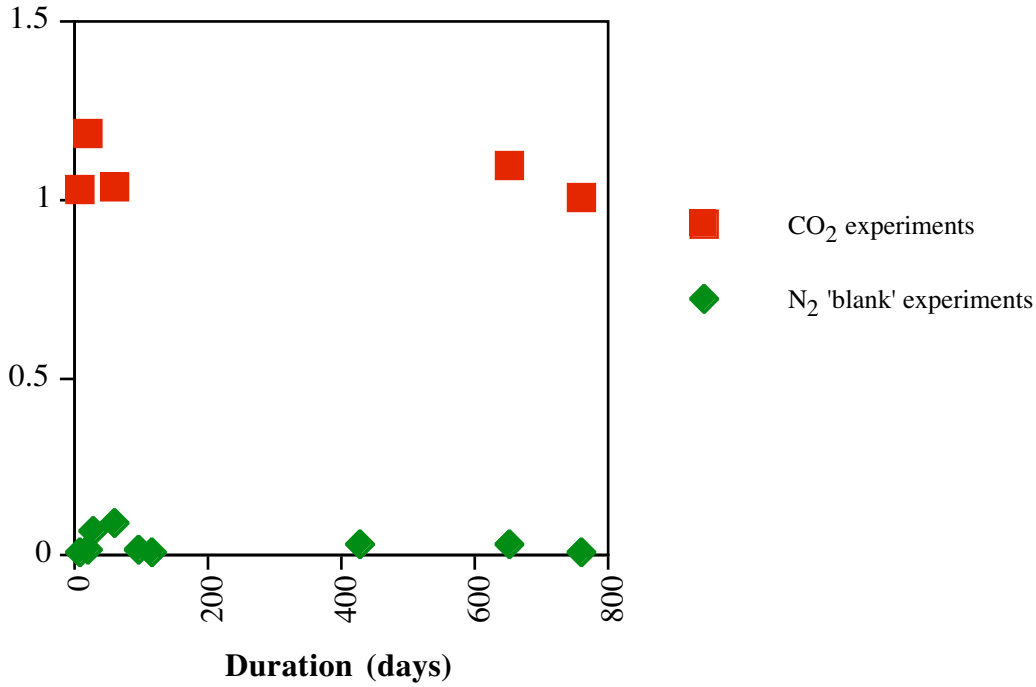

Figure 16 $HCO_3^-$ variation over time. Batch reactors, 37°C, 10 MPa.

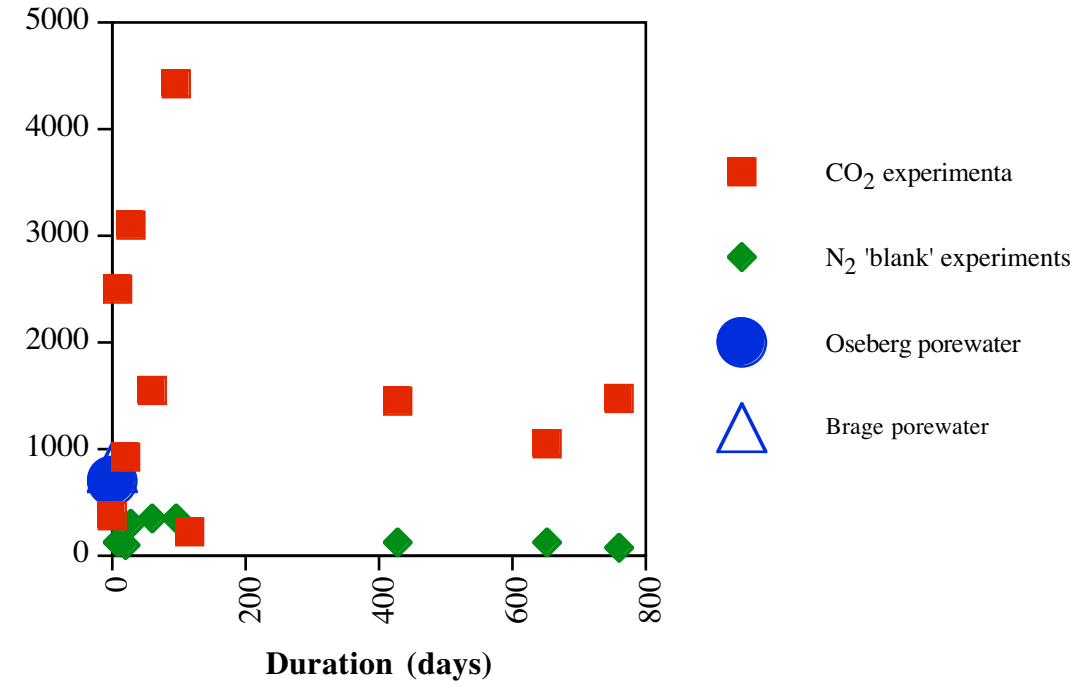


Figure 17 pH variation over time. Batch reactors, 37°C, 10 MPa.

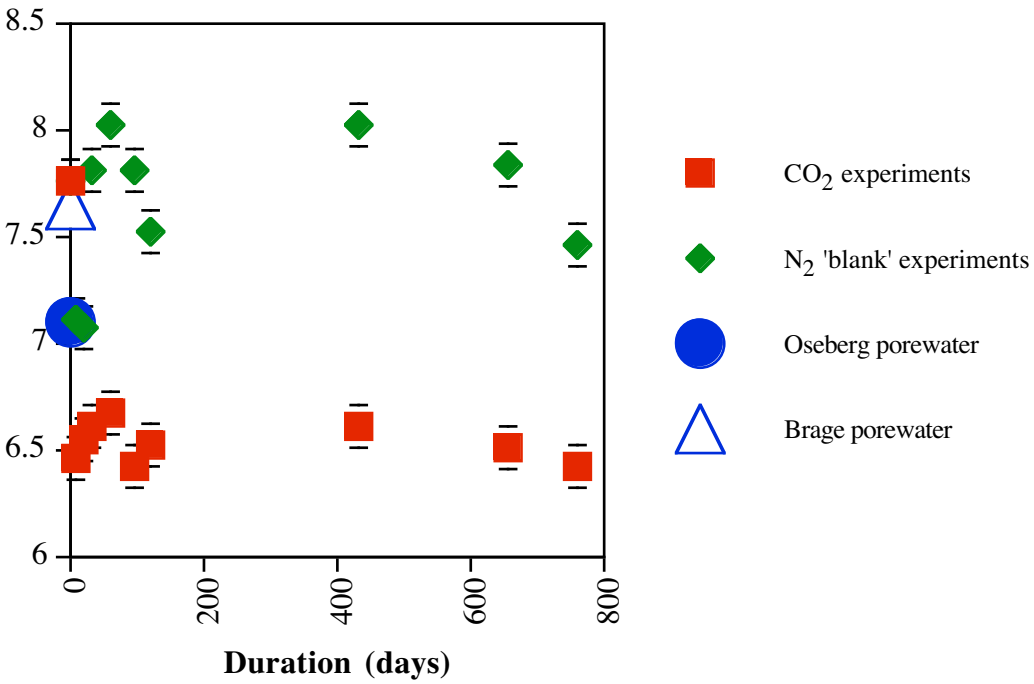

Figure 18 $Cl^-$ variation over time. Batch reactors, 70°C, 10 MPa.

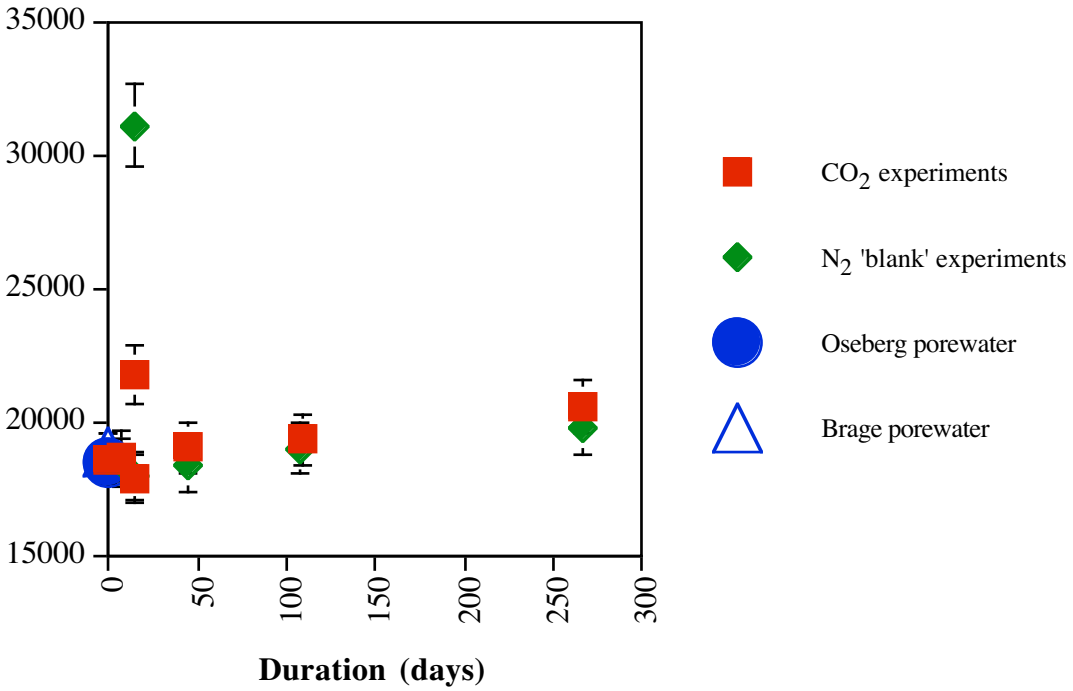


Figure 19 Na variation over time. Batch reactors, 70°C, 10 MPa.

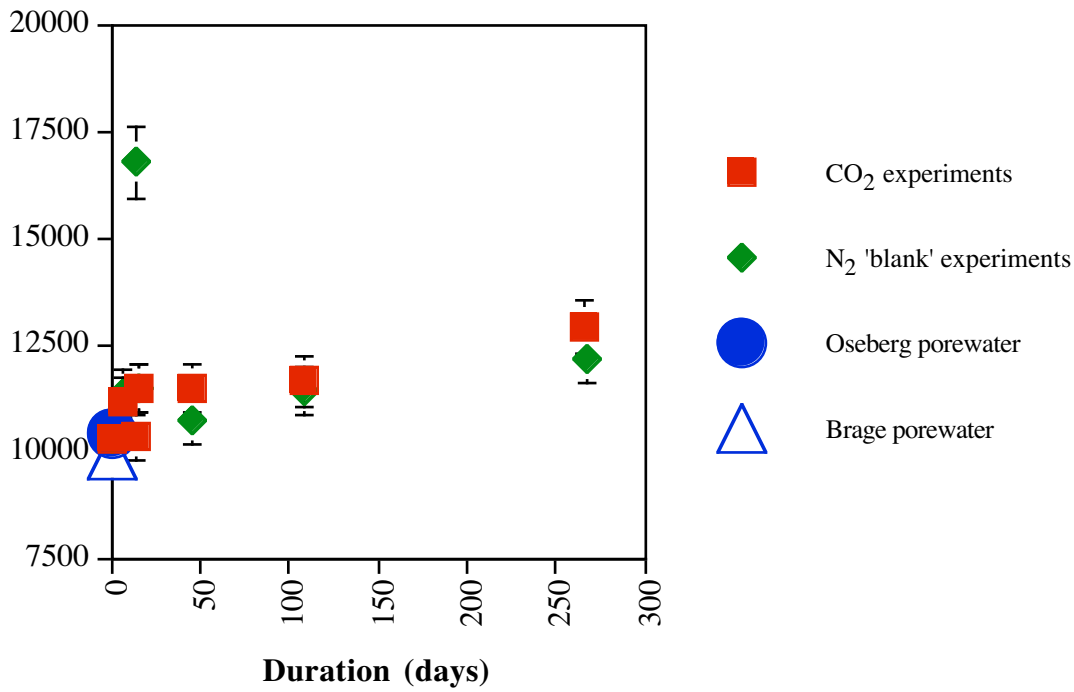

Figure 20 K variation over time. Batch reactors, 70°C, 10 MPa.

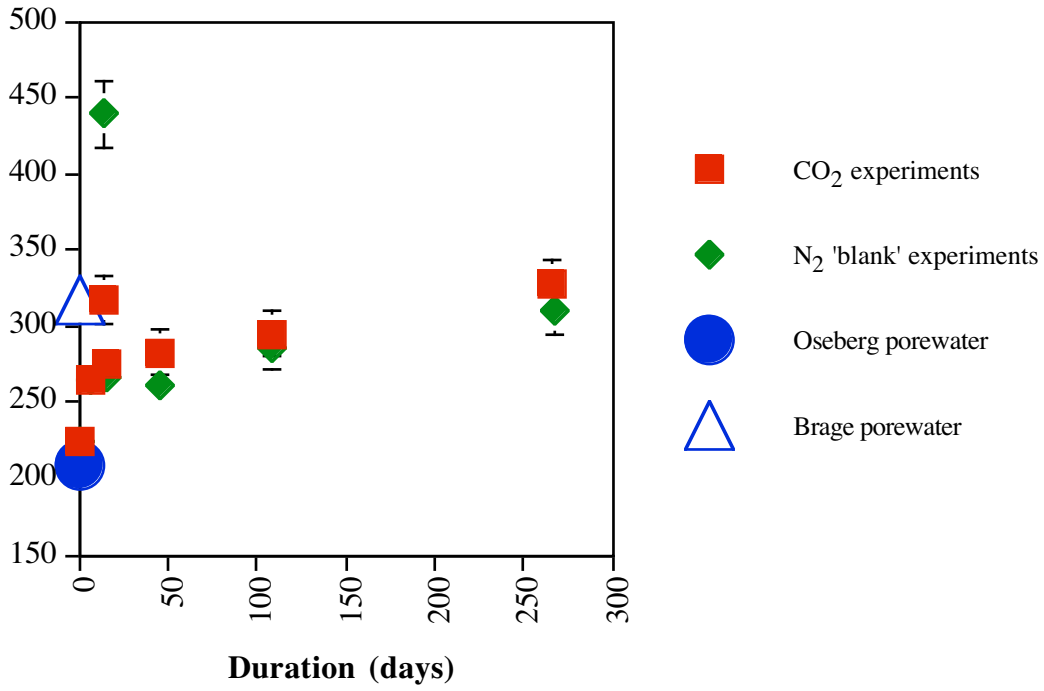


Figure 21 Ca variation over time. Batch reactors, 70°C, 10 MPa.

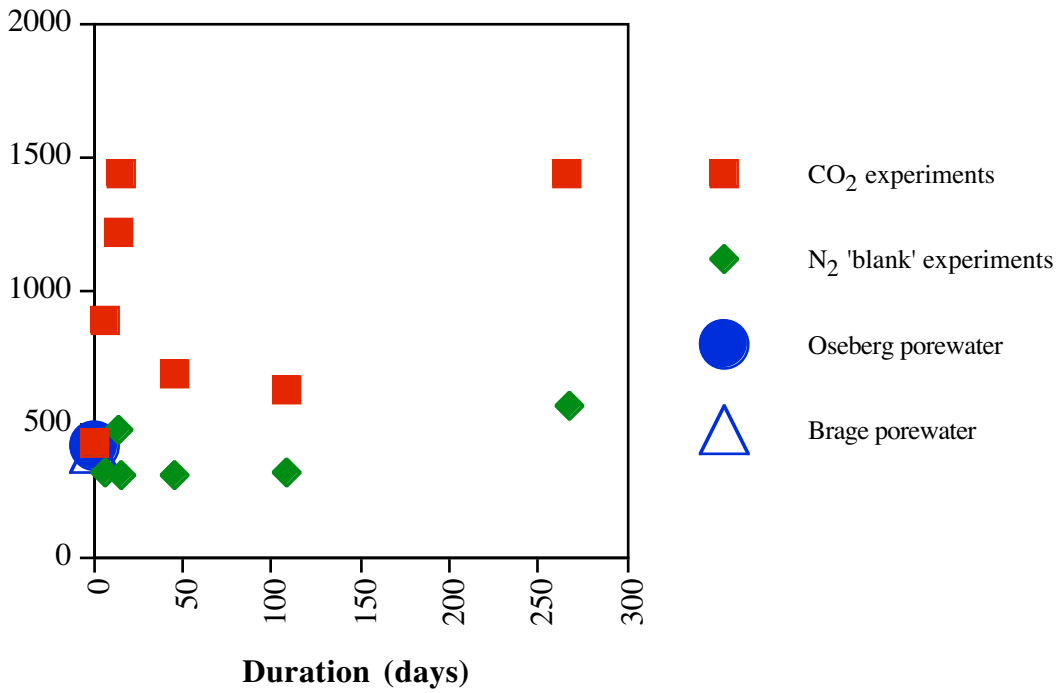

Figure 22 Sr variation over time. Batch reactors, 70°C, 10 MPa.

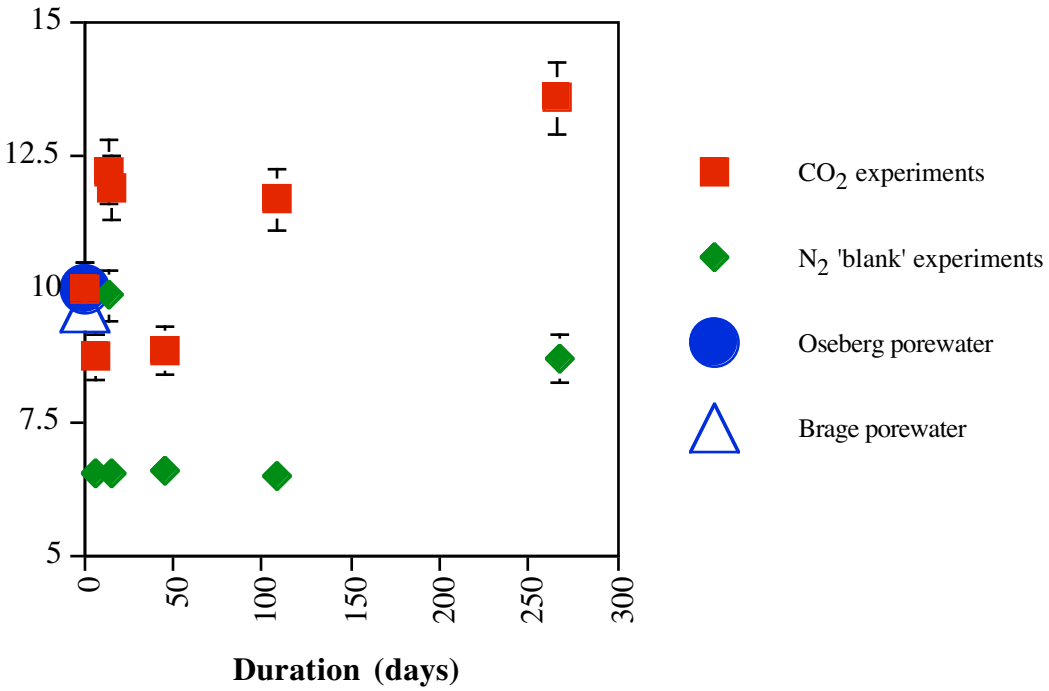


Figure 23 Fe variation over time. Batch reactors, 70°C, 10 MPa.

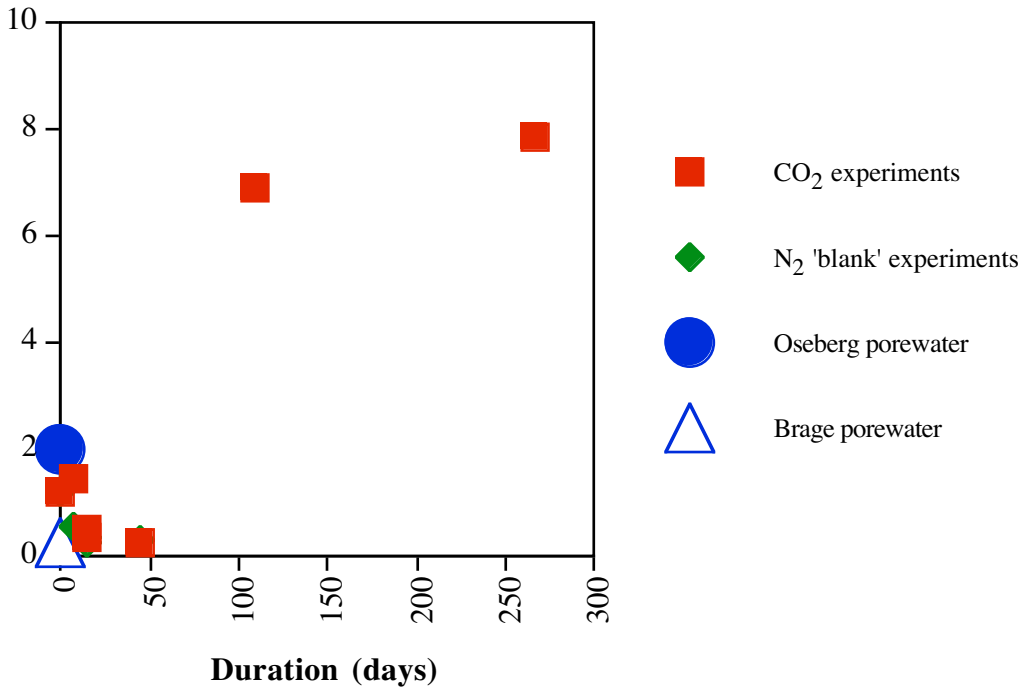

Figure 24 Mn variation over time. Batch reactors, 70°C, 10 MPa.

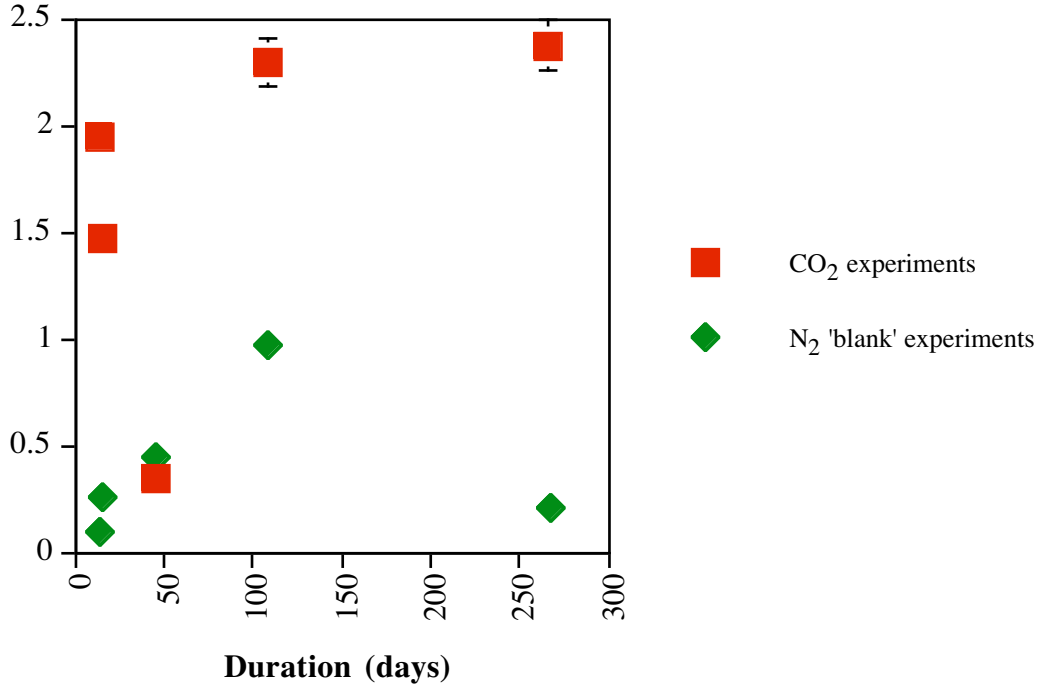


Figure 25 Ba variation over time. Batch reactors, 70°C, 10 MPa.

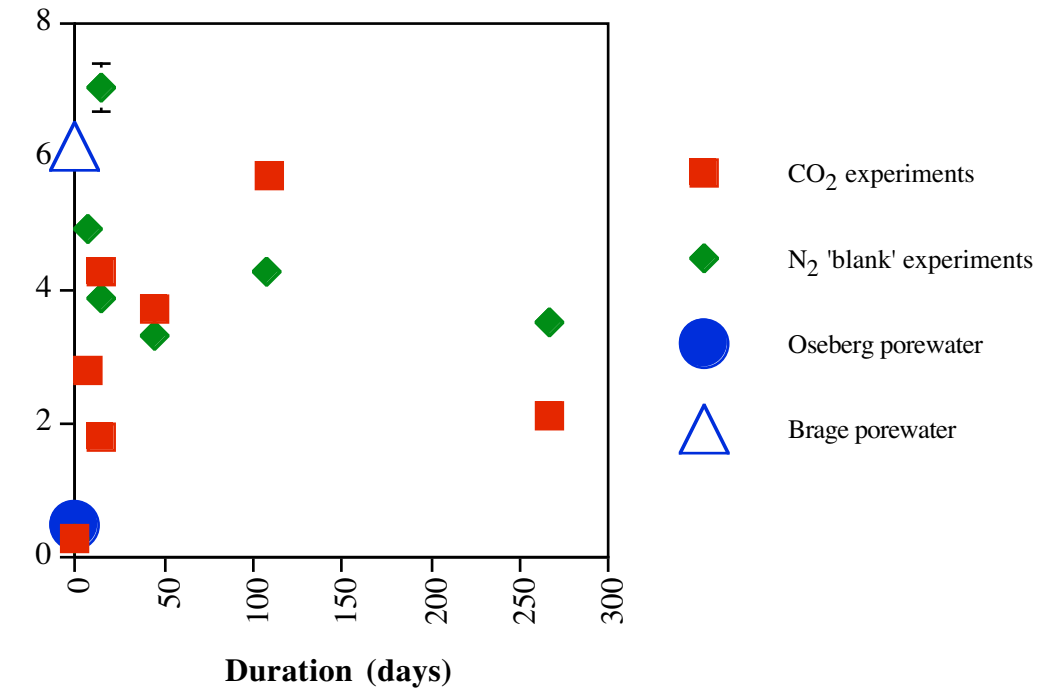

Figure 26 Mg variation over time. Batch reactors, 70°C, 10 MPa.

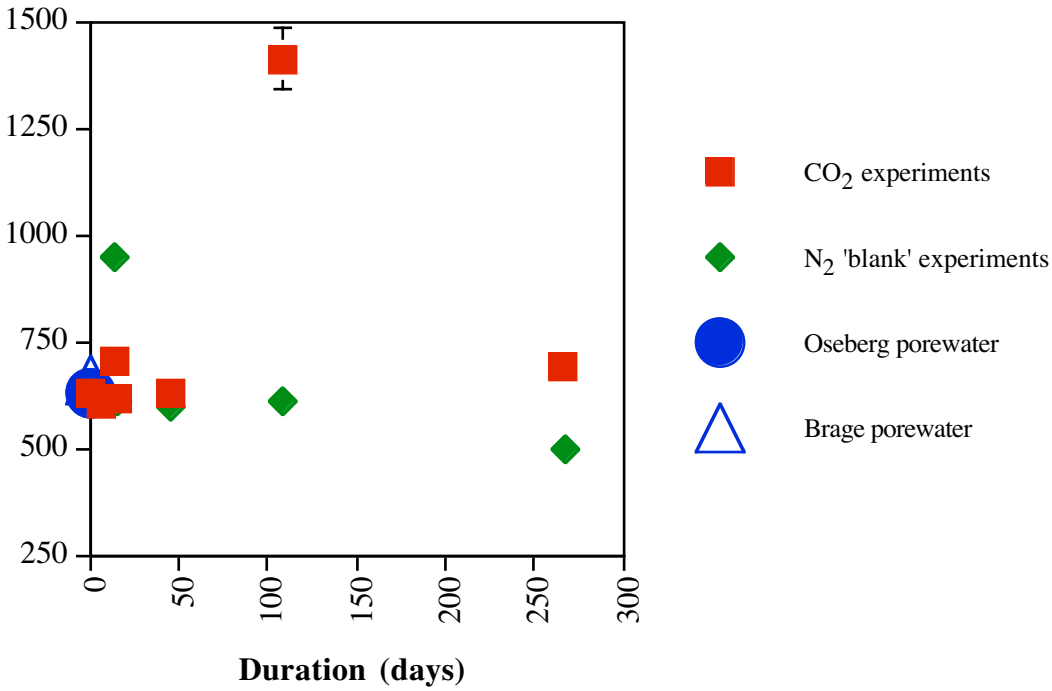


Figure 27 $SiO_2$ variation over time. Batch reactors, 70°C, 10 MPa.

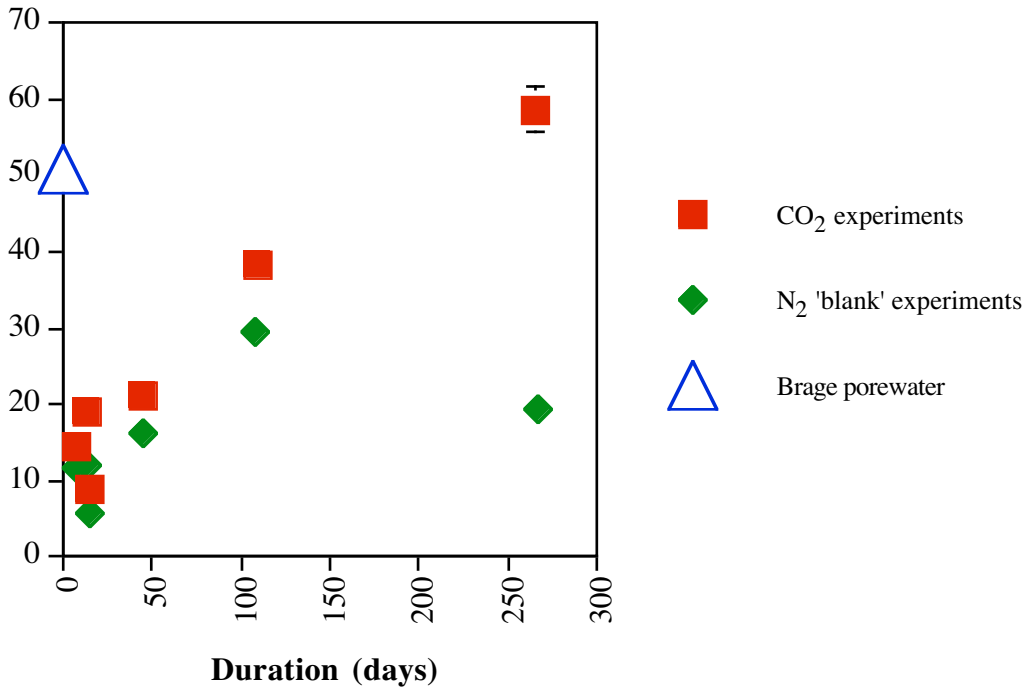

Figure 28 Al variation over time. Batch reactors, 70°C, 10 MPa.

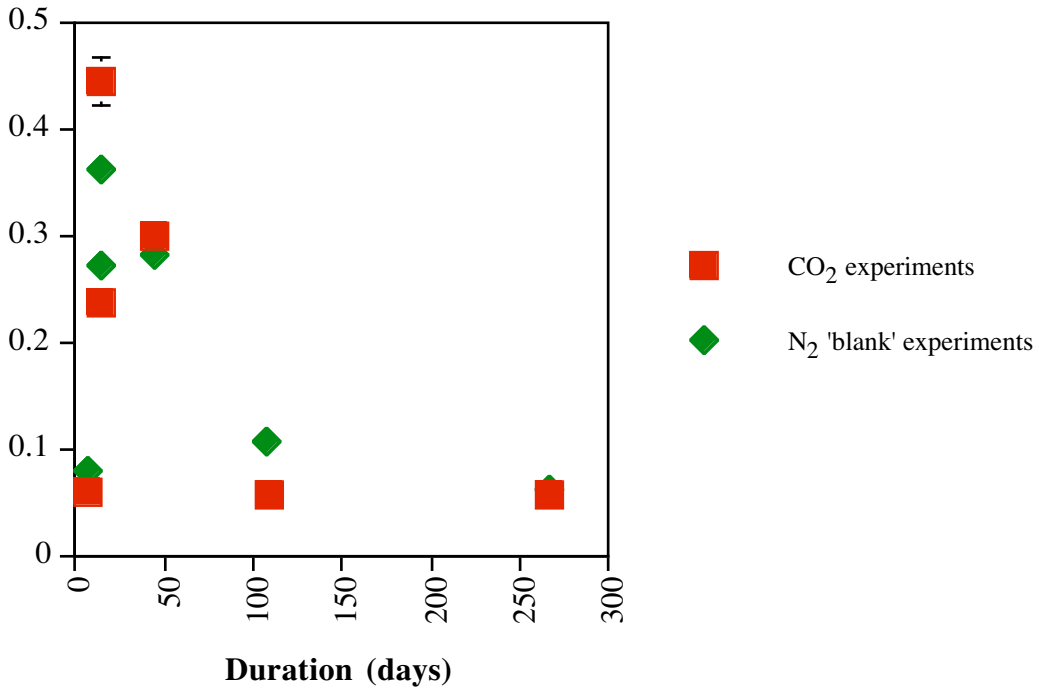


Figure 29 Total S variation over time. Batch reactors, 70°C, 10 MPa.

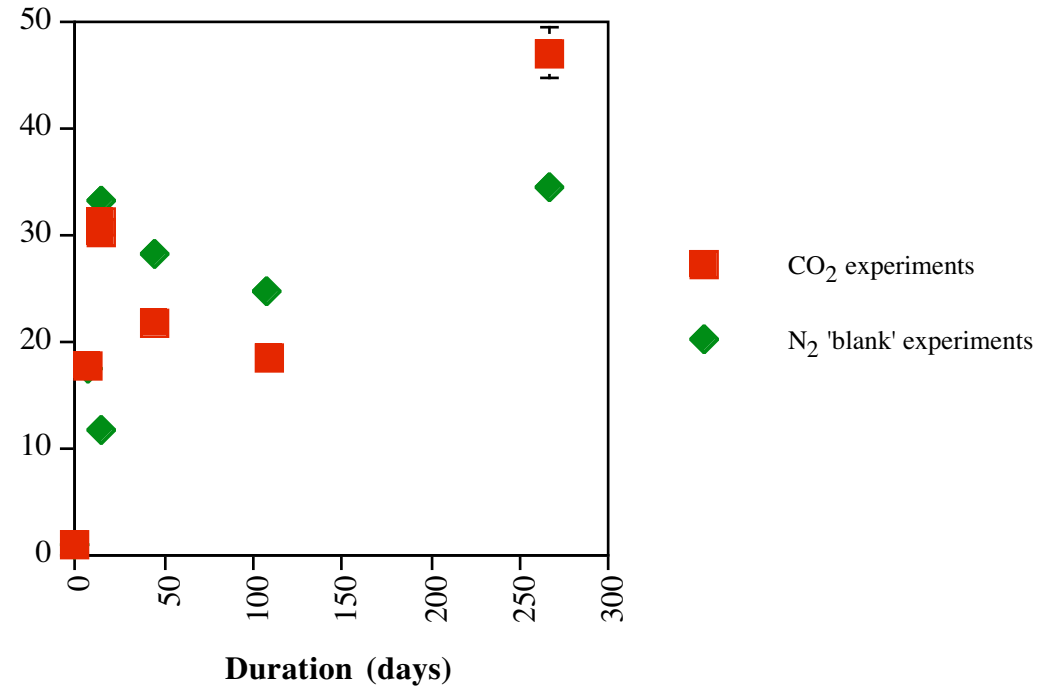

Figure 30 $CO_3^{2-}$ variation over time. Batch reactors, 70°C, 10 MPa.

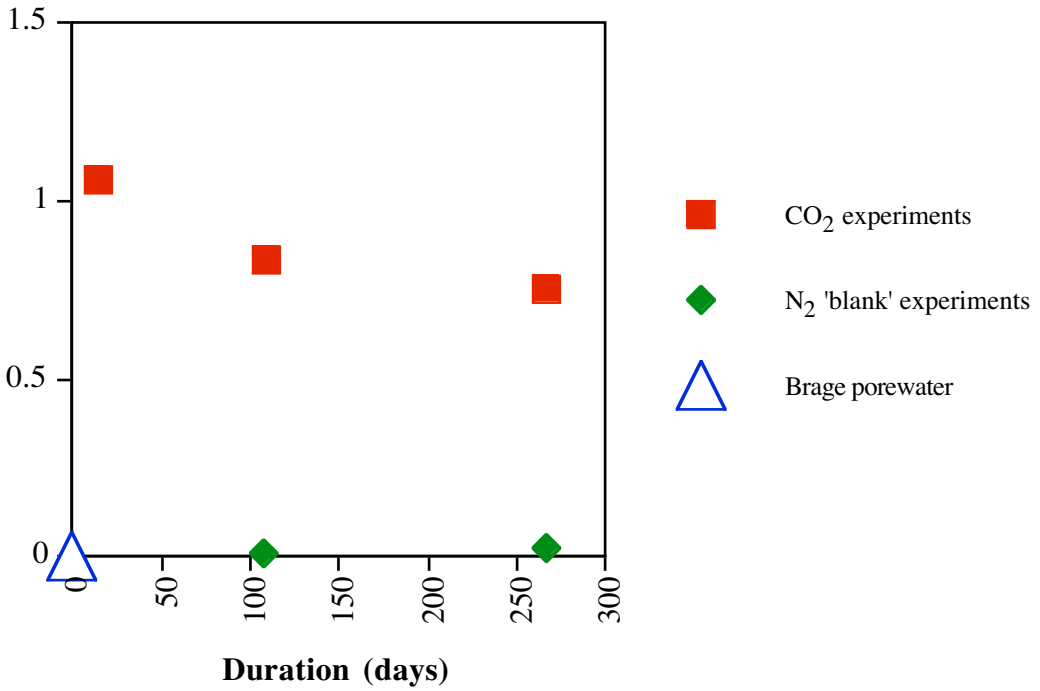


Figure 31 $HCO_3^-$ variation over time. Batch reactors, 70°C, 10 MPa.

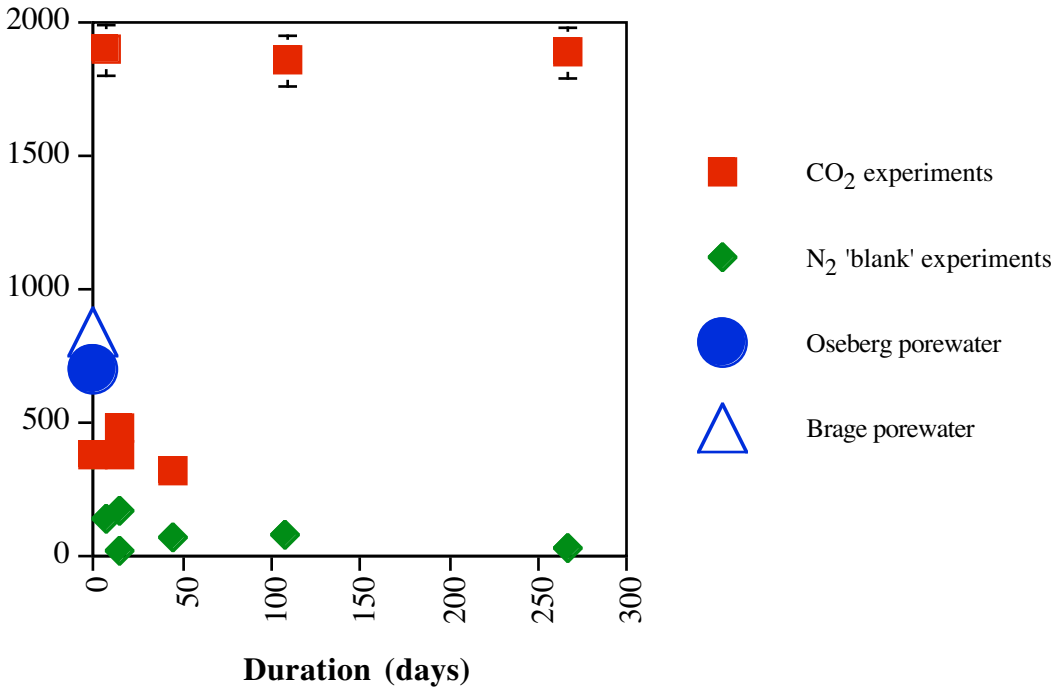

Figure 32 pH variation over time. Batch reactors, 70°C, 10 MPa.

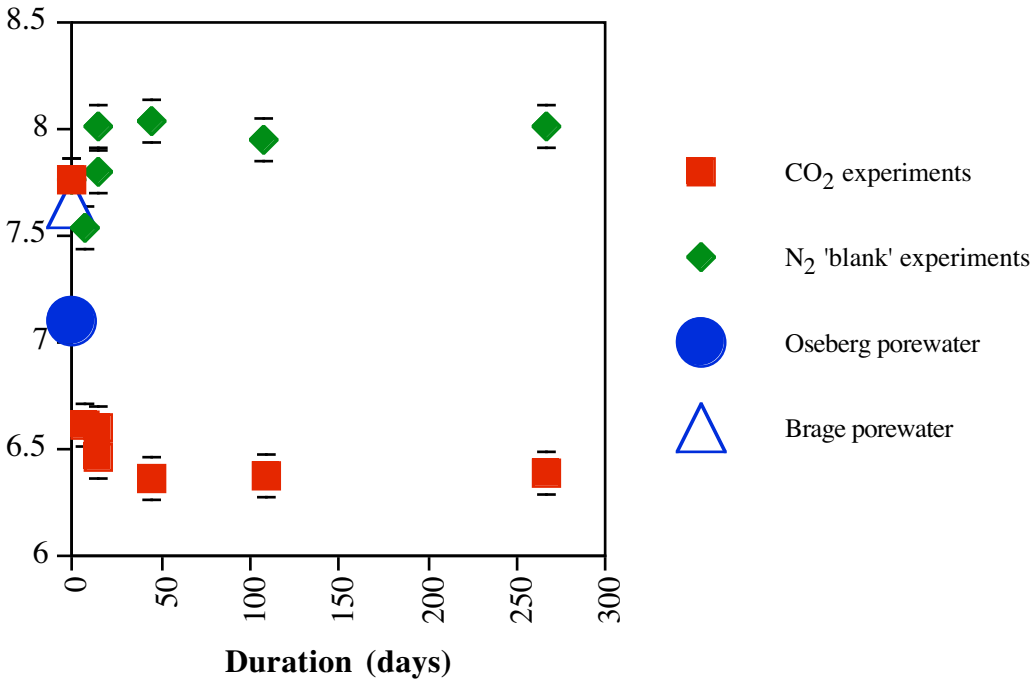


Figure 33 Inlet and outlet pressure variation over time. Column experiment, 70°C, 10 MPa.

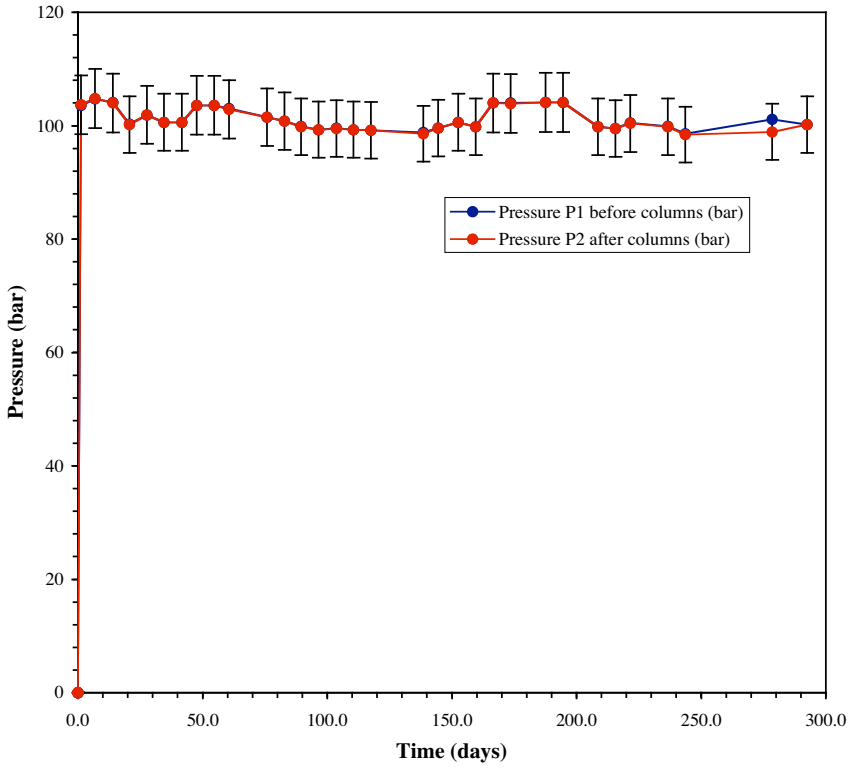

Figure 34 Na and $Cl^-$ variation over time. Column experiment, 70°C, 10 MPa.

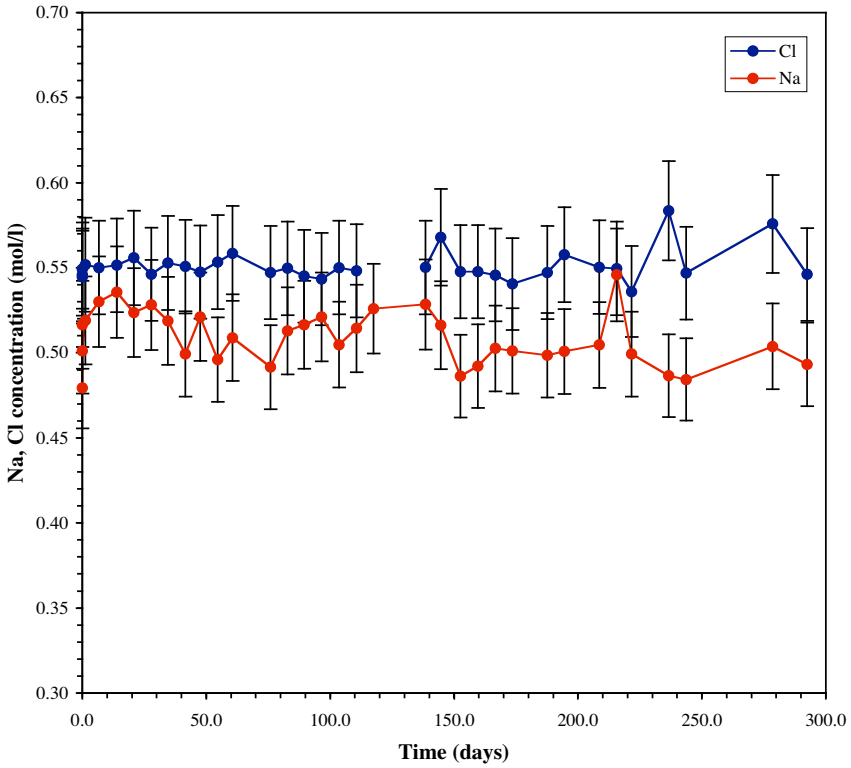


Figure 35 Mg and K variation over time. Column experiment, 70°C, 10 MPa.

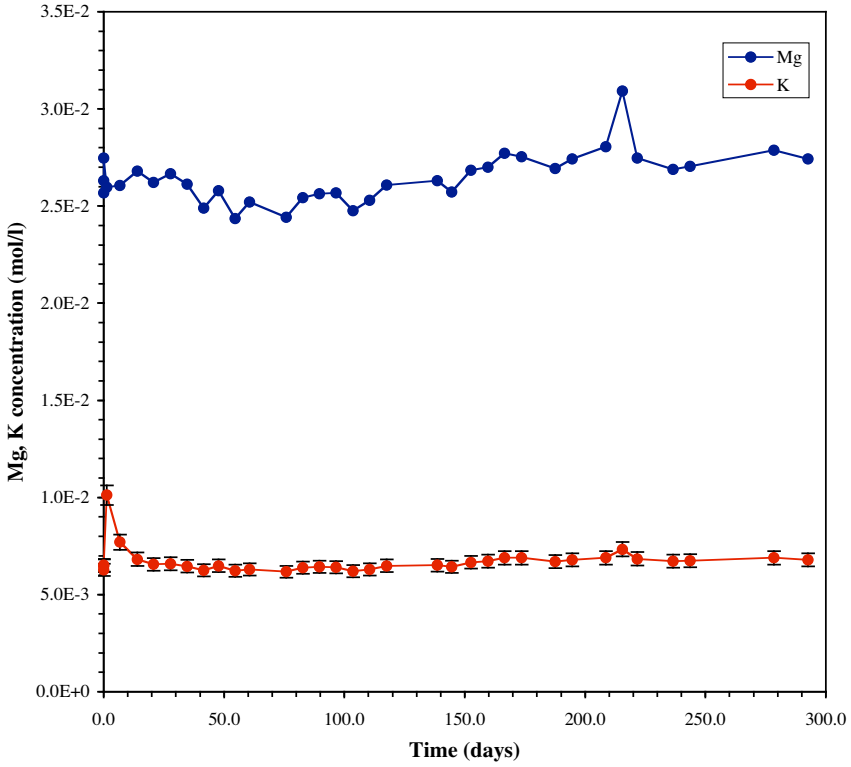

Figure 36 Ca, Ba and Sr variation over time. Column experiment, 70°C, 10 MPa.

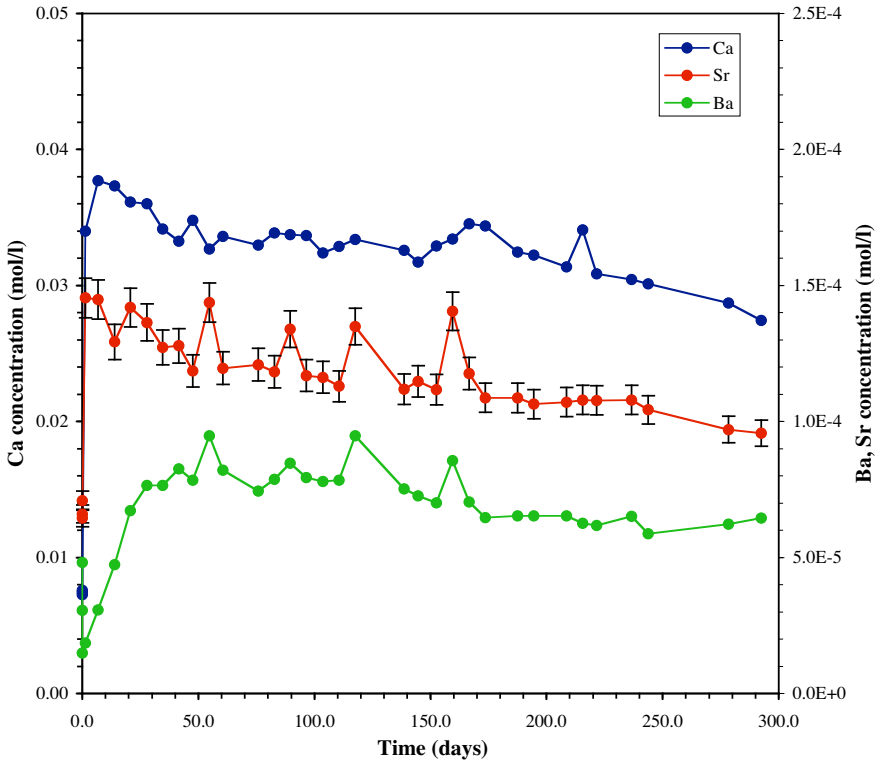


Figure 37 Silica and Al variation over time. Column experiment, 70°C, 10 MPa.

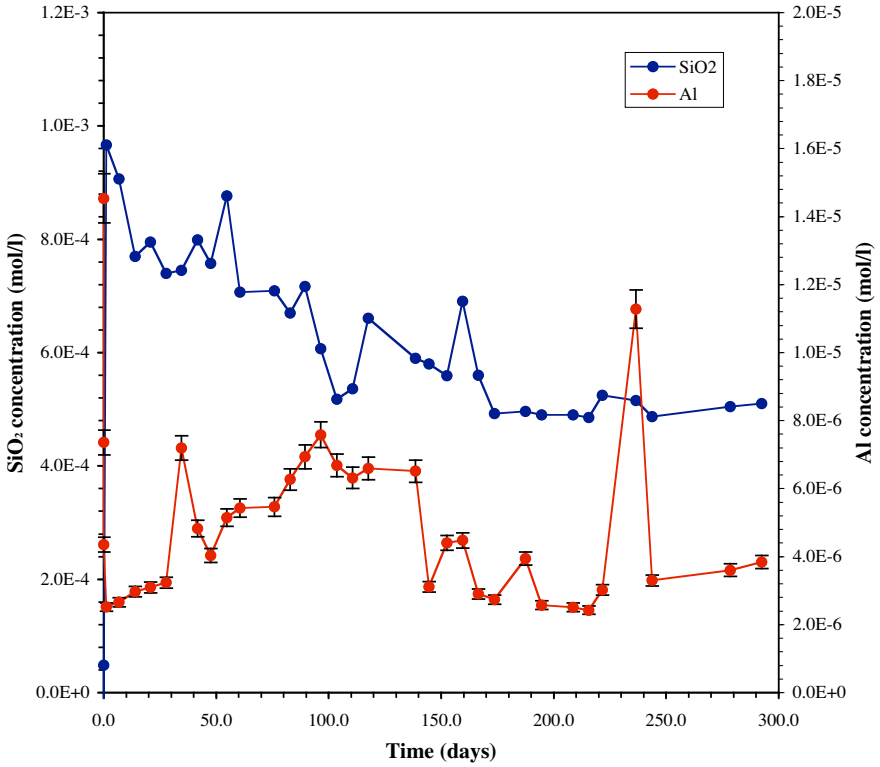

Figure 38 S variation over time. Column experiment, 70°C, 10 MPa.

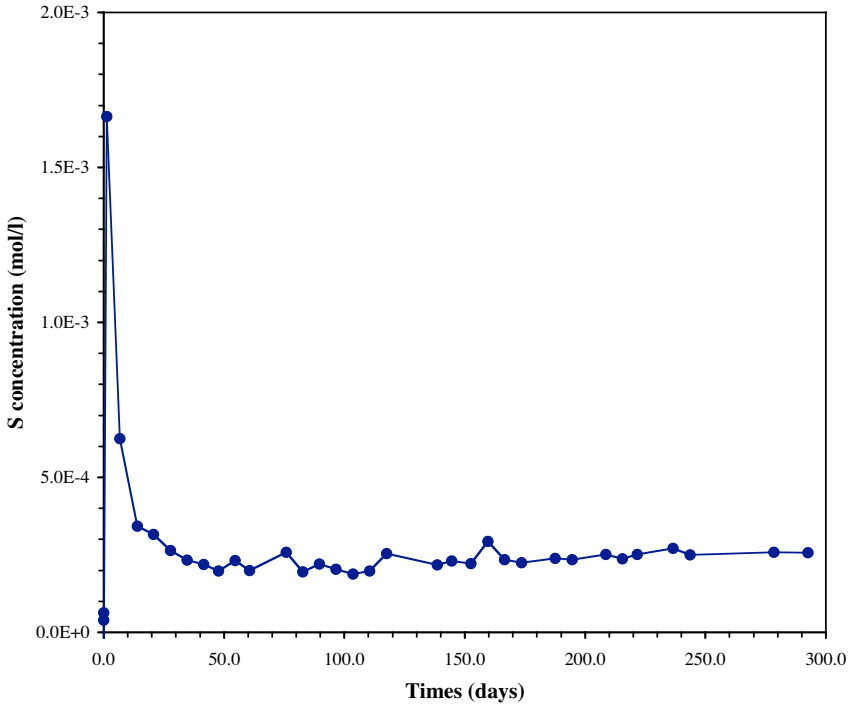


Figure 39 Fe, Mn and Cr variation over time. Column experiment, 70°C, 10 MPa.

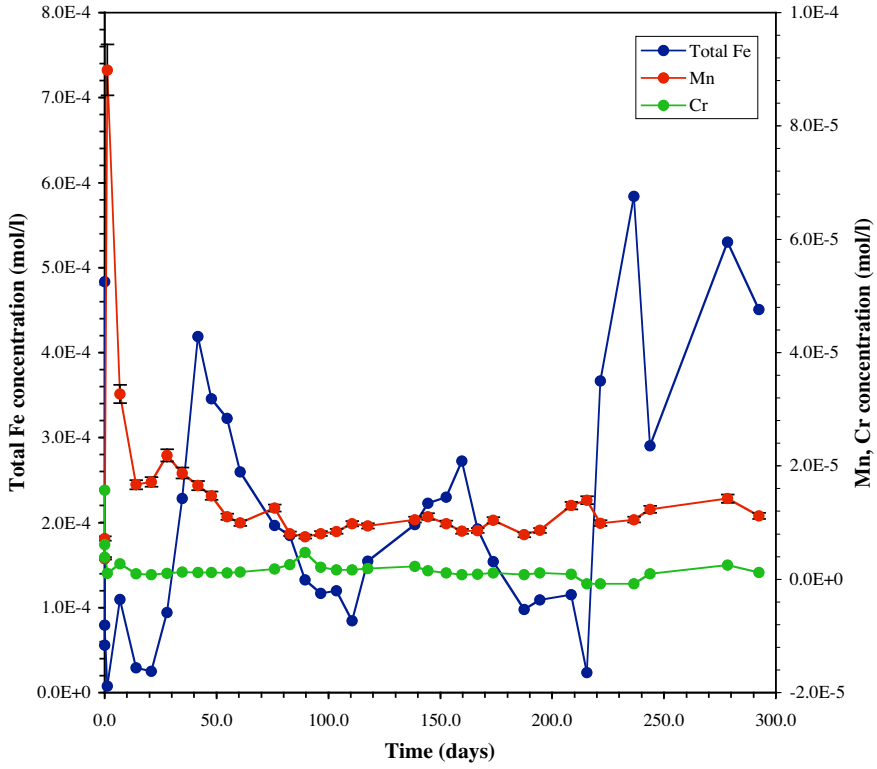

Figure 40 $HCO_3^-$ variation over time. Column experiment, 70°C, 10 MPa.

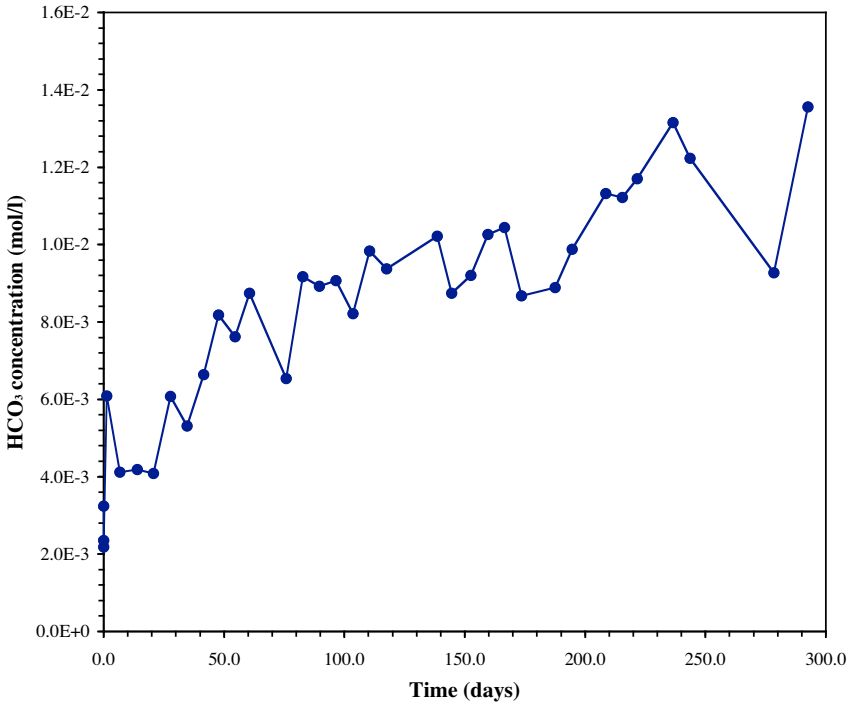


Figure 41 pH variation over time. Column experiment, 70°C, 10 MPa.

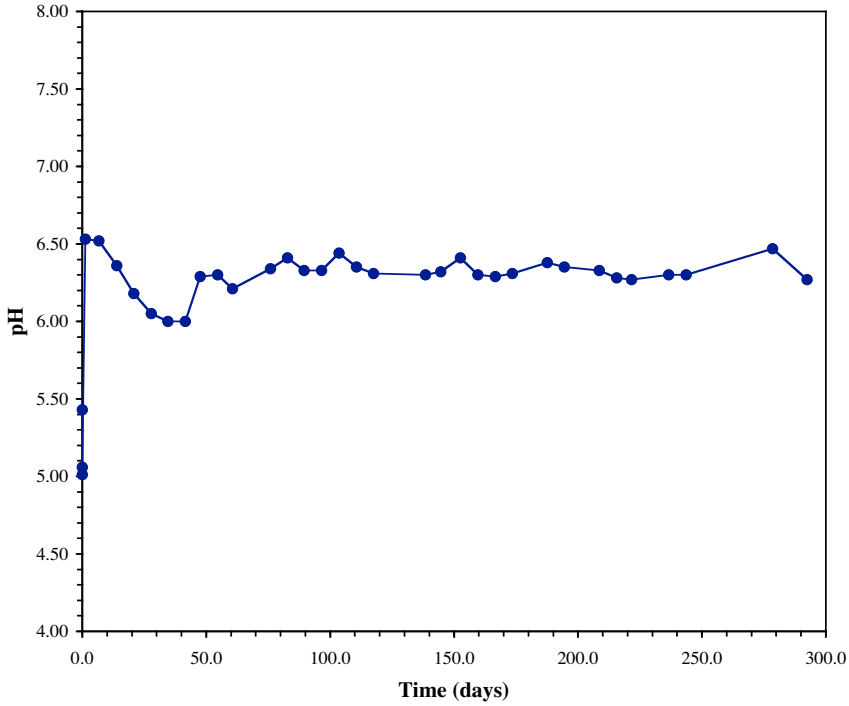

Plate 1 High magnification photomicrograph showing blocky, rhombic Ca-carbonate on lower surface of precipitate from Run 842. Sample G557S2; $CO_2$ experiment, 24 months, 37°C, 10 MPa.

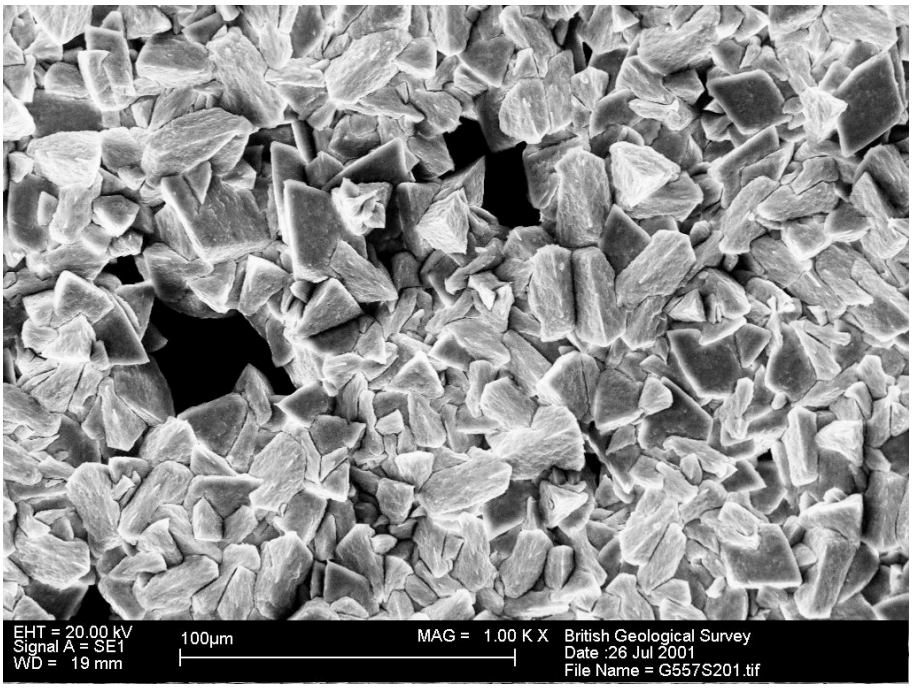


Plate 2 High magnification photomicrograph showing acicular to prismatic Ca-carbonate (possibly aragonite) precipitate on lower surface of precipitate from Run 997. Sample G558S2; $CO_2$ experiment, 1 week, 37°C, 10 MPa. Note that although an interesting precipitate was formed, it was otherwise a 'failed' experiment.

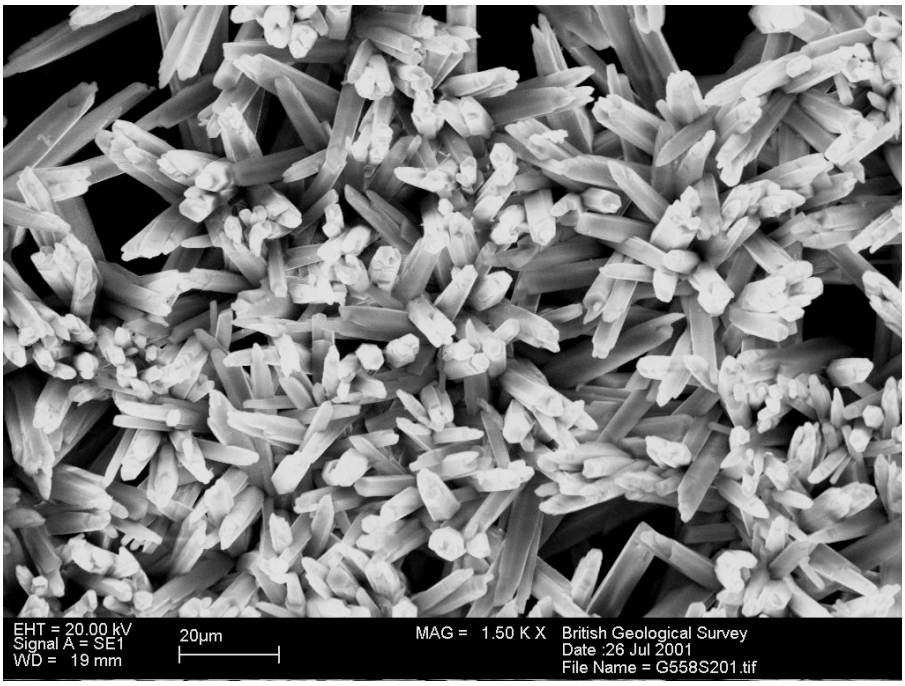

Table 1 Summary of batch experiments undertaken during this study. All used synthetic Utsira porewater (SUP) and were at 10 MPa pressure. Further details can be found in Appendix I.

| Run Number | Temperature (°C) | Duration (days) | Utsira sand (g) | SUP (g) | $CO_2$ or $N_2$ |
|---|---|---|---|---|---|
| 1006 | 37 | 8 | 9.9998 | 99.995 | $CO_2$ |
| 1007 | 37 | 8 | 6.0001 | 59.9961 | $N_2$ |
| 993 | 37 | 19 | 9.9993 | 99.990 | $CO_2$ |
| 994 | 37 | 19 | 6.0009 | 60.0075 | $N_2$ |
| 859 | 37 | 30 | 10.0021 | 100.025 | $CO_2$ |
| 860 | 37 | 30 | 6.0028 | 60.0001 | $N_2$ |
| 838 | 37 | 59 | 10.0032 | 100.015 | $CO_2$ |
| 839 | 37 | 59 | 6.0037 | 60.0261 | $N_2$ |
| 840 | 37 | 96 | 9.9970 | 100.009 | $CO_2$ |
| 841 | 37 | 96 | 5.9973 | 60.0302 | $N_2$ |
| 848 | 37 | 118 | 10.0007 | 100.036 | $CO_2$ |
| 849 | 37 | 118 | 6.0005 | 60.0130 | $N_2$ |
| 846 | 37 | 430 | 10.0001 | 99.995 | $CO_2$ |
| 847 | 37 | 430 | 5.9971 | 60.0069 | $N_2$ |
| 844 | 37 | 654 | 10.0043 | 99.998 | $CO_2$ |
| 845 | 37 | 653 | 5.9982 | 60.0082 | $N_2$ |
| 842 | 37 | 760 | 9.9981 | 99.998 | $CO_2$ |
| 843 | 37 | 760 | 5.9998 | 60.0107 | $N_2$ |
| | | | | | |
| 969 | 70 | 7 | 10.0001 | 100.009 | $CO_2$ |
| 970 | 70 | 7 | 6.0158 | 59.993 | $N_2$ |
| 995 | 70 | 14 | 9.9999 | 99.994 | $CO_2$ |
| 996 | 70 | 14 | 5.9998 | 59.9993 | $N_2$ |
| 973 | 70 | 15 | 10.0007 | 100.014 | $CO_2$ |
| 974 | 70 | 15 | 5.9995 | 60.0252 | $N_2$ |
| 975 | 70 | 45 | 10.0003 | 99.996 | $CO_2$ |
| 976 | 70 | 45 | 6.0003 | 60.0152 | $N_2$ |
| 1001 | 70 | 109 | 10.0000 | 100.001 | $CO_2$ |
| 1002 | 70 | 108 | 5.9999 | 59.9991 | $N_2$ |
| 971 | 70 | 266 | 10.0002 | 100.018 | $CO_2$ |
| 972 | 70 | 267 | 5.9983 | 59.997 | $N_2$ |

Table 2 Modal mineralogical composition of the Utsira sand used in this study (from Pearce et al., 2002).

| Phase | Volumetric % | | Mineral % |
|---|---|---|---|
| | (Average) | Standard deviation | (Average) |
| Quartz | 44.19 | 2.410 | 76.36 |
| K-feldspar | 4.01 | 1.268 | 6.92 |
| Plagioclase | 1.74 | 0.228 | 3.00 |
| Chlorite | 0.77 | 0.217 | 1.33 |
| Mica | 3.02 | 0.877 | 5.22 |
| Zeolite | 0.13 | 0.088 | 0.22 |
| Calcite | 3.90 | 0.707 | 6.73 |
| Ti Oxides | 0.02 | 0.031 | 0.04 |
| Apatite | 0.01 | 0.004 | 0.00 |
| Illmenite | 0.07 | 0.038 | 0.11 |
| Pyrite | 0.03 | 0.014 | 0.05 |
| Porosity | 41.99 | 0.834 | - |

Approx. 1300 grains analysed

Table 3 Recipe for synthetic Utsira porewater (SUP). Weights given for a 25 l volume of SUP.

| Component | Supplier | Grade type | Manufacturers quoted purity | Weight (g) |
|---|---|---|---|---|
| NaCl | BDH | ARISTAR | 99.5% min. assay | 646.6897 |
| KCl | BDH | ARISTAR | 99.5% min. assay | 9.9146 |
| $CaCl_2.2H_2O$ | BDH | AnalaR | 99.5% min. assay | 39.0669 |
| $MgCl_2.6H_2O$ | Fisher Chemicals | - | 99.08% assay | 131.732 |
| $SrCl_2.6H_2O$ | BDH | AnalaR | 98.5% min. assay | 0.7608 |
| $BaCl_2.2H_2O$ | BDH | AnalaR | 99% assay | 0.0227 |
| $FeCl_3.6H_2O$ | BDH | AnalaR | 100.89% assay | 0.2420 |
| $NaHCO_3$ | BDH | AnalaR | 99.5% min. assay | 19.7003 |

Table 4 Analytes and errors.

| Analyte | Detection limits (instrument)# (mg $l^{-1}$) | Detection limits (typical) # mg $l^{-1}$ | mol $l^{-1}$ | Typical percentage ± uncertainty † |
|---|---|---|---|---|
| Li | 0.025 | 0.5 | $7.2 \times 10^{-5}$ | 10 |
| Na | 0.35 | 7 | $3.0 \times 10^{-4}$ | <5 |
| K | 0.5 | 10 | $2.6 \times 10^{-4}$ | <5 |
| Mg | 0.01 | 0.2 | $8.2 \times 10^{-6}$ | <5 |
| Ca | 0.1 | 2 | $5.0 \times 10^{-5}$ | <5 |
| Sr | 0.002 | 0.04 | $4.6 \times 10^{-7}$ | <5 |
| Ba | 0.002 | 0.04 | $2.9 \times 10^{-7}$ | <5 |
| Mn | 0.002 | 0.02 | $3.6 \times 10^{-7}$ | 5-10 |
| Total Fe | 0.01 | 0.2 | $3.6 \times 10^{-7}$ | 5-10 |
| Cr | 0.002 | 0.04 | $7.7 \times 10^{-7}$ | 10 |
| Al | 0.01 | 0.1 | $3.7 \times 10^{-6}$ | 10 |
| Total P | 0.01 | 0.1 | $3.2 \times 10^{-6}$ | N/A |
| Total S | 0.25 | 2.5 | $7.8 \times 10^{-5}$ | 5-10 |
| Si | 0.075 | 0.75 | $2.7 \times 10^{-5}$ | 5-10 |
| $SiO_2$ | 0.16 | 1.6 | $2.7 \times 10^{-5}$ | 5-10 |
| $Cl^-$ | 0.1 | 2 | $5.6 \times 10^{-5}$ | <5 |
| $Br^-$ | 0.03 | 6 | $7.5 \times 10^{-5}$ | 5 |
| $NO_3^-$ | 0.04 | 0.8 | $1.3 \times 10^{-5}$ | 5-10 |
| $SO_4^{2-}$ | 0.3 | 60 | $6.3 \times 10^{-4}$ | 10 |
| $HCO_3^-$ | 22 | 22 | $3.6 \times 10^{-4}$ | 5 |
| $CO_3^{2-}$ | 22 | 22 | $3.6 \times 10^{-4}$ | <5 |
| TOC | 1 | 3.6 | $3.0 \times 10^{-4}$ | N/A |

# Limits of quantification can be described in more than one way. Firstly there is the actual instrument limit for an 'ideal' dilute solution. However, more concentrated solutions (such as the synthetic Utsira porewater) have to be diluted prior to analysis as high concentrations of total dissolved solids cause analytical problems. Dilution causes an effective worsening of the detection limits. During this study, samples were typically diluted 10x or 20x prior to analysis.

† Illustrative uncertainties considered 'typical' for the concentration ranges found in this study. Concentrations <10x the detection limit have uncertainties ≥10%, concentrations >10x the detection limit have uncertainties typically ≤5%.

NA Not applicable, as element was below the detection limit.

# Appendix I

## FLUID CHEMICAL ANALYTICAL DATA FROM THE BATCH EXPERIMENTS

## BGS EXPERIMENTS - STARTING SOLUTIONS

| | | OSEBERG | BRAGE | SUP | | | SUP | SUP | | | | |
|---|---|---|---|---|---|---|---|---|---|---|---|---|
| | | Oseberg composition from Task 0 report | Average of analyses conducted at BGS | Synthetic Utsira Porewater - starting solution Initial composition at make up (29/7/99) SUP for expts § | E641A / SUP § | E642 / SUP § | Synthetic Utsira Porewater starting solution (Average of 'E641A / SUP' E642 / SUP' and 'SUP for expts') | Synthetic Utsira Porewater - stock solution held in lab (at about 20°C). Batch made on 29/7/99 Compositional variation over time | | | | |
| Sampling date | | | | | | | | 14/10/99 § | 11/11/99 | 18/12/00 | 4/5/01 | 5/9/01 |
| Age of SUP | | | | 0 days | 0 days | 0 days | 0 days | 77 days | 105 days | 508 days | 645 days | 769 days |
| Main LIMS number | | | 06678-00001 | 06423-00017 | 06423-00007 | 06423-00014 | - | 06423-00018 | 06448-00005 | 06859-00001 | 10001-00001 | 10104-00001 |
| pH (≈ 20 °C) | | 7.1 | 7.65 | 7.72 | 7.77 | 7.83 | 7.77 | 7.72 | 7.92 | 7.98 | 7.90 | 8.17 |
| Li | mg/l | - | 1.77 | - | - | - | - | - | - | - | - | - |
| Na | mg/l | 10392 | 9934 | 10502 | 9829 | 10588 | 10306 | 9179 | 10682 | 11119 | 11388 | 11389 |
| K | mg/l | 208 | 317 | 226 | 228 | 220 | 225 | 241 | 220 | 232 | 241 | 255 |
| Mg | mg/l | 630 | 664 | 646 | 614 | 639 | 633 | 586 | 640 | 611 | 607 | 625 |
| Ca | mg/l | 426 | 412 | 440 | 429 | 428 | 432 | 334 | 347 | 307 | 281 | 269 |
| Sr | mg/l | 10 | 9.65 | 10.2 | 9.62 | 10.3 | 10.0 | 7.52 | 8.10 | 6.05 | 5.61 | 5.48 |
| Ba | mg/l | 0.5 | 6.17 | 0.32 | 0.42 | 0.20 | 0.31 | 1.10 | 1.82 | 0.38 | 0.38 | 0.395 |
| Mn | mg/l | - | <0.02 | - | - | - | - | - | - | - | 0.05 | <0.040 |
| Total Fe | mg/l | 2 | 0.28 | 1.50 | <0.2 | 2.12 | 1.21 | 1.98 | 11.5 | 0.53 | 0.27 | <0.20 |
| Cr | mg/l | - | - | - | - | - | - | - | - | - | <0.04 | <0.040 |
| Al | mg/l | - | <0.1 | 0.06 | 0.54 | 0.44 | 0.35 | 0.05 | 7.00 | 0.10 | 0.38 | 0.04 |
| Total P | mg/l | - | <0.1 | - | - | - | - | - | - | - | - | - |
| Total S | mg/l | - | <2.5 | 1.18 | 1.34 | 0.62 | 1.05 | <1.0 | 1.55 | <5.0 | <5.00 | <7.00 |
| Si | mg/l | - | 23.7 | <1.50 | 0.58 | 0.58 | 0.58 | <1.50 | <0.30 | <1.5 | <1.50 | <1.5 |
| $SiO_2$ | mg/l | - | 50.7 | <3.21 | 1.23 | 1.23 | 1.23 | <3.21 | <0.64 | <3.2 | <3.21 | <3.21 |
| Cl | mg/l | 18482 | 18921 | 18589 | 18679 | 18709 | 18659 | 18575 | 18650 | 18811 | 18388 | 18772 |
| Br | mg/l | - | 71.5 | <6 | <6 | <6 | <2.00 | <6.0 | <6.0 | <7.5 | <6.00 | <6.00 |
| $NO_3$ | mg/l | - | 8.40 | - | - | - | - | - | - | - | - | - |
| $SO_4$ | mg/l | ND | <60 | <60 | <3 | <60 | <2.00 | <60 | <60 | <75 | <60.0 | <60.0 |
| $HCO_3$ * | mg/l | 707 | 842 | 395 | 388 | 374 | 386 | 334 | 285 | 203 | 115 | 86.0 |
| Ionic balance | % | - | -3.07 | 0.67 | -2.67 | 0.62 | - | -5.78 | 1.03 | 1.97 | 4.15 | 3.28 |
| TIC ($CO_3^{2-}$) | mol/l | - | 0.0030 | - | - | - | - | - | - | - | - | |
| TOC | mol/l | | <0.0003 | - | - | - | - | - | - | - | - | |

LIMS = Laboratory Information Management System
ND = Not detected
* = Analyses done several days after sampling so be aware of possible decreases over time due to loss of $CO_2$ to the atmosphere. Alkalinity measurements by potentiometric titration.
§ = Si and Al specially re-analysed on 1/10/01 with improved background corrections. This was done after the preserved samples had been in store for over a year.

## INFORMATION FROM BGS BATCH EXPERIMENTS AT 37°C

| | | OSEBERG | BRAGE | SUP | 1 WEEK REACTION | | 1 WEEK REACTION | | 3 WEEKS REACTION | | 1 MONTH REACTION | | 2 MONTHS REACTION | | 3 MONTHS REACTION | | 4 MONTHS REACTION | | 14 MONTHS REACTION | | 21 MONTHS REACTION | | 24 MONTHS REACTION | |
|---|---|---|---|---|---|---|---|---|---|---|---|---|---|---|---|---|---|---|---|---|---|---|---|---|
| | | Oseberg composition from Task 0 report | Average of analyses conducted at BGS | Synthetic Utsira Porewater starting solution (Average of 'E641A / SUP' E642 / SUP' and 'SUP for expts') | Run 997 $CO_2$ expt 10 MPa $CO_2$ | Run 998 Blank 10 MPa $N_2$ | Run 1006 $CO_2$ expt 10 MPa $CO_2$ | Run 1007 Blank 10 MPa $N_2$ | Run 993 $CO_2$ expt 10 MPa $CO_2$ | Run 994 Blank 10 MPa $N_2$ | Run 859 $CO_2$ expt 10 MPa $CO_2$ | Run 860 Blank 10 MPa $N_2$ | Run 838 § $CO_2$ expt 10 MPa $CO_2$ | Run 839 § Blank 10 MPa $N_2$ | Run 840 $CO_2$ expt 10 MPa $CO_2$ | Run 841 Blank 10 MPa $N_2$ | Run 848 * § $CO_2$ expt 10 MPa $CO_2$ | Run 849 § Blank 10 MPa $N_2$ | Run 846 ** § $CO_2$ expt 10 MPa $CO_2$ | Run 847 ** § Blank 10 MPa $N_2$ | Run 844 $CO_2$ expt 10 MPa $CO_2$ | Run 845 Blank 10 MPa $N_2$ | Run 842 $CO_2$ expt 10 MPa $CO_2$ | Run 843 Blank 10 MPa $N_2$ |
| Start date | | | | | 14/5/01 | 14/5/01 | 30/5/01 | 30/5/01 | 19/4/01 | 19/4/01 | 5/10/99 | 5/10/99 | 6/8/99 | 6/8/99 | 6/8/99 | 6/8/99 | 6/8/99 | 6/8/99 | 6/8/99 | 6/8/99 | 6/8/99 | 6/8/99 | 6/8/99 | 6/8/99 |
| End date | | | | | 21/5/01 | 21/5/01 | 7/6/01 | 7/6/01 | 8/5/02 | 8/5/02 | 4/11/99 | 4/11/99 | 4/10/99 | 4/10/99 | 10/11/99 | 10/11/99 | 3/12/99 | 3/12/99 | 9/10/00 | 9/10/00 | 11/5/01 | 10/5/01 | 4/9/01 | 4/9/01 |
| Exact duration | | | | 0 days | Failed runs | | 8 days | 8 days | 19 days | 19 days | 30 days | 30 days | 59 days | 59 days | 96 days | 96 days | 118 days | 118 days | 430 days | 430 days | 654 days | 653 days | 760 days | 760 days |
| Main LIMS number | | - | 06678-00001 | - | 10001-00019 | 10001-00020 | 10001-00022 | 10001-00024 | 10001-00011 | 10001-00013 | 06448-00003 | 06448-00004 | 06423-00016# | 06423-00015# | 06448-00001 | 06448-00002 | 06784-00003 | 06784-00004 | 06784-00001 | 06784-00002 | 10001-00003 | 10001-00005 | 10104-00003 | 10104-00005 |
| pH (@ 20 °C) | | 7.1 | 7.65 | 7.77 | | | 6.46 | 7.11 | 6.55 | 7.08 | 6.62 | 7.82 | 6.68 | 8.03 | 6.43 | 7.82 | 6.53 | 7.53 | 6.62 †† | 8.03 †† | 6.51 | 7.84 | 6.43 | 7.46 |
| pH (in-situ) | | | | | | | | | | | | | | | | | | | | | | | 4.35 ## | 4.40 ## |
| Li | mg/l | | 1.77 | | - | - | - | - | - | - | - | - | - | - | - | - | - | - | - | - | - | - | - | - |
| Na | mg/l | 10392 | 9934 | 10306 | 10936 | 10416 | 10314 | 10215 | 10499 | 10293 | 9326 | 9400 | 10438 | 9979 | 10226 | 10528 | 10774 | 11071 | 10798 | 10662 | 11434 | 11387 | 11860 | 11133 |
| K | mg/l | 208 | 317 | 225 | 274 | 270 | 266 | 280 | 273 | 282 | 228 | 226 | 277 | 251 | 240 | 239 | 277 | 276 | 272 | 262 | 281 | 256 | 297 | 275 |
| Mg | mg/l | 630 | 664 | 633 | 619 | 628 | 598 | 650 | 613 | 659 | 580 | 578 | 659 | 622 | 625 | 629 | 594 | 608 | 582 | 573 | 619 | 589 | 645 | 606 |
| Ca | mg/l | 426 | 412 | 432 | 925 | 299 | 1653 | 311 | 1779 | 314 | 1577 | 332 | 1817 | 372 | 1840 | 376 | 1774 | 323 | 1505 | 288 | 1685 | 307 | 1709 | 299 |
| Sr | mg/l | 10 | 9.65 | 10.0 | 8.05 | 6.09 | 11.4 | 6.32 | 12.1 | 6.40 | 13.6 | 7.84 | 17.1 | 9.16 | 16.7 | 9.29 | 15.0 | 7.68 | 14.3 | 7.02 | 15.4 | 7.04 | 16.2 | 7.29 |
| Ba | mg/l | 0.5 | 6.17 | 0.31 | 2.97 | 4.32 | 2.44 | 4.98 | 2.29 | 4.89 | 2.12 | 4.22 | 2.78 | 3.80 | 2.44 | 3.70 | 2.11 | 3.59 | 1.14 | 3.11 | 1.01 | 2.35 | 0.972 | 2.63 |
| Mn | mg/l | - | <0.02 | - | 1.16 | 0.22 | 1.57 | 0.23 | 2.06 | 0.27 | - | - | - | - | - | - | - | - | - | - | 2.37 | 0.234 | 2.23 | 0.228 |
| Total Fe | mg/l | 2 | 0.28 | 1.21 | 0.30 | 0.29 | 0.65 | 0.30 | 1.81 | 0.30 | 0.71 | 1.41 | 6.48 | 0.40 | 5.72 | 9.07 | 1.10 | 0.545 | 2.33 | 0.538 | 1.59 | 0.266 | 0.25 | <0.20 |
| Cr | mg/l | - | - | - | <0.04 | <0.04 | <0.04 | <0.04 | <0.04 | <0.04 | - | - | - | - | - | - | - | - | - | - | <0.04 | <0.04 | <0.04 | <0.04 |
| Al | mg/l | - | <0.1 | 0.35 | 0.37 | 0.39 | 0.50 | 0.37 | 0.41 | 0.30 | <2.00 | <2.00 | 0.57 | 0.46 | <2.00 | 1.94 | 1.43 | 0.27 | 0.33 | 0.73 | 0.39 | 0.29 | 0.100 | 0.042 |
| Total P | mg/l | - | <0.1 | - | - | - | - | - | - | - | - | - | - | - | - | - | - | - | - | - | - | - | - | - |
| Total S | mg/l | - | <2.5 | 1.05 | 13.5 | 10.4 | 17.8 | 10.8 | 22.0 | 11.5 | 23.3 | 11.2 | 33.2 | 15.3 | 34.1 | 16.9 | 38.5 | 16.0 | 38.4 | 17.7 | 50.3 | 23.9 | 64.2 | 24.1 |
| Si | mg/l | - | 23.7 | 0.58 | 3.11 | 2.12 | 3.46 | 2.11 | 4.07 | 2.35 | 2.36 | 0.87 | 4.95 | 3.30 | 3.23 | 0.87 | 6.33 | 3.5 | 9.31 | 4.22 | 10.2 | 3.94 | 12.4 | 5.01 |
| $SiO_2$ | mg/l | - | 50.7 | 1.23 | 6.64 | 4.53 | 7.40 | 4.51 | 8.70 | 5.03 | 5.06 | 1.86 | 10.59 | 7.06 | 6.91 | 1.86 | 13.54 | 7.49 | 19.92 | 9.03 | 21.8 | 8.42 | 26.6 | 10.7 |
| Cl | mg/l | 18482 | 18921 | 18659 | 19099 | 18600 | 18266 | 18277 | 18453 | 18698 | 18166 | 17952 | 18849 | 18549 | 18556 | 18621 | 17230 | 17489 | 18510 | 17681 | 18737 | 18317 | 18974 | 18773 |
| Br | mg/l | - | 71.5 | <2.00 | <6.00 | <6.00 | <6.00 | <6.00 | <6.00 | <6.00 | <2.00 | <6.00 | <6.00 | <6.00 | <6.00 | <6.00 | <7.5 | <7.5 | <7.5 | <7.5 | <6.00 | <6.00 | <6.00 | <6.00 |
| $NO_3$ | mg/l | - | 8.40 | - | - | - | - | - | - | - | - | - | - | - | - | - | - | - | - | - | - | - | - | - |
| $SO_4$ | mg/l | ND | <60 | <2.00 | <60.0 | <60.0 | <60.0 | <60.0 | <60.0 | <60.0 | <2.00 | <60.00 | 66.8 | <60.0 | 68.2 | <60.00 | <75 | <75 | 96.0 | <75 | <60.0 | <60.0 | <60.0 | <60.0 |
| $HCO_3$ *** | mg/l | 707 | 842 | 386 | 1360 | 132 | 2500 | 119 | 935 | 114 | 3102 | 300 | 1558 | 368 | 4423 | 349 | 232 | - | 1461 | 129 | 1062 | 123 | 1491 | 90 |
| Ionic balance | % | - | -3.07 | - | 1.67 | 0.00 | 2.74 | 0.31 | 5.93 | <0.39 | -2.27 | -3.25 | 4.20 | -1.77 | -0.20 | 0.43 | 11.23 | 5.89 | 4.54 | 3.06 | 7.94 | 4.35 | 8.40 | 2.32 |
| TIC ($CO_2^2$) † | mol/l | - | 0.0030 | - | - | 0.00883 | 1.03 | 0.0143 | 1.19 | 0.0222 | 0.562 ? | 0.074 | 1.04 | 0.0946 | 0.466 ? | 0.0235 | 0.648 ? | 0.00864 | - | 0.0254 | 1.10 | 0.0285 | 1.01 | 0.011 |
| TOC | mol/l | - | <0.0003 | - | - | - | - | - | - | - | - | - | - | - | - | - | - | - | - | - | - | - | - | - |

LIMS = Laboratory Information Management System
ND = Not detected
BD = Below detection
* = Sample valve blocked. Had to sample on its side through $CO_2$ valve. NaOH sample could be low on $CO_2$ due to pressure dropping during sampling.
** = Run 846 sample valve blocked. This time depressurised the entire experiments *before* sampling any fluids. Same procedure applied to Run 847.
*** = Analyses done several days after sampling so be aware of possible decreases over time due to loss of $CO_2$ to the atmosphere Alkalinity measurements by potentiometric titration.
† = $CO_2$-rich solutions captured in 4M NaOH whilst at 10 Mpa pressure. Potentiometric titrations represent total inorganic carbon (i.e. $CO_2$, $H_2CO_3$, $HCO_3^-$, $CO_3^{2-}$ etc).
†† = Only 2 point pH calibration rather than the usual 3 point calibration.
# = LIMS numbers transposed during analysis
## = 'Experimental' method employed to generate this data - treat with caution
§ = Si and Al specially re-analysed on 1/10/01 with improved background corrections. For samples from Runs 838 and 839, this was done after the preserved samples had been in store for over a year.
? = Measured concentrations appear lower than expected.

## INFORMATION FROM BGS BATCH EXPERIMENTS AT 70°C

| | | OSEBERG | BRAGE | SUP | 1 WEEK REACTION | | 2 WEEKS REACTION | | 2 WEEKS REACTION | | 1.5 MONTHS REACTION | | 3.5 MONTHS REACTION | | 9 MONTHS REACTION | |
|---|---|---|---|---|---|---|---|---|---|---|---|---|---|---|---|---|
| | | Oseberg composition from Task 0 report | Average of analyses conducted at BGS | Synthetic Utsira Porewater starting solution (Average of 'E641A / SUP' E642 / SUP' and 'SUP for expts') | Run 969 $CO_2$ expt 10 MPa $CO_2$ | Run 970 Blank 10 MPa $N_2$ | Run 995 $CO_2$ expt 10 MPa $CO_2$ | Run 996 Blank 10 MPa $N_2$ | Run 973 $CO_2$ expt 10 MPa $CO_2$ | Run 974 Blank 10 MPa $N_2$ | Run 975 $CO_2$ expt 10 MPa $CO_2$ | Run 976 Blank 10 MPa $N_2$ | Run 1001 $CO_2$ expt 10 MPa $CO_2$ | Run 1002 Blank 10 MPa $N_2$ | Run 971 $CO_2$ expt 10 MPa $CO_2$ | Run 972 Blank 10 MPa $N_2$ |
| Start date | | | | | 11/12/00 | 11/12/00 | 20/4/01 | 20/4/01 | 15/12/00 | 15/12/00 | 18/12/00 | 18/12/00 | 14/5/01 | 14/5/01 | 11/12/00 | 11/12/00 |
| End date | | | | | 18/12/00 | 18/12/00 | 3/5/01 | 4/5/01 | 30/1/01 | 30/1/01 | 1/2/01 | 1/2/01 | 31/8/01 | 30/8/01 | 3/9/01 | 4/9/01 |
| Exact duration | | | | 0 days | 7 days | 7 days | 14 days | 14 days | 15 days | 15 days | 45 days | 45 days | 109 days | 108 days | 266 days | 267 days |
| Main LIMS number | | | 06678-00001 | - | 06859-00002 | 06859-00003 | 10001-00015 | 10001-00018 | 10001-00007 | 10001-00008 | 10001-00009 | 10001-00010 | 10104-00011 | 10104-00013 | 10104-00007 | 10104-00009 |
| pH (≈ 20 °C) | | 7.1 | 7.65 | 7.77 | 6.62 | 7.54 | 6.60 | 7.80 | 6.46 | 8.01 | 6.36 | 8.04 | 6.38 | 7.95 | 6.39 | 8.02 |
| pH (in-situ) | | | | | | | | | | | | | | | 4.40 # | 4.50 # |
| Li | mg/l | - | 1.77 | - | - | - | - | - | - | - | - | - | - | - | - | - |
| Na | mg/l | 10392 | 9934 | 10306 | 11181 | 11326 | 10327 | 16752 | 11457 | 11488 | 11455 | 10690 | 11632 | 11419 | 12909 | 12186 |
| K | mg/l | 208 | 317 | 225 | 264 | 264 | 317 | 439 | 275 | 267 | 283 | 262 | 295 | 286 | 327 | 310 |
| Mg | mg/l | 630 | 664 | 633 | 608 | 625 | 709 | 950 | 618 | 611 | 635 | 603 | 1417 | 612 | 693 | 500 |
| Ca | mg/l | 426 | 412 | 432 | 892 | 320 | 1221 | 484 | 1439 | 313 | 693 | 312 | 634 | 319 | 1445 | 577 |
| Sr | mg/l | 10 | 9.65 | 10.0 | 8.7 | 6.58 | 12.2 | 9.89 | 11.9 | 6.58 | 8.86 | 6.60 | 11.7 | 6.50 | 13.6 | 8.71 |
| Ba | mg/l | 0.5 | 6.17 | 0.31 | 2.8 | 4.94 | 4.28 | 7.05 | 1.82 | 3.88 | 3.75 | 3.33 | 5.75 | 4.28 | 2.14 | 3.52 |
| Mn | mg/l | - | <0.02 | - | - | - | 1.95 | 0.10 | 1.48 | 0.26 | 0.35 | 0.45 | 2.30 | 0.984 | 2.38 | 0.218 |
| Total Fe | mg/l | 2 | 0.28 | 1.21 | 1.46 | 0.58 | 0.53 | 0.37 | 0.34 | 0.25 | 0.27 | 0.29 | 6.92 | <0.20 | 7.84 | <0.20 |
| Cr | mg/l | - | - | - | - | - | <0.04 | <0.04 | <0.04 | <0.04 | <0.04 | <0.04 | <0.04 | <0.04 | <0.04 | <0.04 |
| Al | mg/l | - | <0.1 | <2.00 | 0.06 | 0.08 | 0.24 | 0.36 | 0.45 | 0.27 | 0.30 | 0.28 | 0.059 | 0.109 | 0.059 | 0.063 |
| Total P | mg/l | - | <0.1 | - | | | | | | | | | | | | |
| Total S | mg/l | - | <2.5 | 1.05 | 17.7 | 17.6 | 31.3 | 33.3 | 30.4 | 11.8 | 21.8 | 28.2 | 18.6 | 24.8 | 47.1 | 34.5 |
| Si | mg/l | - | 23.7 | BD | 6.67 | 5.43 | 8.92 | 5.66 | 4.08 | 2.71 | 9.86 | 7.61 | 17.8 | 13.8 | 27.4 | 8.98 |
| $SiO_2$ | mg/l | - | 50.7 | BD | 14.27 | 11.62 | 19.1 | 12.1 | 8.73 | 5.80 | 21.1 | 16.3 | 38.1 | 29.5 | 58.6 | 19.2 |
| Cl | mg/l | 18482 | 18921 | 18659 | 18760 | 18528 | 21868 | 31166 | 17963 | 18063 | 19119 | 18381 | 19377 | 19057 | 20616 | 19841 |
| Br | mg/l | - | 71.5 | <2.00 | <7.5 | <7.5 | <12.00 | <6.00 | <6.00 | <6.00 | <6.00 | <6.00 | <6.00 | <6.00 | <6.00 | <6.00 |
| $NO_3$ | mg/l | - | 8.40 | - | - | - | - | - | - | - | - | - | - | - | - | - |
| $SO_4$ | mg/l | ND | <60 | <2.00 | <75 | 280 | <120 | 78.3 | <60.0 | <60.0 | <60.0 | <60.0 | <60.0 | <60.0 | <60.0 | <60.0 |
| $HCO_3$ *** | mg/l | 707 | 842 | 386 | 1900 | 144 | 487 | 27.0 | 378 | 172 | 324 | 74.7 | 1860 | 83.0 | 1890 | 28.0 |
| Ionic balance | % | - | -3.07 | - | 2.40 | 3.30 | -4.15 | -2.24 | 10.1 | 5.56 | 4.14 | 1.65 | 4.95 | 2.85 | 6.65 | 4.11 |
| TIC ($CO_3^{2-}$) † | mol/l | - | 0.0030 | - | ? | ? | 1.06 | - | | | | | 0.834 | 0.011 | 0.755 | 0.025 |
| TOC | mol/l | - | <0.0003 | - | - | - | - | - | - | - | - | - | | | | |

LIMS = Laboratory Information Management System
ND = Not detected
BD = Below detection
# = A new and 'experimental' analytical method was employed to generate this data - treat with caution
† = $CO_2$-rich solutions captured in 4M NaOH whilst at 10 Mpa pressure. Potentiometric titrations represent total inorganic carbon (i.e. $CO_2$, $H_2CO_3$, $HCO_3^-$, $CO_3^{2-}$ etc).
? = Measured concentrations appear lower than expected.

# Appendix II

## FLUID CHEMICAL ANALYTICAL DATA FROM THE COLUMN EXPERIMENT

**INFORMATION FROM BGS FLOW EXPERIMENT - Part 1 of 2**

**RUN 958: 70°C, 0.1MPa**
**$CO_2$ saturated SACS water, 4x60cm Columns**

| | | |
|---|---|---|
| **Initial solid + PEEK column wt =** | 736.63 | g |
| **Initial PEEK column wt =** | 570.602 | g |
| **Initial solid wt =** | 166.028 | g |
| **Initial Fluid vol =** | 45.39 | $cm^3$ |
| **Mean Porosity =** | 42.01 | % |
| **Mean Flow rate** | 0.5 | $cm^3.hr^{-1}$ |

| **Sample Code** | **958/blk** | **958/blank** | **958/final blk** | **958/1** | **958/2** | **958/3** | **958/4** | **958/5** | **958/6** | **958/7** | **958/8** | **958/9** | **958/10** | **958/11** | **958/12** | **958/13** | **958/14** | **958/15** | **958/16** |
|---|---|---|---|---|---|---|---|---|---|---|---|---|---|---|---|---|---|---|---|
| **Time (hours)** | 0.0 | 0.0 | 0.0 | 30.0 | 162.0 | 334.5 | 498.0 | 666.0 | 830.0 | 999.0 | 1143.0 | 1312.0 | 1455.0 | 1647.8 | 1820.5 | 1986.7 | 2149.0 | 2316.6 | 2486.6 |
| **Time (Days)** | 0.0 | 0.0 | 0.0 | 1.3 | 6.8 | 13.9 | 20.8 | 27.8 | 34.6 | 41.6 | 47.6 | 54.7 | 60.6 | 68.7 | 75.9 | 82.8 | 89.5 | 96.5 | 103.6 |
| **Sample volume (ml)** | 21.0 | - | - | 17.0 | 21.7 | 14.8 | 21.1 | 21.5 | 21.5 | 21.5 | 21.0 | 21.0 | 21.0 | - | 14.1 | 21.7 | 22.1 | 22.2 | 23.0 |
| **Pressure P, before columns (bar)** | - | - | - | 103.6 | 104.7 | 104.1 | 100.3 | 101.9 | 100.6 | 100.6 | 103.6 | 103.6 | 103.0 | 100.3 | 101.5 | 100.8 | 99.9 | 99.3 | 99.6 |
| **Pressure P, after columns (bar)** | - | - | - | 103.7 | 104.8 | 104.0 | 100.2 | 101.9 | 100.6 | 100.6 | 103.6 | 103.6 | 102.9 | 100.3 | 101.5 | 100.8 | 99.8 | 99.3 | 99.5 |
| **pH** | 5.43 | 5.01 | 5.06 | 6.53 | 6.52 | 6.36 | 6.18 | 6.05 | 6 | 6 | 6.29 | 6.3 | 6.21 | 6.3 | 6.34 | 6.41 | 6.33 | 6.33 | 6.44 |
| **Concentrations in p.p.m.** | | | | | | | | | | | | | | | | | | | |
| **Ca** | 304.0 | 290.9 | 298.0 | 1362.5 | 1511.0 | 1495.8 | 1448.3 | 1443.3 | 1368.6 | 1333.2 | 1394.8 | 1310.0 | 1347.3 | n/s | 1321.1 | 1357.4 | 1352.4 | 1349.4 | 1298.9 |
| **Mg** | 624.2 | 639.3 | 667.6 | 631.3 | 633.3 | 651.5 | 637.3 | 648.4 | 635.3 | 605.0 | 627.2 | 591.9 | 613.1 | n/s | 593.9 | 618.1 | 623.2 | 624.2 | 602.0 |
| **Na** | 11872.6 | 11023.1 | 11519.1 | 11933.2 | 12186.7 | 12314.9 | 12039.2 | 12142.2 | 11928.1 | 11480.7 | 11982.6 | 11401.9 | 11698.8 | n/s | 11300.9 | 11791.8 | 11876.6 | 11980.6 | 11604.9 |
| **K** | 245.4 | 253.5 | 254.5 | 395.9 | 301.0 | 266.6 | 256.5 | 257.6 | 252.5 | 244.4 | 253.5 | 243.4 | 246.4 | n/s | 241.4 | 249.5 | 251.5 | 250.5 | 242.4 |
| **Cl** | 19349.6 | 19305.1 | 19470.8 | 19563.7 | 19499.1 | 19550.6 | 19705.1 | 19363.7 | 19596.0 | 19524.3 | 19411.2 | 19614.2 | 19799.0 | n/s | 19398.1 | 19488.0 | 19322.3 | 19262.7 | 19501.1 |
| **$SO_4$** | <60.60 | <60.60 | <60.60 | 88.68 | 84.44 | <60.60 | <60.60 | <60.60 | <60.60 | <60.60 | <60.60 | <60.60 | <60.60 | n/s | <60.60 | <60.60 | <60.60 | <60.60 | <60.60 |
| **Si** | 1.36 | <1.52 | <1.52 | 27.14 | 25.46 | 21.62 | 22.34 | 20.78 | 20.92 | 22.44 | 21.28 | 24.61 | 19.85 | n/s | 19.93 | 18.81 | 20.12 | 17.05 | 14.55 |
| **$SiO_2$** | 2.91 | <3.24 | <3.24 | 58.07 | 54.47 | 46.25 | 47.79 | 44.45 | 44.76 | 48.02 | 45.53 | 52.66 | 42.47 | n/s | 42.63 | 40.24 | 43.05 | 36.48 | 31.14 |
| **Total Fe** | 27.00 | 3.12 | 4.44 | 0.44 | 6.11 | 1.64 | 1.40 | 5.25 | 12.77 | 23.40 | 19.32 | 18.03 | 14.50 | n/s | 10.98 | 10.33 | 7.42 | 6.52 | 6.70 |
| **Mn** | 0.40 | 0.20 | 0.20 | 4.94 | 1.80 | 0.92 | 0.94 | 1.20 | 1.03 | 0.91 | 0.81 | 0.61 | 0.55 | n/s | 0.69 | 0.44 | 0.41 | 0.44 | 0.46 |
| **Al** | 0.39 | 0.20 | 0.12 | 0.07 | 0.07 | 0.08 | 0.08 | 0.09 | 0.19 | 0.13 | 0.11 | 0.14 | 0.15 | n/s | 0.15 | 0.17 | 0.19 | 0.20 | 0.18 |
| **$HCO_3$** | 197.96 | 143.42 | 133.32 | 371.68 | 251.49 | 255.53 | 249.47 | 370.67 | 324.21 | 405.01 | 498.94 | 464.60 | 533.28 | n/s | 398.95 | 559.54 | 544.39 | 553.48 | 500.96 |
| **Br** | <6.06 | <6.06 | <6.06 | <6.06 | <6.06 | <6.06 | <6.06 | <6.06 | <6.06 | <6.06 | <6.06 | <6.06 | <6.06 | n/s | <6.06 | <6.06 | <6.06 | <6.06 | <6.06 |
| **S** | 2.03 | 1.25 | <5.05 | 53.38 | 20.05 | 11.00 | 10.14 | 8.45 | 7.49 | 7.03 | 6.33 | 7.42 | 6.41 | n/s | 8.28 | 6.27 | 7.08 | 6.51 | 6.03 |
| **Ba** | 6.61 | 4.20 | 2.04 | 2.55 | 4.23 | 6.50 | 9.22 | 10.51 | 10.51 | 11.35 | 10.77 | 13.02 | 11.28 | n/s | 10.23 | 10.81 | 11.62 | 10.89 | 10.70 |
| **Sr** | 6.21 | 5.78 | 5.65 | 12.74 | 12.69 | 11.33 | 12.44 | 11.96 | 11.15 | 11.20 | 10.39 | 12.59 | 10.48 | n/s | 10.59 | 10.36 | 11.74 | 10.24 | 10.18 |
| **Cr** | 0.82 | 0.20 | 0.32 | 0.06 | 0.14 | 0.05 | 0.04 | 0.06 | 0.07 | 0.06 | 0.06 | 0.06 | 0.07 | n/s | 0.10 | 0.14 | 0.25 | 0.11 | 0.09 |
| **Concentrations in mol/l** | | | | | | | | | | | | | | | | | | | |
| **Ca** | 7.59E-03 | 7.26E-03 | 7.43E-03 | 3.40E-02 | 3.77E-02 | 3.73E-02 | 3.61E-02 | 3.60E-02 | 3.41E-02 | 3.33E-02 | 3.48E-02 | 3.27E-02 | 3.36E-02 | n/s | 3.30E-02 | 3.39E-02 | 3.37E-02 | 3.37E-02 | 3.24E-02 |
| **Mg** | 2.57E-02 | 2.63E-02 | 2.75E-02 | 2.60E-02 | 2.60E-02 | 2.68E-02 | 2.62E-02 | 2.67E-02 | 2.61E-02 | 2.49E-02 | 2.58E-02 | 2.43E-02 | 2.52E-02 | n/s | 2.44E-02 | 2.54E-02 | 2.56E-02 | 2.57E-02 | 2.48E-02 |
| **Na** | 5.16E-01 | 4.79E-01 | 5.01E-01 | 5.19E-01 | 5.30E-01 | 5.36E-01 | 5.24E-01 | 5.28E-01 | 5.19E-01 | 4.99E-01 | 5.21E-01 | 4.96E-01 | 5.09E-01 | n/s | 4.92E-01 | 5.13E-01 | 5.17E-01 | 5.21E-01 | 5.05E-01 |
| **K** | 6.28E-03 | 6.48E-03 | 6.51E-03 | 1.01E-02 | 7.70E-03 | 6.82E-03 | 6.56E-03 | 6.59E-03 | 6.46E-03 | 6.25E-03 | 6.48E-03 | 6.23E-03 | 6.30E-03 | n/s | 6.17E-03 | 6.38E-03 | 6.43E-03 | 6.41E-03 | 6.20E-03 |
| **Cl** | 5.46E-01 | 5.45E-01 | 5.49E-01 | 5.52E-01 | 5.50E-01 | 5.51E-01 | 5.56E-01 | 5.46E-01 | 5.53E-01 | 5.51E-01 | 5.48E-01 | 5.53E-01 | 5.59E-01 | n/s | 5.47E-01 | 5.50E-01 | 5.45E-01 | 5.43E-01 | 5.50E-01 |
| **$SO_4$** | <6.31E-04 | <6.31E-04 | <6.31E-04 | 9.23E-04 | 8.79E-04 | <6.31E-04 | <6.31E-04 | <6.31E-04 | <6.31E-04 | <6.31E-04 | <6.31E-04 | <6.31E-04 | <6.31E-04 | n/s | <6.31E-04 | <6.31E-04 | <6.31E-04 | <6.31E-04 | <6.31E-04 |
| **Si** | 4.85E-05 | <5.39E-05 | <5.39E-05 | 9.66E-04 | 9.06E-04 | 7.70E-04 | 7.95E-04 | 7.40E-04 | 7.45E-04 | 7.99E-04 | 7.58E-04 | 8.76E-04 | 7.07E-04 | n/s | 7.09E-04 | 6.70E-04 | 7.16E-04 | 6.07E-04 | 5.18E-04 |
| **$SiO_2$** | 4.85E-05 | <5.39E-05 | <5.39E-05 | 9.66E-04 | 9.07E-04 | 7.70E-04 | 7.95E-04 | 7.40E-04 | 7.45E-04 | 7.99E-04 | 7.58E-04 | 8.76E-04 | 7.07E-04 | n/s | 7.09E-04 | 6.70E-04 | 7.16E-04 | 6.07E-04 | 5.18E-04 |
| **Total Fe** | 4.83E-04 | 5.59E-05 | 7.95E-05 | 7.85E-06 | 1.09E-04 | 2.94E-05 | 2.50E-05 | 9.41E-05 | 2.29E-04 | 4.19E-04 | 3.46E-04 | 3.23E-04 | 2.60E-04 | n/s | 1.97E-04 | 1.85E-04 | 1.33E-04 | 1.17E-04 | 1.20E-04 |
| **Mn** | 7.21E-06 | 3.68E-06 | 3.70E-06 | 8.99E-05 | 3.27E-05 | 1.67E-05 | 1.72E-05 | 2.19E-05 | 1.88E-05 | 1.65E-05 | 1.48E-05 | 1.10E-05 | 9.95E-06 | n/s | 1.26E-05 | 8.03E-06 | 7.54E-06 | 8.07E-06 | 8.44E-06 |
| **Al** | 1.45E-05 | 7.36E-06 | 4.35E-06 | 2.52E-06 | 2.66E-06 | 2.97E-06 | 3.09E-06 | 3.24E-06 | 7.20E-06 | 4.83E-06 | 4.03E-06 | 5.14E-06 | 5.43E-06 | n/s | 5.46E-06 | 6.27E-06 | 6.93E-06 | 7.58E-06 | 6.69E-06 |
| **$HCO_3$** | 3.24E-03 | 2.35E-03 | 2.18E-03 | 6.09E-03 | 4.12E-03 | 4.19E-03 | 4.09E-03 | 6.07E-03 | 5.31E-03 | 6.64E-03 | 8.18E-03 | 7.61E-03 | 8.74E-03 | n/s | 6.54E-03 | 9.17E-03 | 8.92E-03 | 9.07E-03 | 8.21E-03 |
| **Br** | <7.58E-05 | <7.58E-05 | <7.58E-05 | <7.58E-05 | <7.58E-05 | <7.58E-05 | <7.58E-05 | <7.58E-05 | <7.58E-05 | <7.58E-05 | <7.58E-05 | <7.58E-05 | <7.58E-05 | n/s | <7.58E-05 | <7.58E-05 | <7.58E-05 | <7.58E-05 | <7.58E-05 |
| **S** | 6.34E-05 | 3.91E-05 | <1.57E-04 | 1.66E-03 | 6.25E-04 | 3.43E-04 | 3.16E-04 | 2.63E-04 | 2.33E-04 | 2.19E-04 | 1.97E-04 | 2.31E-04 | 2.00E-04 | n/s | 2.58E-04 | 1.96E-04 | 2.21E-04 | 2.03E-04 | 1.88E-04 |
| **Ba** | 4.82E-05 | 3.06E-05 | 1.48E-05 | 1.85E-05 | 3.08E-05 | 4.73E-05 | 6.71E-05 | 7.66E-05 | 7.66E-05 | 8.27E-05 | 7.84E-05 | 9.48E-05 | 8.22E-05 | n/s | 7.45E-05 | 7.87E-05 | 8.46E-05 | 7.93E-05 | 7.79E-05 |
| **Sr** | 7.09E-05 | 6.60E-05 | 6.45E-05 | 1.45E-04 | 1.45E-04 | 1.29E-04 | 1.42E-04 | 1.36E-04 | 1.27E-04 | 1.28E-04 | 1.19E-04 | 1.44E-04 | 1.20E-04 | n/s | 1.21E-04 | 1.18E-04 | 1.34E-04 | 1.17E-04 | 1.16E-04 |
| **Cr** | 1.57E-05 | 3.88E-06 | 6.10E-06 | 1.09E-06 | 2.74E-06 | 1.01E-06 | 8.35E-07 | 1.09E-06 | 1.30E-06 | 1.20E-06 | 1.22E-06 | 1.11E-06 | 1.28E-06 | n/s | 1.85E-06 | 2.60E-06 | 4.72E-06 | 2.12E-06 | 1.69E-06 |

**n/s = No Sample**

**INFORMATION FROM BGS FLOW EXPERIMENT - Part 2 of 2**

**RUN 958: 70°C, 0.1MPa**
**$CO_2$ saturated SACS water, 4x60cm Columns**

| | | |
|---|---|---|
| **Initial solid + PEEK column wt =** | 736.63 | g |
| **Initial PEEK column wt =** | 570.602 | g |
| **Initial solid wt =** | 166.028 | g |
| **Initial Fluid vol =** | 45.39 | $cm^3$ |
| **Mean Porosity =** | 42.01 | % |
| **Mean Flow rate** | 0.5 | $cm^3.hr^{-1}$ |

| **Sample Code** | **958/17** | **958/18** | **958/19** | **958/20** | **958/21** | **958/22** | **958/23** | **958/24** | **958/25** | **958/26** | **958/27** | **958/28** | **958/29** | **958/30** | **958/31** | **958/32** | **958/33** |
|---|---|---|---|---|---|---|---|---|---|---|---|---|---|---|---|---|---|
| **Time (hours)** | 2653.1 | 2821.1 | 3325.1 | 3469.1 | 3661.1 | 3829.6 | 3998.1 | 4166.1 | 4501.1 | 4669.1 | 5005.1 | 5173.1 | 5318.1 | 5678.1 | 5848.1 | 6682.9 | 7020.1 |
| **Time (Days)** | 110.5 | 117.5 | 138.5 | 144.5 | 152.5 | 159.6 | 166.6 | 173.6 | 187.5 | 194.5 | 208.5 | 215.5 | 221.6 | 236.6 | 243.7 | 278.5 | 292.5 |
| **Sample volume (ml)** | 22.6 | 23.0 | 21.8 | 22.0 | 21.5 | 22.5 | 20.0 | - | 22.0 | 22.2 | 22.0 | 21.5 | 22.7 | 22.0 | 22.9 | 12.0 | 22.0 |
| **Pressure $P_1$ before columns (bar)** | 99.3 | 99.2 | 98.8 | 99.6 | 100.6 | 99.8 | 104.0 | 104.0 | 104.1 | 104.1 | 99.8 | 99.5 | 100.5 | 99.9 | 98.6 | 101.1 | 100.2 |
| **Pressure $P_3$ after columns (bar)** | 99.3 | 99.2 | 98.6 | 99.6 | 100.6 | 99.8 | 104.0 | 103.9 | 104.1 | 104.1 | 99.8 | 99.5 | 100.4 | 99.8 | 98.4 | 98.9 | 100.2 |
| **pH** | 6.35 | 6.31 | 6.3 | 6.32 | 6.41 | 6.3 | 6.29 | 6.31 | 6.38 | 6.35 | 6.33 | 6.28 | 6.27 | 6.3 | 6.3 | 6.47 | 6.27 |
| **Concentrations in p.p.m.** | | | | | | | | | | | | | | | | | |
| **Ca** | 1317.0 | 1338.3 | 1305.9 | 1271.6 | 1319.1 | 1339.3 | 1384.7 | 1377.6 | 1300.9 | 1291.8 | 1257.5 | 1366.5 | 1236.2 | 1220.1 | 1207.0 | 1151.4 | 1098.9 |
| **Mg** | 615.1 | 634.3 | 639.3 | 625.2 | 652.5 | 656.5 | 673.7 | 669.6 | 654.5 | 666.6 | 681.8 | 751.4 | 667.6 | 653.5 | 657.5 | 677.7 | 666.6 |
| **Na** | 11825.1 | 12092.7 | 12148.3 | 11869.5 | 11178.7 | 11316.0 | 11554.4 | 11521.1 | 11462.5 | 11513.0 | 11602.9 | 12548.2 | 11477.6 | 11187.8 | 11135.3 | 11582.7 | 11339.3 |
| **K** | 246.4 | 253.5 | 254.5 | 251.5 | 260.6 | 262.6 | 269.7 | 269.7 | 261.6 | 265.6 | 269.7 | 286.8 | 267.7 | 262.6 | 263.6 | 269.7 | 265.6 |
| **Cl** | 19432.4 | <20.2 | 19505.1 | 20130.3 | 19417.3 | 19419.3 | 19347.6 | 19158.7 | 19401.1 | 19767.7 | 19511.2 | 19481.9 | 19004.2 | 20686.8 | 19385.9 | 20411.1 | 19358.7 |
| **$SO_4$** | <60.60 | <60.60 | <60.60 | <60.60 | <60.60 | <60.60 | <60.60 | <60.60 | <60.60 | <60.60 | <60.60 | <60.60 | <60.60 | <60.60 | <60.60 | <60.60 | <60.60 |
| **Si** | 15.07 | 18.56 | 16.57 | 16.28 | 15.71 | 19.41 | 15.72 | 13.82 | 13.94 | 13.77 | 13.77 | 13.64 | 14.74 | 14.48 | 13.68 | 14.18 | 14.34 |
| **$SiO_2$** | 32.24 | 39.71 | 35.46 | 34.83 | 33.62 | 41.51 | 33.63 | 29.57 | 29.83 | 29.46 | 29.46 | 29.18 | 31.53 | 30.99 | 29.26 | 30.33 | 30.67 |
| **Total Fe** | 4.73 | 8.64 | 11.05 | 12.45 | 12.85 | 15.21 | 10.76 | 8.60 | 5.47 | 6.09 | 6.44 | 1.32 | 20.48 | 32.60 | 16.21 | 29.60 | 25.16 |
| **Mn** | 0.54 | 0.52 | 0.58 | 0.61 | 0.54 | 0.47 | 0.47 | 0.57 | 0.43 | 0.47 | 0.71 | 0.77 | 0.54 | 0.58 | 0.68 | 0.78 | 0.62 |
| **Al** | 0.17 | 0.18 | 0.18 | 0.08 | 0.12 | 0.12 | 0.08 | 0.07 | 0.11 | 0.07 | 0.07 | 0.07 | 0.08 | 0.30 | 0.09 | 0.10 | 0.10 |
| **$HCO_3$** | 599.94 | 571.66 | 623.17 | 533.28 | 561.56 | 626.20 | 637.31 | 529.24 | 542.37 | 602.97 | 690.84 | 684.78 | 714.07 | 802.95 | 746.39 | 565.60 | 827.19 |
| **Br** | <6.06 | <6.06 | <6.06 | <6.06 | <6.06 | <6.06 | <6.06 | <6.06 | <6.06 | <6.06 | <6.06 | <6.06 | <6.06 | <6.06 | <6.06 | <6.06 | <6.06 |
| **S** | 6.34 | 8.15 | 6.97 | 7.38 | 7.12 | 9.39 | 7.52 | 7.21 | 7.66 | 7.51 | 8.05 | 7.63 | 8.07 | 8.68 | 8.00 | 8.28 | 8.22 |
| **Ba** | 10.76 | 13.02 | 10.32 | 9.99 | 9.63 | 11.77 | 9.68 | 8.88 | 8.96 | 8.97 | 8.97 | 8.59 | 8.48 | 8.93 | 8.05 | 8.54 | 8.86 |
| **Sr** | 9.89 | 11.82 | 9.80 | 10.05 | 9.79 | 12.32 | 10.30 | 9.53 | 9.52 | 9.32 | 9.39 | 9.46 | 9.44 | 9.46 | 9.14 | 8.50 | 8.39 |
| **Cr** | 0.08 | 0.10 | 0.12 | 0.08 | 0.06 | 0.04 | 0.05 | 0.06 | 0.04 | 0.06 | 0.05 | <0.04 | <0.04 | <0.04 | 0.05 | 0.13 | 0.06 |
| **Concentrations in mol/l** | | | | | | | | | | | | | | | | | |
| **Ca** | 3.29E-02 | 3.34E-02 | 3.26E-02 | 3.17E-02 | 3.29E-02 | 3.34E-02 | 3.45E-02 | 3.44E-02 | 3.25E-02 | 3.22E-02 | 3.14E-02 | 3.41E-02 | 3.08E-02 | 3.04E-02 | 3.01E-02 | 2.87E-02 | 2.74E-02 |
| **Mg** | 2.53E-02 | 2.61E-02 | 2.63E-02 | 2.57E-02 | 2.68E-02 | 2.70E-02 | 2.77E-02 | 2.75E-02 | 2.69E-02 | 2.74E-02 | 2.80E-02 | 3.09E-02 | 2.75E-02 | 2.69E-02 | 2.70E-02 | 2.79E-02 | 2.74E-02 |
| **Na** | 5.14E-01 | 5.26E-01 | 5.28E-01 | 5.16E-01 | 4.86E-01 | 4.92E-01 | 5.03E-01 | 5.01E-01 | 4.99E-01 | 5.01E-01 | 5.05E-01 | 5.46E-01 | 4.99E-01 | 4.87E-01 | 4.84E-01 | 5.04E-01 | 4.93E-01 |
| **K** | 6.30E-03 | 6.48E-03 | 6.51E-03 | 6.43E-03 | 6.66E-03 | 6.72E-03 | 6.90E-03 | 6.90E-03 | 6.69E-03 | 6.79E-03 | 6.90E-03 | 7.34E-03 | 6.85E-03 | 6.72E-03 | 6.74E-03 | 6.90E-03 | 6.79E-03 |
| **Cl** | 5.48E-01 | <5.70E-04 | 5.50E-01 | 5.68E-01 | 5.48E-01 | 5.48E-01 | 5.46E-01 | 5.40E-01 | 5.47E-01 | 5.58E-01 | 5.50E-01 | 5.50E-01 | 5.36E-01 | 5.84E-01 | 5.47E-01 | 5.76E-01 | 5.46E-01 |
| **$SO_4$** | <6.31E-04 | <6.31E-04 | <6.31E-04 | <6.31E-04 | <6.31E-04 | <6.31E-04 | <6.31E-04 | <6.31E-04 | <6.31E-04 | <6.31E-04 | <6.31E-04 | <6.31E-04 | <6.31E-04 | <6.31E-04 | <6.31E-04 | <6.31E-04 | <6.31E-04 |
| **Si** | 5.36E-04 | 6.61E-04 | 5.90E-04 | 5.80E-04 | 5.59E-04 | 6.91E-04 | 5.60E-04 | 4.92E-04 | 4.96E-04 | 4.90E-04 | 4.90E-04 | 4.86E-04 | 5.25E-04 | 5.16E-04 | 4.87E-04 | 5.05E-04 | 5.10E-04 |
| **$SiO_2$** | 5.37E-04 | 6.61E-04 | 5.90E-04 | 5.80E-04 | 5.59E-04 | 6.91E-04 | 5.60E-04 | 4.92E-04 | 4.96E-04 | 4.90E-04 | 4.90E-04 | 4.86E-04 | 5.25E-04 | 5.16E-04 | 4.87E-04 | 5.05E-04 | 5.10E-04 |
| **Total Fe** | 8.47E-05 | 1.55E-04 | 1.98E-04 | 2.23E-04 | 2.30E-04 | 2.72E-04 | 1.93E-04 | 1.54E-04 | 9.80E-05 | 1.09E-04 | 1.15E-04 | 2.36E-05 | 3.67E-04 | 5.84E-04 | 2.90E-04 | 5.30E-04 | 4.50E-04 |
| **Mn** | 9.80E-06 | 9.43E-06 | 1.05E-05 | 1.11E-05 | 9.82E-06 | 8.47E-06 | 8.60E-06 | 1.04E-05 | 7.85E-06 | 8.64E-06 | 1.30E-05 | 1.40E-05 | 9.89E-06 | 1.05E-05 | 1.23E-05 | 1.42E-05 | 1.12E-05 |
| **Al** | 6.32E-06 | 6.59E-06 | 6.51E-06 | 3.11E-06 | 4.40E-06 | 4.48E-06 | 2.90E-06 | 2.74E-06 | 3.94E-06 | 2.57E-06 | 2.51E-06 | 2.43E-06 | 3.02E-06 | 1.13E-05 | 3.30E-06 | 3.60E-06 | 3.85E-06 |
| **$HCO_3$** | 9.83E-03 | 9.37E-03 | 1.02E-02 | 8.74E-03 | 9.20E-03 | 1.03E-02 | 1.04E-02 | 8.67E-03 | 8.89E-03 | 9.88E-03 | 1.13E-02 | 1.12E-02 | 1.17E-02 | 1.32E-02 | 1.22E-02 | 9.27E-03 | 1.36E-02 |
| **Br** | <7.58E-05 | <7.58E-05 | <7.58E-05 | <7.58E-05 | <7.58E-05 | <7.58E-05 | <7.58E-05 | <7.58E-05 | <7.58E-05 | <7.58E-05 | <7.58E-05 | <7.58E-05 | <7.58E-05 | <7.58E-05 | <7.58E-05 | <7.58E-05 | <7.58E-05 |
| **S** | 1.98E-04 | 2.54E-04 | 2.17E-04 | 2.30E-04 | 2.22E-04 | 2.93E-04 | 2.35E-04 | 2.25E-04 | 2.39E-04 | 2.34E-04 | 2.51E-04 | 2.38E-04 | 2.52E-04 | 2.71E-04 | 2.50E-04 | 2.58E-04 | 2.56E-04 |
| **Ba** | 7.84E-05 | 9.48E-05 | 7.52E-05 | 7.27E-05 | 7.01E-05 | 8.57E-05 | 7.05E-05 | 6.47E-05 | 6.53E-05 | 6.53E-05 | 6.53E-05 | 6.26E-05 | 6.18E-05 | 6.51E-05 | 5.87E-05 | 6.22E-05 | 6.45E-05 |
| **Sr** | 1.13E-04 | 1.35E-04 | 1.12E-04 | 1.15E-04 | 1.12E-04 | 1.41E-04 | 1.18E-04 | 1.09E-04 | 1.09E-04 | 1.06E-04 | 1.07E-04 | 1.08E-04 | 1.08E-04 | 1.08E-04 | 1.04E-04 | 9.70E-05 | 9.57E-05 |
| **Cr** | 1.63E-06 | 1.86E-06 | 2.29E-06 | 1.50E-06 | 1.15E-06 | 8.35E-07 | 8.93E-07 | 1.11E-06 | 7.96E-07 | 1.15E-06 | 8.74E-07 | <7.77E-07 | <7.77E-07 | <7.77E-07 | 9.52E-07 | 2.54E-06 | 1.18E-06 |

**n/s = No Sample**